Electronic Supplementary Material (ESI) for Dalton Transactions.

Supplemental information for:

Design of porphyrin-based ligands for the assembly of [*d*-block metal:calcium] bimetallic centers

Matthieu Koepf, Jesse J. Bergkamp, Anne-Lucie Teillout, Manuel Jose Llansola-Portoles, Gerdenis Kodis, Ana L. Moore, Devens Gust, and Thomas A. Moore

Contribution of the

Center for Bio-Inspired Solar Fuel Production,

Department of Chemistry and Biochemistry, Arizona State University, Tempe, AZ 85287, USA

Table of content

1 Experimental procedures

1.1 Materials and methods

Dipyrrylmethane was prepared according to a previously published procedure.[1] 2-nitrobenzaldehyde, trifluoroacetic acid (TFA), 1,2-dicyno-4,5-dichloroquinone (DDQ), tin chloride ($SnCl_2$), zinc acetate dihydrate ($ZnOAc.2H_2O$), N-bromosuccinimide (NBS), potassium phosphate tribasique (K_3PO_4), sodium tetraphenylborate ($NaBPh_4$), 2-(1H-Benzotriazole-1-yl)-1,1,3,3-tetramethyluronium hexafluorophosphate (HBTU), *p*-toluenesulfonic acid (*p*-TSA), methyl-2-formylbenzoate, citric acid, and boron trifluoride etherate ($BF_3.Et_2O$) complex were purchased from Alfa-Aesar. Triethylamine (TEA), chloroacethyl chloride($ClCH_2COCl$), tetrahydrofuran (THF) stabilized with BHT, dimethylformamide (DMF), benzene, 4,13-diaza-18-crown-6, 4-aza-18-crown-6, and benzaldehyde were obtained from Acros Organics. Methyl-2-carboxyphenylboronic acid was purchased from Aldrich. Palladium(0) *tetrakis*-triphenylphosphine ($Pd(PPh_3)_4$) and zinc(0) powder ~ 40 mesh were obtained from Strem Chemicals. Hydrochloric acid (HCl, 37% aqueous solution), ammonium hydroxide (28 % aqueous solution), glacial acetic acid (AcOH), Sodium bicarbonate ($NaHCO_3$), sodium sulfate (Na_2SO_4), potassium carbonate (K_2CO_3), potassium hydroxide (KOH), pyridine, and ethylene glycol were obtained from JT-Baker. Chloroform ($CHCl_3$) stabilized with ethanol, toluene, dichloromethane stabilized with amylenes (CH_2Cl_2), hexanes, methanol (MeOH), acetone, ethyl acetate (EtOAc) were obtained from BDH and absolute ethanol from Decon labs. All the reagents were purchased with ACS grade quality or higher, and were used without further purification for synthesis purposes. Solvents were distilled prior to use. Dichloromethane, hexane and ethyl acetate were distilled over calcium chloride. Dioxane and THF were distilled over sodium and were stored under Argon (Ar). Analytical thin layer chromatography (TLC) was conducted on glass-coated silica gel 60 F254 plates obtained from EMD-Millipore. Column chromatography were conducted on silica gel (SiO_2, 43–60 μm) provided by Silicycle. Unless specified, the 43–60 μm silica gel was used as stationary phase for the columns as well as the adsorption support for dry loading. Celite® 545 was purchased from EMD-Millipore.

Mass spectrometry was conducted on an Voyager DE STR MALDI-TOF spectrometer from Applied Biosystems using tertiophene or trans-2-[3-(4-tert-Butylphenyl)-2-methyl-2-propenylidene]malononitrile (DCTB) as ionization matrix. High res SM was conducted on a JEOL LCmate mass spectrometer using ESI ionization mode. ^1H NMR were conducted on Varian spectrometers operating at 400 or 500 MHz in the appropriate deuterated solvents. Residual solvent peaks or TMS were used to calibrate the chemical shifts. UV–Visible spectroscopy was performed using a Shimadzu UV-2550 UV–Visible spectrophotometer.

1.2 Preparation of ligands 1a and 1b

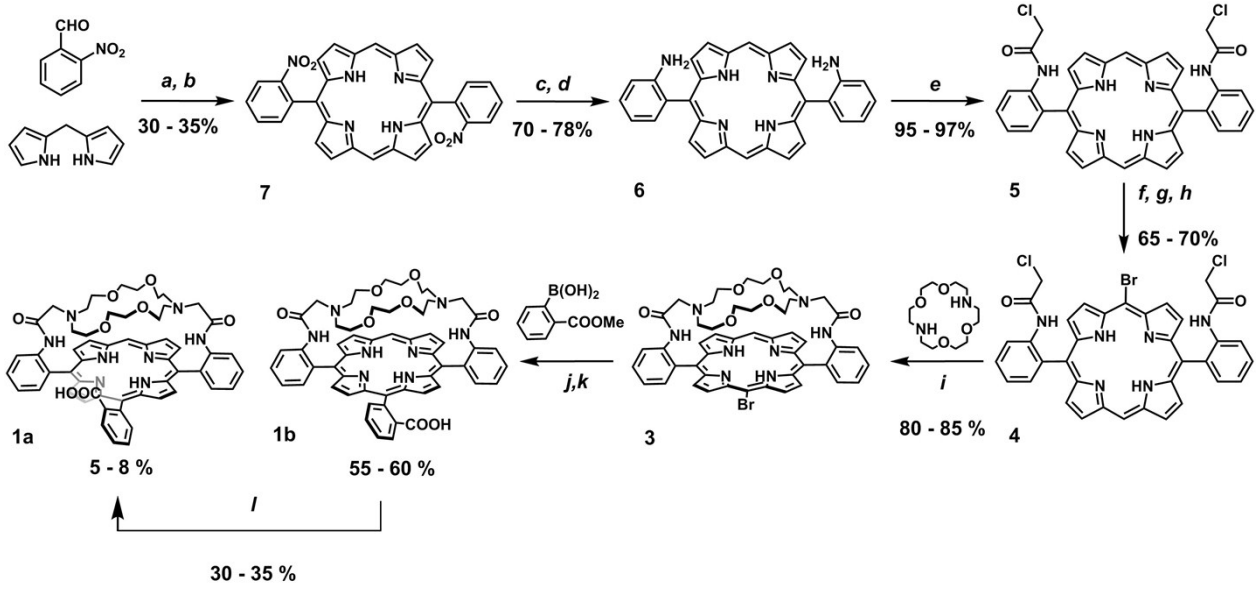

Scheme 1. Synthetic scheme for ligands **1a** and **1b**. *a)* TFA (trifluoroacetic acid), $CHCl_3$, Ar (argon), RT (room temperature); *b)* DDQ (2,3-dichloro-5,6-dcyano-1,4-benzoquionone), $CHCl_3$, RT; *c)* $SnCl_2$, HCl, Ar, 65°C; *d)* SiO_2, Toluene, Ar, 90°C; *e)* $ClCH_2COCl$, K_2CO_3, CH_2Cl_2, Ar, O°C - RT; *f)* $Zn(OAc)_2$ (zinc(II) acetate), DMF (dimethylformamide), 45°C; *g)* NBS (N-bromosuccinimide), pyridine, $CHCl_3$, Ar, 0°C; *h)* TFA, CH_2Cl_2, RT; *i)* EtOH (ethanol), Ar, 70°C; *j)* $Pd(PPh_3)_4$, K_3PO_4, dioxane, Ar, 80°C ; *k)* KOH, MeOH (methanol), THF, H_2O, Ar, 45°C; *l)* $NaBPh_4$, pyridine-toluene 1-4, Ar, 90°C.

General synthetic strategy

In brief, the 5,15-bis(2-nitrophenyl)porphyrin (**7**) was obtained as a mixture of two atropisomers by direct condensation of dipyrrylmethane[2] and 2-nitrobenzaldehyde under acid catalysis. The nitro groups were subsequently reduced to amines using tin(II) chloride in acidic conditions. Thermal treatment of the resulting mixture in the presence of silica, according to the protocol described by Lindsey[3], yielded the desired α,α-atropisomer (**6**) as the major product. After isolation, **6** was acylated with chloroacetyl chloride at low temperature and the resulting derivative (**5**) was brominated with *N*-bromosuccinimide. Treatment of the mono-bromo macrocycle (**4**) with 4,13-diaza-18-crown-6 in refluxing ethanol gave the capped porphyrin (**3**) in good yield. The latter was engaged in a palladium-catalyzed Suzuki coupling with 2-(carboxymethyl)phenylboronic acid to yield the methyl-ester form of ligands: **1a-OMe** and **1b-OMe**. The ratio of **1a-OMe**/**1b-OMe** was estimated to be 1/8 by ^{1}H-NMR spectroscopy (see section 2.1). The two atropisomers **1a** and **1b** could only be separated after the hydrolysis of the esters. The final ligands **1a** and **1b** were stable at room temperature, showing no detectable interconversion in solution over days. However, at elevated temperatures (>80 °C) the atropisomers underwent dynamic exchange and rapidly re-equilibrated into the initial **1a**/**1b** ratio of 1/8. The final proportion of **1a** in the mixture could be increased by annealing either pure **1b** or the initial mixture of both **1a** and **1b** atropisomers in the presence of sodium tetraphenylborate in a pyridine-toluene (1-4) mixture. Under these conditions the ratio of the atropisomers equilibrated at roughly

1a/**1b** ~ 1/2 and thus permitted isolation of the desired conformer **1a** in higher quantity (*cf.* SI section 2.2).

Synthesis of 5,15-bis-(2-nitrophenyl)porphyrin 7

In a two-neck 1L round bottom flask, 2-nitrobenzaldehyde (552 mg, 3.65 mmol) was dissolved in chloroform (720 mL), the solution was sparged with nitrogen for 15 minutes and dipyrrylmethane (600 mg, 3.65 mmol) was added. The mixture was further sparged with nitrogen for 15 minutes and trifluoroacetic acid (2.4 mL, 3.55 g, 31 mmol) was added. The solution was sparged with nitrogen for another 5 minutes, then it was stirred in the dark, under a nitrogen atmosphere, for 1 hour at room temperature. 1,2-dicyano-4,5-dichloro-1,4-benzoquinone (3.0 g, 13.2 mmol) was added and the mixture was stirred at room temperature for 1 hour. Triethylamine (4 mL) was added and the mixture was extracted with water (3 x 400 mL). The organic layer was collected, dried over sodium sulfate, filtered and the solvent was evaporated under reduced pressure. The crude product was purified on column chromatography (SiO_2, CH_2Cl_2-hexanes 7-3) to yield the desired 5,15-bis-(2-nitrophenyl) porphyrin as a mixture of two atropisomers (376.6 mg, 0.68 mmol, 37 %). The ^{1}H-NMR spectrum of the obtained porphyrins mixture was in good agreement with the previously reported data.[4]

^{1}H-NMR (400 MHz, $CDCl_3$) δ 10.28 (s, 2H), 9.36 (d, *J* = 4.7 Hz, 4H), 8.84 (d, *J* = 4.6 Hz, 4H), 8.55 – 8.40 (m, 2H), 8.35 – 8.22 (m, 2H), 8.09 – 7.90 (m, 4H), -3.10 (s, 2H).

Synthesis of 5,15-bis(2-aminophenyl)porphyrin 6

In a 100 mL round bottom flask, 5,15-bis-(2-nitrophenyl)porphyrin **7** (340 mg, 0.62 mmol) was dissolved in concentrated hydrochloric acid (37% aqueous solution, 30 ml), tin(II) chloride dihydrate (1.04 g, 4.62 mmol) was added and the mixture was stirred at room temperature for 3 hours. It was treated with a concentrated aqueous ammonium hydroxide solution until the pH was stabilized at 7. The aqueous layer was extracted with a CH_2Cl_2-EtOAc 4-1 mixture (2 x 200 mL). The combined organic layers were dried over Na_2SO_4, filtered and the solvent was evaporated. The crude material was purified by column chromatography (SiO_2) with the following elution gradient: CH_2Cl_2-hexane (8-2) – CH_2Cl_2 – CH_2Cl_2-1% acetone. The 5,15-bis(2-aminophenyl)porphyrin was obtained as two bands, the first eluted with pure CH_2Cl_2 corresponded to the αβ isomer (151.4 mg, 0.31 mmol, 50%), the second band eluted with the use of CH_2Cl_2-1% acetone corresponded to the desired αα isomer (140.3 mg, 0.29 mmol, 47%). The ^{1}H-NMR spectra of the prepared porphyrins were in good agreement with the previously reported data.[5]

αβ-5,15-bis-(2-aminophenyl)porphyrin

^{1}H-NMR (400 MHz, $CDCl_3$) δ 10.27 (s, 2H), 9.38 (d, *J* = 4.6 Hz, 4H), 9.10 (d, *J* = 4.6 Hz, 4H), 7.90 (dd, *J* = 7.4, 1.6 Hz, 2H), 7.72 – 7.56 (m, 2H), 7.25 – 7.10 (m, 4H), 3.58 (s, 4H), -3.13 (s, 2H).

αα-5,15-bis-(2-aminophenyl)porphyrin

^{1}H-NMR (400 MHz, $CDCl_3$) δ 10.27 (brs, 2H), 9.37 (d, *J* = 4.6, 4H), 9.10 (d, *J* = 4.6 Hz, 4H), 7.95 (dd, *J* = 7.4, 1.6 Hz, 1H), 7.90 (dd, *J* = 7.4, 1.6 Hz, 1H), 7.66 – 7.60 (m, 2H), 7.24 –7.18 (m, 2H), 7.16 –7.12 (m, 2H), 3.57 (s, 2H), 3.52 (s, 2H), -3.13 (s, 2H).

Isomerization of αβ-5,15-bis-(2-aminophenyl)porphyrin

A two-neck 250 mL round bottom flask equipped with a dean stark condenser was charged with silica (12 g) and toluene (70 mL). The silica slurry was refluxed under Ar for 2 hours and 25 mL of a mixture of toluene and water was collected in the dean-stark apparatus. The temperature was reduced to 80 °C and the αβ-5,15-bis-(2-aminophenyl) porphyrin was added (270 mg, 0.55 mg). The slurry was stirred at 80 °C, under Ar, for 10h. The mixture was cooled down to room temperature and filtered on a silica short plug (SiO_2, CH_2Cl_2). The remaining αβ-5,15-bis-(2-aminophenyl) porphyrin was eluted with CH_2Cl_2 (53 mg, 0.11 mmol, 20%). The desired αα-5,15-bis-(2-aminophenyl) porphyrin was then eluted with CH_2Cl_2-1% acetone (199 mg, 0.41 mmol, 74%). The ^{1}H-NMR spectra of the isomerized porphyrin perfectly matched the spectra of the as-prepared porphyrins.

Synthesis of αα-5,15-bis-(2-(2-chloroacethyl)aminophenyl)porphyrin 5

In a 100 mL round bottom flask, αα-5,15-bis-(2-aminophenyl) porphyrin **6** (365 mg, 0.74 mmol) was dissolved in chloroform (60 mL). Potassium carbonate (0.92 g, 8.7 mmol) was added to the solution and the mixture was cooled to 0 °C under nitrogen. Chloroacethyl chloride (0.32 mL, 460 mg, 4.1 mmol) was added and the mixture was further stirred at 0 °C for 10 minutes. The reaction mixture was warmed up to room temperature then quenched with the slow addition of water (30 mL). The organic layer was collected and further washed with 5% $NaHCO_3$ solution (1 x 50 mL), saturated ammonium chloride solution (1 x 50 mL) and water (1 x 50 mL). The organic layer was collected, dried over Na_2SO_4, filtered and the solvent was evaporated. The crude material was filtered over a silica short plug (SiO_2, CH_2Cl_2-1% acetone) to yield the desired product as a bright purple crystalline solid (474 mg, 0.73 mmol, 99%).

^{1}H-NMR (400 MHz, $CDCl_3$) δ 10.34 (s, 2H), 9.42 (d, *J* = 4.6 Hz, 4H), 8.98 (d, *J* = 4.6 Hz, 4H), 8.74 (d, *J* = 7.5 Hz, 2H), 8.16 (s, 2H), 8.09 (dd, *J* = 7.5, 1.6 Hz, 2H), 7.90 (ddd, *J* = 8.7, 7.7, 1.6 Hz, 2H), 7.62 (td, *J* = 7.5, 1.2 Hz, 2H), 3.42 (s, 4H), -3.09 (s, 2H).

Synthesis of αα-5,15-bis-(2-(2-chloroacethyl)aminophenyl)-10-bromoporphyrin 4

a) zinc insertion

αα-5,15-bis-(2-(2-chloroacethyl)aminophenyl)porphyrin **5** (302 mg, 0.47 mmol) was dissolved in tetrahydrofuran and zinc acetate (3.01 g, 13.7 mmol) was added. The mixture was stirred at 30 °C for 30 minutes after which TLC analysis (SiO_2, CH_2Cl_2-0.5% acetone) indicated complete metallation of the porphyrin. The porphyrin was precipitated in water (200 mL) and the solid was recovered by filtration. The solid was thoroughly washed with water (200 mL), dissolved in CH_2Cl_2-THF 5-1 (200 mL) and the organic layer was further extracted with water (3 x 100 mL). The organic layer was recovered, dried over Na_2SO_4, filtered and the solvent was evaporated under reduced pressure. The obtained compound was used in the following step without further purification (333 mg, 0.47 mmol, 100 %).

b) bromation

The metallated porphyrin (333 mg, 0.47 mmol) was dissolved in chloroform (150 mL) containing 1% v/v of pyridine. The solution was cooled to 0 °C and *N*-bromosuccinimide (75 mg, 0.42 mmol) was added. The reaction mixture was stirred at 0 °C for 15 minutes before being quenched by the addition of acetone (20 mL). The mixture was washed with water (3 x 100 mL), the organic layer was collected, dried

over Na_2SO_4, filtered, and the solvent was evaporated under reduced pressure. The crude solid was partly dissolved in CH_2Cl_2 (100 mL), trifluoroacetic acid (15 mL) was added and the mixture was stirred at room temperature for 15 minutes. The mixture was extracted with water (2 x 100 mL), diluted sodium hydroxide solution (1% aqueous, 2 x 50 mL) and water (1 x 100 mL). The organic layer was collected, dried over Na_2SO_4, filtered and the solvent was evaporated under reduced pressure. Column chromatography (SiO_2, CH_2Cl_2-0.5% acetone) yielded three major fractions in the following order:

αα-5,15-bis-(2-(2-chloroacethyl)aminophenyl)-10,20-dibromoporphyrin (72.6 mg, 90 µmol, 19%)

^{1}H-NMR (400 MHz, $CDCl_3$) δ 9.54 (d, *J* = 4.9 Hz, 4H), 8.68 (d, *J* = 4.9 Hz, 4H), 8.62 (dd, *J* = 8.5, 1.1 Hz, 2H), 7.96 – 7.88 (m, 4H), 7.84 – 7.77 (m, 2H), 7.55 – 7.49 (m, 2H), 3.36 (s, 4H), -2.70 (s, 2H).

MS (MALDI-TOF, positive) calcd for $C_{36}H_{24}Br_2Cl_2N_6O_2$ [M^+] *m/z(*100%) 799.97, found *m/z*(100%) 800.03.

αα-5,15-bis-(2-(2-chloroacethyl)aminophenyl)-10-bromoporphyrin (219.9 mg, 0.30 mmol, 64%)

^{1}H-NMR (400 MHz, $CDCl_3$) δ 10.17 (s, 1H), 9.73 (d, *J* = 4.8 Hz, 2H), 9.29 (d, *J* = 4.7 Hz, 2H), 8.88 – 8.84 (m, 4H), 8.70 (d, *J* = 8.4 Hz, 1H), 8.06 (brs, 2H), 8.05 – 7.95 (m, 4H), 7.92 – 7.86 (m, 2H), 7.59 (td, *J* = 7.5, 1.2 Hz, 2H), 3.41 (s, 4H), -2.94 (s, 2H).

MS (MALDI-TOF, positive) calcd for $C_{36}H_{25}BrCl_2N_6O_2$ [M^+] *m/z(*100%) 722.06, found *m/z*(100%) 722.04.

αα-5,15-bis-(2-(2-chloroacethyl)aminophenyl)porphyrin (24.1 mg, 80 µmol, 17%); ^{1}H NMR spectrum matched the spectrum of the as-prepared compound.

Synthesis of strapped porphyrin 3

A two-neck 1L round bottom flask equipped with a reflux condenser was charged with αα-5,15-bis-(2-(2-chloroacethyl)aminophenyl)-10-bromoporphyrin **4** (185 mg, 0.26 mmol), 4,13-diaza-18-crown-6 (400 mg, 1.52 mmol) and absolute ethanol (650 mL). After sparging the suspension with argon for 20 minutes it was gently refluxed at 60 °C under argon. The progression of the reaction was followed by TLC (SiO_2, CH_2Cl_2-5% acetone). After 4 days of gentle reflux no more starting material remained. The solvent was evaporated under reduced pressure and the crude solid was dissolved in dichloromethane (300 mL). The mixture was extracted with water (2 x 200 mL) dried over Na_2SO_4, filtered and the solvent was evaporated. Column chromatography (SiO_2, elution gradient: CH_2Cl_2-15% acetone to CH_2Cl_2-20% acetone) was conducted and the desired strapped porphyrin was obtained as the second eluted compound. Recrystallization from CH_2Cl_2-hexanes yielded porphyrin **3** as bright purple crystals (210.7 mg, 0.23 mmol, 88%).

^{1}H-NMR (400 MHz, $CDCl_3$) δ 10.18 (s, 1H), 9.74 (d, *J* = 4.8 Hz, 2H), 9.29 (d, *J* = 4.6 Hz, 2H), 8.99 (s, 2H), 8.96 – 8.91 (m, 4H), 8.83 – 8.69 (m, 2H), 7.98 (dd, *J* = 7.5, 1.5 Hz, 2H), 7.91 – 7.84 (m, 2H), 7.62 – 7.45 (m, 2H), 2.81 – 2.43 (m, 4H), 2.13 (brs, 2H), 1.65 (brs, 2H), 1.46 (brs, 12H), 0.86 (brs, 2H), 0.25 (brs, 6H), -2.84 (s, 2H).

MS (MALDI-TOF, positive) calcd for $C_{48}H_{49}BrN_8O_6$ [M^+] *m/z(*100%) 914.29, found *m/z*(100%) 914.47.

Synthesis of strapped porphyrins 1a-OMe and 1b-OMe

Synthesis of the methyl ester porphyrins (mixtures of atopisomers)

An oven-dried 3-neck 100 mL round bottom flask equipped with a reflux condenser was charged with porphyrin **3** (90 mg, 98.5 µmol), methyl-2-carboxyphenylboronic acid (90 mg, 0.5 mmol), finely grounded anhydrous potassium phosphate tribasic (232 mg, 0.87 mmol) and freshly distilled dioxane (50 mL). The slurry was sparged with argon for 30 min and palladium(0) *tetrakis*-triphenylphosphine was added. The mixture was stirred at 85 – 90 °C under argon; the progression of the reaction was followed by TLC analysis (SiO_2, CH_2Cl_2-15% acetone). After 4h no starting materials remained, the reaction mixture was cooled down to room temperature and the solvent was evaporated. The crude solid was dissolved in dichloromethane, and the mixture was extracted with saturated aqueous ammonium chloride solution (2 x 50 mL), and water (1 x 50 mL). The organic phase was collected, dried over Na_2SO_4, filtered and the solvent was evaporated under reduced pressure. The crude product was purified by column chromatography (SiO_2, elution gradient: CH_2Cl_2-10% acetone to CH_2Cl_2-20% acetone); the desired strapped-porphyrin was eluted as a mixture of atropisomers (second band collected). Recrystallization from CH_2Cl_2-hexanes yielded compound **1-OMe** (mixture of atropisomers) as bright purple crystals (64.5 mg, 67 µmol, 68%).

Note: due to the small relative quantity of the *cis* atropisomer in the initial mixture (**3a**/**3b** ~ 1/9) and due to the partial overlap the signals of the two atropisomers, the following ^{1}H NMR signals are characteristic for the major *trans* atropisomer.

^{1}H-NMR (400 MHz, $CDCl_3$) δ 10.19 (s, 1H), 9.33 (d, *J* = 4.7 Hz, 2H), 9.02 (s, 2H), 8.98 (d, *J* = 4.6 Hz, 2H), 8.82 (d, *J* = 4.8 Hz, 2H), 8.69 (d, *J* = 4.8 Hz, 3H), 8.43 – 8.34 (m, 1H), 8.34 – 8.24 (m, 1H), 8.06 (dd, *J* = 7.6, 1.5 Hz, 2H), 7.99 – 7.88 (m, 2H), 7.88 – 7.80 (m, 2H), 7.58 – 7.53 (m, 2H), 2.80 (s, 3H), 2.62 (s, 4H), 1.54 (s, 15H), 0.48 (s, 6H), -2.73 (s, 2H).

MS (MALDI-TOF, positive) calcd for $C_{56}H_{56}N_8O_8$ [M^+] *m/z(*100%) 968.42, found *m/z*(100%) 968.61.

Saponification of the methyl ester and isolation of atropisomers 1a and 1b

In a 25 mL round bottom flask, porphyrin **2** was dissolved in tetrahydrofuran (3 mL), and a solution of potassium hydroxide (2 M in ethanol-water 8-2, 5 mL) was added. The mixture was stirred at room temperature and the evolution of the reaction was followed by TLC analysis (SIO_2, CH_2Cl_2-20% acetone). After 4 hours all the starting material was converted. The mixture was diluted with CH_2Cl_2 (25 mL) and the organic phase was extracted with an aqueous citric acid solution (5 % m/v, 1 x 25 mL) and water (2 x 25 mL). The organic layer was collected, dried over Na_2SO_4, filtered and the solvent was evaporated under reduced pressure. The crude solid was purified by column chromatography (SiO_2, CH_2Cl_2-20 % acetone). Two bands were collected, the first (major) was assigned to the *trans*-atropisomer (**1b**), the second was assigned to the *cis*-atropisomer (**1a**). Recrystallization for CH_2Cl_2-hexanes yielded the desired porphyrins as bright purple crystals.

1b (19.3 mg, 20.2 µmol, 93%).

^{1}H-NMR (400 MHz, $CDCl_3$) δ 10.14 (s, 1H), 9.28 (d, *J* = 4.7 Hz, 2H), 8.97 – 8.92 (m, 3H), 8.78 (d, *J* = 4.8 Hz, 2H), 8.69 – 8.57 (m, 4H), 8.28 (m, 2H), 7.99 (d, *J* = 7.4 Hz, 2H), 7.90 –7.80 (m, 4H), 7.54 – 7.49 (m, 2H), 2.58 (s, 4H), 2.04 – 0.4 (br.m, 24H), -2.86 (s, 2H).

MS (MALDI-TOF, positive) calcd for $C_{55}H_{54}N_8O_8$ [M^+] *m/z(*100%) 954.41, found *m/z*(100%) 954.52.

HRMS (ESI-TOF, positive) calcd for $C_{55}H_{55}N_8O_8$ [M + H^+] *m/z(*100%) 955.4143, found *m/z*(100%) 955.4181.

1a (1.8 mg, 1.6 µmol, 7%).

^{1}H-NMR (500 MHz, $CDCl_3$) δ 10.21 (s, 1H), 9.41 (s, 2H), 9.33 (d, *J* = 4.6 Hz, 2H), 8.95 (d, *J* = 4.6 Hz, 2H), 8.85 (d, *J* = 4.7 Hz, 2H), 8.77 (d, *J* = 8.0 Hz, 2H), 8.75 (d, *J* = 4.7 Hz, 2H), 8.50 (d, *J* = 8.0 Hz, 1H), 7.97 (d, *J* = 8.0 Hz, 2H), 7.96 – 7.89 (m, 2H), 7.86 – 7.84 (m, 2H), 7.79 – 7.77 (m, 1H), 7.53 – 7.51 (m, 2H), 3.23 – 3.04 (m, 2H), 2.89 – 2.85 (m, 2H), 2.81 (d, *J* = 17.4 Hz, 2H), 2.80 – 2.74 (m, 2H), 2.68 – 2.64 (m, 2H), 2.55 (d, *J* = 17.4 Hz, 2H), 1.37 – 1.32 (m, 4H), 1.28 – 1.21 (m, 2H), 0.86 – 0.76 (m, 2H), 0.70 – 0.65 (m, 2H), 0.63 – 0.58 (m, 2H), -0.21 – 0.17 (m, 2H), -0.92 – -0.87 (m, 2H), -2.82 (s, 2H).

MS (MALDI-TOF, positive) calcd for $C_{55}H_{54}N_8O_8$ [M^+] *m/z(*100%) 954.41, found *m/z*(100%) 954.44.

HRMS (ESI-TOF, positive) calcd for $C_{55}H_{55}N_8O_8$ [M + H^+] *m/z(*100%) 955.4143, found *m/z*(100%) 955.4152.

Note: the saponification step can be executed directly after the Suzuki coupling reaction, purification of the methyl ester precursor mixture (porphyrin **2**). Residual palladium and boronic acid impurities can be conveniently removed by a short plug filtration (SiO_2, CH_2Cl_2-25% acetone) before saponification. During the final column chromatography purification conducted after saponification (SiO_2, CH_2Cl_2-20 % acetone) a first band eluted rapidly and could be attributed the product resulting for the debromination of the starting material. No decrease in the isolated yields of compounds **1a** and **1b** was otherwise noticed.

Isomerization of 1b

In a 50 mL three-neck round bottom flask, equipped with a reflux condenser, the porphyrin atropisomer **1b** (50 mg, 52.3 µmol) and sodium tetraphenylborate (100 mg, 0.29 mmol) were dissolved in a mixture of toluene-20% pyridine (10 mL). The mixture was purged with argon (vacuum-argon cycles, 3 times) and gently refluxed at 100 – 105 °C for 4 hours under argon. The mixture was cooled down to room temperature and the solvent was evaporated. The residue was purified on a column chromatography (SiO_2, CH_2Cl_2-acetone 1-1) to yield, after recrystallization from CH_2Cl_2-hexanes, **1b** atropisomer (32 mg, 33.5 µmol, 64%, first band eluted) and **1a** atropisomer (17 mg, 17.8 µmol, 34%).

Note: under similar conditions and treatment but in the absence of sodium tetraphenylborate the yields obtained after column chromatography and recrystallization were: **1b** (42 mg, 44 µmol, 85%) and **1a** (6 mg, 6.3 µmol, 12 %). In all cases the ^{1}H NMR, and MS of ligands **1a** and **1b** recovered after the described annealing processes were similar to the spectra obtained for the products isolated directly after saponification of the ester precursors. The compounds were therefore used without distinction for the physico-chemical studies reported in this work.

1.3 Preparation of the precursor 12

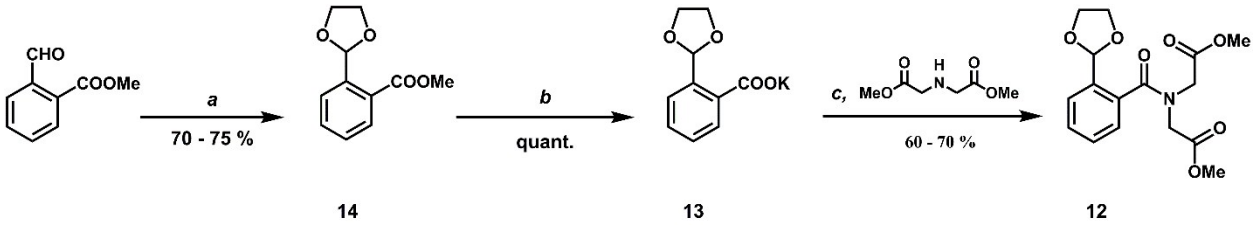

Scheme 2. Synthetic scheme for the functionalized precursor **12**. *a*) ethylene glycol, benzene, *p*-toluene sulfonic acid, Ar, reflux 12 h (Dean-Stark), Ar; *b)* KOH, THF, MeOH, H_2O, 5h; *c)* 2-(1H-Benzotriazole-1-yl)-1,1,3,3-tetramethyluronium hexafluorophosphate (HBTU), DMF, RT, N_2.

Synthesis of methyl-2-carboxyphenyldioxolane 14

A two-neck 250 mL round bottom flask equipped with a Dean-Stark condenser was charged with methyl-2-formylbenzoate (4.0 g, 24.4 mmol), ethylene glycol (1.75 mL, 1.94 g, 31.3 mmol) and benzene (100 mL). The mixture was sparged with argon for 15 minutes and *p*-toluene sulfonic acid (0.137 g, 0.80 mmol) was added. The reaction mixture refluxed, under argon, for 12 hours. During this time the water/benzene mixture that was collected in the Dean-Stark condenser was discarded every 4 hours. The solution was cooled down to room temperature and the organic phase was extracted with 5% aqueous $NaHCO_3$ solution (3 x 100 mL). The organic layer was collected, dried over Na_2SO_4, filtered and the solvent was evaporated under reduced pressure. The crude oil was purified by filtration over a silica short plug (SiO_2, CH_2Cl_2) to yield the desired compound as a pale yellow oil (3.74 g, 18 mmol, 74%).

^{1}H-NMR (400 MHz, $CDCl_3$) δ 7.87 (dd, *J* = 7.8, 1.4 Hz, 1H), 7.76 (dd, *J* = 7.8, 1.4 Hz, 1H), 7.54 (td, *J* = 7.6, 1.4 Hz, 1H), 7.41 (td, *J* = 7.6, 1.4 Hz, 1H), 6.60 (s, 1H), 4.06 (s, 4H), 3.92 (s, 3H).

Saponification of the methyl-2-carboxyphenyldioxolane 13

In a 100 mL round bottom flask, methyl-2-carboxyphenyldioxolane **14** (1.69 g, 8.12 mmol) was dissolved in tetrahydrofuran (5 mL). Potassium hydroxide (0.48 g, 8.6 mmol) dissolved in a methanolic solution (8-2 methanol-water mixture, 5 mL) was added and the mixture was stirred at room temperature for 5h, after which no starting material remained according to TLC analysis (SiO_2, CH_2Cl_2). The solvent was evaporated under reduced pressure and the crude solid was dried via azeotropic distillation with toluene, to yield a white solid (1.91 g, quant.). The compound was immediately used in the following step without further purification.

Synthesis of 2-N,N-bis(2-methoxyacetonyl)amidophenyldioxolane 12

The potassium salt of the 2-carboxyphenyldioxolane **13** (2.33 g, 10 mmol) was suspended in dry dimethylformamide (30 mL). 2-(1H-Benzotriazole-1-yl)-1,1,3,3-tetramethyluronium hexafluorophosphate (HBTU) (4 g, 10.5 mmol) was added portion-wise (4 x 1g) over 5 minutes and the mixture was stirred

until all the solid dissolved (15 minutes). *N,N*-bis-(2-metoxyacethyl)amine (2 g, 12.4 mmol) was added and the mixture was stirred for 10 hours at room temperature, under nitrogen. The mixture was poured into water (100 mL) and the aqueous phase was extracted with diethyl ether until only traces of the desired product remained in the aqueous phase (4 x 100 mL). The combined organic layers were dried over Na_2SO_4, filtered and the solvent was evaporated under reduced pressure. Column chromatography (SiO_2, CH_2Cl_2-1% acetone) yielded the desired product (third band) as a thick oil (2.15 g, 6.37 mmol, 64%).

^{1}H-NMR (400 MHz, $CDCl_3$) δ 7.63 (dd, *J* = 7.7, 1.4 Hz, 1H), 7.44 (td, *J* = 7.5, 1.5 Hz, 1H), 7.39 (td, *J* = 7.5, 1.5 Hz, 1H), 7.30 – 7.27 (m, 1H), 5.90 (s, 1H), 4.85 – 4.45 (br s, 2H), 4.30 – 3.95 (br m, 6H), 3.78 (s, 3H), 3.68 (s, 3H).

1.4 Preparation of ligands 2a and 2b

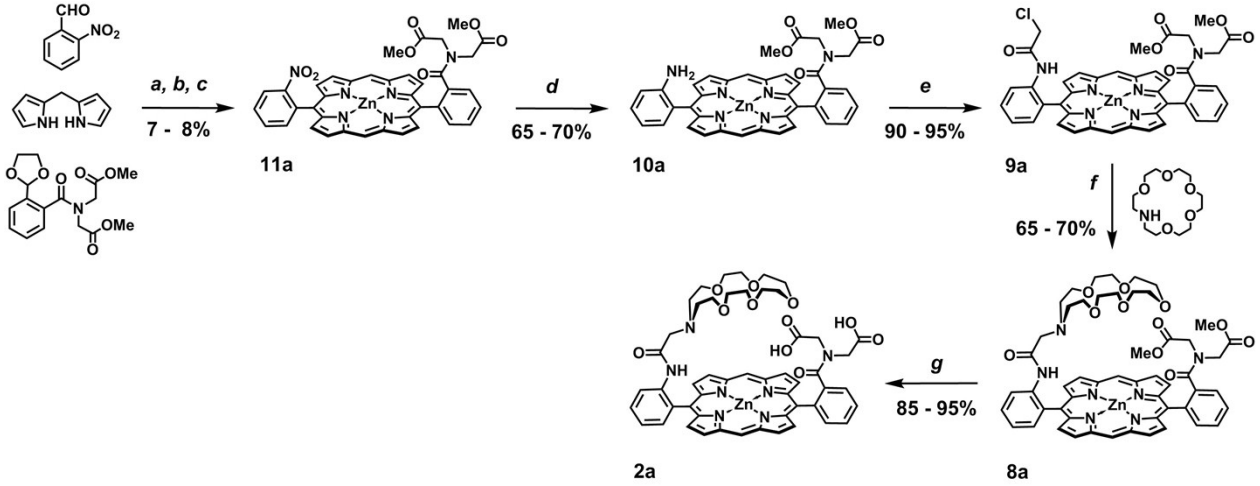

Scheme 3. Synthetic scheme for ligand **2a**. The same synthetic strategy was followed to prepare ligand **2b**, starting from the atropisomer **11b** (for which the nitro group and diester substituents are facing towards the two opposite sides of the porphyrin macrocycle). *a)* $BF_3.Et_2O$, CH_3Cl, Ar, RT; *b)* DDQ, $CHCl_3$, RT; *c)* $Zn(OAc)_2$, $CHCl_3$, MeOH, RT; *d*) Zn, AcOH (acetic acid), CH_2Cl_2, THF, Ar, RT; *e)* $ClCH_2COCl$, K_2CO_3, CH_2Cl_2, Ar, O°C - RT; *f)* EtOH, Ar, 70°C; *g)* NaOH, MeOH, H_2O, Ar, RT.

General synthetic strategy

The precursor porphyrin (**11**) was obtained as a mixture of two atropisomers from the statistical acid-catalyzed condensation of dipyrrylmethane with 2-nitrobenzaldeyhde and the acetal derivative of dimethyl 2,2'-(2-formylbenzamido)diacetate. Each atropisomer of the desired mixed-porphyrin, **11a** and **11b**, could be isolated in its pure form after column chromatography. Importantly, only relatively slow rates of interconversion between the two atropisomers were observed above 60°C. The latter could thus be engaged in further reactions in their pure forms and were not subjected to significant re-equilibration during the subsequent synthetic steps. Reduction of the nitro functionality was conducted using zinc(0) in the presence of acetic acid at room temperature. Next, the amino-porphyrin **10a**(or **10b**) was acylated with chloroacetyl chloride at low temperature, followed by treatment of the resulting derivative **9a**(or **9b**) with 4-aza-18-crown-6 in gently refluxing methanol. Finally, saponification of the diester led to the desired ligands **2a**(or **2b**).

Synthesis of 5-(2-nitrophenyl)-15-(2-N,N-(bis-2-methoxyacethyl)amidophenyl)porphyrins 11a and 11b

The atropisomers **11a** and **11b** were more easily separated as their zinc complexes. Therefore, we first isolated the two isomers as a mixture of the free base porphyrins and subsequently metallated macrocycles before separation.

a) Condensation of the porphyrin macrocycle

A 4 L three-neck flask was charged with 2-nitrobenzaldehyde (0.964 g, 6.4 mmol), 2-*N,N*-bis(2-methoxyacetonyl)amidophenyldioxolane **12** (2.15 g, 6.4 mmol), chloroform (2.4 L), and the mixture was sparged with argon under vigorous stirring for 45 minutes. Dipyrrylmethane (1.865 g, 12.8 mmol) was added and the solution was further sparged with argon for 15 minutes. Boron trifluoride diethyl ether complex (380 µL, 429 mg, 3 mmol) dissolved in deoxygenated chloroform (5 mL) was added and the mixture stirred under argon for 4 hours. 2-3-dichloro-4,6-dicyano-1,4-benzoquinone (6 g, 26.4 mmol) was added and the mixture was stirred at room temperature for 2 hours. Triethylamine (1 mL) was added and the organic phase was extracted with 5% aqueous $NaHCO_3$ solution (3 x 1.5 L). The organic layer was collected, dried over Na_2SO_4, filtered and the solvent was evaporated under reduced pressure. The crude mixture was purified by column chromatography (SIO_2, elution gradient: CH_2Cl_2-1% acetone to CH_2Cl_2-4% acetone). The desired porphyrin was collected as a mixture of the two thermally stable atropisomers **11a** and **11b** (third band eluted; 433.3 mg, 0.62 mmol, 9.7%).

^{1}H-NMR was poorly informative due to the overlapping signals of the two atropisomers which resulted in a complex pattern of signals over the entire range of the spectra.

MS (MALDI-TOF, positive) calcd for $C_{39}H_{30}N_6O_7$ [M^+] *m/z(*100%) 694.22, found *m/z*(100%) 694.09.

*b) Metallation of 5-(2-nitrophenyl)-15-(2-N,N-(bis-2-methoxyacethyl)amidophenyl)porphyrin and isolation of the pure atropisomers **11a** and **11b***

The mixture of the two atropisomers (433.3 mg, 0.62 mmol) and zinc acetate dihydrate (2.5 g, 11.5 mmol) were suspended in a chloroform-methanol 1-3 mixture (70 mL). The slurry was stirred for 10 h at room temperature and TLC analysis (SiO_2, $CHCl_3$-EtOAc 8-2) confirmed the full metallation of the porphyrins. The solvent was evaporated and the crude residue taken in chloroform-5% methanol (200 mL). The organic layer was washed with water (3 x 200 mL), collected, dried over Na_2SO_4, filtered and the solvent was evaporated under reduced pressure. Column chromatography (SiO_2, Toluene-EtOAc 8-2), followed by recrystallization from CH_2Cl_2-hexanes, yielded the two atropisomers in their pure form.

Note: due to the higher solubility of the material in chlorinated solvents the crude was loaded on the column using $CHCl_3$-EtOAc 7-3; the column was subsequently run with the solvents mixture indicated above.

αα'-5-(2-nitrophenyl)-15-(2-*N,N*-(bis-2-methoxyacethyl)amidophenyl)-zinc-porphyrin (197.2 mg, 0.26 mmol, 42%) was obtained as the first major band (**11a**).

^{1}H-NMR (400 MHz, $CDCl_3$) δ 10.23 (br. s, 2H), 9.47 – 9.30 (m, 4H), 9.10 (br. s, 2H), 8.90 (d, *J* = 4.5 Hz, 2H), 8.71 (d, *J* = 7.5 Hz, 1H), 8.47 – 8.38 (m, 2H), 8.06 – 7.94 (m, 3H), 7.84 (td, *J* = 7.7, 1.3 Hz, 1H), 7.63 (dd, *J* = 7.7, 1.4 Hz, 1H), 3.67 (br. s, 1H), 3.38 – 3.10 (br. s, 3H + 1H), 2.20 (br. s, 1H), 1.92 (br. s, 1H), 1.03 (s, 3H).

MS (MALDI-TOF, positive) calcd for $C_{39}H_{28}N_6O_7Zn$ [M^+] *m/z(*100%) 756.13, found *m/z*(100%) 756.49.

αβ'-5-(2-nitrophenyl)-15-(2-*N,N*-(bis-2-methoxyacethyl)amidophenyl)-zinc-porphyrin (234.6 mg, 0.31 mmol, 50%) was obtained as the second major band (**11b**).

MS (MALDI-TOF, positive) calcd for $C_{39}H_{28}N_6O_7Zn$ [M^+] *m/z(*100%) 756.13, found *m/z*(100%) 756.49.

Synthesis of αα'-5-(2-aminophenyl)-15-(2-N,N-(bis-2-methoxyacethyl)amidophenyl)-zinc-porphyrin 10a

In a two-neck 25 mL flask equipped with a 10 mL addition funnel, αα'-5-(2-nitrophenyl)-15-(2-*N,N*-(bis-2-methoxyacethyl)amidophenyl)-zinc-porphyrin **11a** (21 mg, 28 μmol) was dissolved in a mixture of tetrahydrofuran-dichloromethane 1-1 (8 mL). Zinc powder (50 mg) was added and a solution of 10% glacial acetic acid in dichloromethane (4 mL) was added dropwise over 20 minutes, while stirring vigorously the suspension at room temperature. After complete addition, TLC analysis (SiO_2, CH_2Cl_2-10% EtOAc) indicated the remaining presence of unreacted nitro porphyrin; additional zinc powder (50 mg) was added and the mixture further stirred for another 30 minutes at room temperature. After that time, TLC analysis still indicated the presence of unreacted starting material. Another 50 mg of zinc powder was added and the mixture further stirred at room temperature for 30 minutes, after what TLC analysis showed that only traces amount of staring material was left. The zinc powder was filtered off and the mixture diluted to 100 mL with dichloromethane. It was washed with a 5% aqueous $NaHCO_3$ solution (100 mL) and water (100 mL). The organic layer was collected, dried over Na_2SO_4, filtered and the solvent was evaporated under reduced pressure. Column chromatography (SiO_2, elution gradient: CH_2Cl_2-EtOAc 8-2 to CH_2Cl_2-EtOAc 4-2) yielded the desired compound **10a** (16 mg, 22 μmol, 79%) as a deep purple solid (third eluted compound).

^{1}H-NMR (400 MHz, $CDCl_3$-MeOD 4-1) δ 10.21 (s, 2H), 9.38 (d, *J* = 4.4 Hz, 2H), 9.35 (d, *J* = 4.4 Hz, 2H), 9.11 (d, *J* = 4.4 Hz, 2H), 8.97 (br. s, 2H), 8.30 – 8.24 (m, 1H), 7.94 (dd, *J* = 7.4, 1.6 Hz, 1H), 7.93 – 7.83 (m, 2H), 7.80 (dd, *J* = 7.4, 1.8 Hz, 1H), 7.64 (td, *J* = 7.8, 1.6 Hz, 1H), 7.28 – 7.16 (m, 2H), 4.23 (s, 2H), 3.27 – 3.24 (br. s, 3H + 2H), 2.77 (s, 3H).

Note: due to the presence of deuterated methanol the labile protons form the amino groups are not observed.

MS (MALDI-TOF, positive) calcd for $C_{39}H_{30}N_6O_5Zn$ [M^+] *m/z(*100%) 726.16, found *m/z*(100%) 726.49.

Synthesis of αβ'-5-(2-aminophenyl)-15-(2-N,N-(bis-2-methoxyacethyl)amidophenyl)-zinc-porphyrin 10b

αβ'-5-(2-aminophenyl)-15-(2-*N,N*-(bis-2-methoxyacethyl)amidophenyl)-zinc-porphyrin was prepared following the same procedure as described for αα'-5-(2-aminophenyl)-15-(2-*N,N*-(bis-2-methoxyacethyl)amidophenyl)-zinc-porphyrin, using the following reactants and solvent quantities: αα'-

5-(2-nitrophenyl)-15-(2-N,N-(bis-2-methoxyacethyl)amidophenyl)-zinc-porphyrin **11b** (65 mg, 87 µmol), tetrahydrofuran-dichloromethane 1-1 (20 mL), 10% glacial acetic acid in dichloromethane (10 mL), zinc powder (4 x 50 mg). Column chromatography (SiO_2, elution gradient: CH_2Cl_2-EtOAc 8-2 to CH_2Cl_2-EtOAc 4-2) yielded the desired compound **10b** (44 mg, 61 µmol, 70 %) as a deep purple solid (third eluted compound).

^{1}H-NMR (400 MHz, $CDCl_3$) δ 10.21 (s, 2H), 9.38 – 9.35 (m, 4H), 9.04 (br s, 2H), 9.02 (d, *J* = 4.5 Hz, 2H), 8.50 – 8.40 (m, 1H), 7.94 – 7.83 (m, 2H), 7.80 (d, *J* = 7.5 Hz, 1H), 7.77 – 7.71 (m, 1H), 7.57 (td, *J* = 7.8, 1.5 Hz, 1H), 7.16 (td, *J* = 7.5, 1.1 Hz, 1H), 6.91 (d, *J* = 8.1 Hz, 1H), 4.06 (br. s, 1H), 3.24 (s, 2 + 1H), 3.16 (s, 3H), 3.05 (br. s, 1H), 2.90 (br s, 1H), 1.89 (s, 3H).

MS (MALDI-TOF, positive) calcd for $C_{39}H_{30}N_6O_5Zn$ [M^+] *m/z(*100%) 726.16, found *m/z*(100%) 726.49.

Synthesis of αα'-5-(2-(2-chloroactyl)aminophenyl)-15-(2-N,N-(bis-2-methoxyacethyl)amidophenyl)-zinc-porphyrin 9a

A 50 mL round bottom flask, was charged with αα'-5-(2-aminophenyl)-15-(2-*N,N*-(bis-2-methoxyacethyl)amidophenyl)-zinc-porphyrin **10a** (40 mg, 55 µmol), potassium carbonate (36.4 mg, 0.28 mmol) and dichloromethane (10 mL). The mixture was cooled down to 0 °C under argon and 2-chloroacethylchloride (8.6 µL, 12.2 mg, 11 µmol) was added. The mixture was stirred under argon at 0 °C. The evolution of the reaction was followed by TLC analysis (SiO_2, CH_2Cl_2-1% EtOAc). After 1 hour no staring material remained. The mixture was diluted to 100 mL with dichloromethane and the organic phase was washed with a 5% $NaHCO_3$ aqueous solution (1 x 100 mL) and water (1x 100 mL). The organic layer was collected, dried over Na_2SO_4, filtered and the solvent was evaporated under reduced pressure. Column chromatography (SiO_2, CH_2Cl_2-7% EtOAc) followed by recrystallization form CH_2Cl_2-hexannes, yielded the desired compound **9a** as deep purple crystals (second eluted compound, 40.6 mg, 51 µmol, 92 %).

^{1}H-NMR (400 MHz, $CDCl_3$) δ 10.28 (s, 2H), 9.42 – 9.37 (m, 4H), 9.06 (br. s, 2H), 9.01 (d, *J* = 4.5 Hz, 2H), 8.72 (d, *J* = 8.3 Hz, 1H), 8.42 – 8.34 (m, 1H), 8.23 (s, 1H), 8.19 (dd, *J* = 7.5, 1.5 Hz, 1H), 7.94 – 7.83 (m, 3H), 7.81 – 7.74 (m, 1H), 7.66 – 7.58 (m, 1H), 4.13 (br s, 1H), 3.74 (br. s, 1H), 3.33 (s, 2H), 3.25 –3.05 (br. s, 3H + 2H), 2.24 (s, 3H).

MS (MALDI-TOF, positive) calcd for $C_{31}H_{41}ClN_6O_6Zn$ [M^+] *m/z(*100%) 802.13, found *m/z*(100%) 802.43.

Synthesis of αβ'-5-(2-(2-chloroactyl)aminophenyl)-15-(2-N,N-(bis-2-methoxyacethyl)amidophenyl)-zinc-porphyrin 9b

αβ'-5-(2-(2-chloroactyl)aminophenyl)-15-(2-*N,N*-(bis-2-methoxyacethyl)amidophenyl)-zinc-porphyrin **9b** was prepared following the same procedure as described for αα'-5-(2-(2-chloroactyl)aminophenyl)-15-(2-*N,N*-(bis-2-methoxyacethyl)amidophenyl)-zinc-porphyrin **9a** with the following reactants and solvent quantities: αα'-5-(2-aminophenyl)-15-(2-*N,N*-(bis-2-methoxyacethyl)amidophenyl)-zinc-porphyrin **10b** (32 mg, 44 µmol), potassium carbonate (29 mg, 0.22 mmol), chloroacethyl chloride (6.9 µL, 9.7 mg, 88 µmol), dichloromethane (10 mL). Purification was conducted using column chromatography (SiO_2, elution gradient: CH_2Cl_2-5% EtOAc to CH_2Cl_2-10% EtOAc)

followed by recrystallization from CH_2Cl_2-hexanes to yield the desired product **9b** as deep purple crystals (30.8 mg, 40 µmol, 91%).

^{1}H-NMR (400 MHz, $CDCl_3$) δ 10.29 (s, 2H), 9.46 – 9.38 (m, 4H), 9.09 (d, *J* = 4.5 Hz, 2H), 8.99 (d, *J* = 4.5 Hz, 2H), 8.76 (d, *J* = 8.4 Hz, 1H), 8.47 (dd, *J* = 7.0, 1.5 Hz, 1H), 8.16 (s, 1H), 8.07 (dd, *J* = 7.5, 1.6 Hz, 1H), 7.92 (td, *J* = 7.5, 1.7 Hz, 1H), 7.90 – 7.82 (m, 2H), 7.78 – 7.70 (m, 1H), 7.59 (td, *J* = 7.5, 1.3 Hz, 1H), 4.20 – 2.60 (m,9H), 1.90 (s, 3H).

Between 3.6 and 4.3 ppm a complex pattern is observed with a very broad baseline signal overalling two well defined singlet centered at 3.34 and 3.17 ppm respectively. We can attribute the broad signal to the two slowly exchanging C*H*$_2$COOMe arms, the singlet centered at 3.34 ppm to the protons of the C**H**$_2$Cl and the singlet centered at 3.17 ppm to one of the COOC*H*$_3$ groups. The theoretical total integration should be 9 protons; we observed 8.6 on the normalized spectra which is explained by the broadening of the signal associated to the two C*H*$_2$COOMe groups.

MS (MALDI-TOF, positive) calcd for $C_{31}H_{41}ClN_6O_6Zn$ [M^+] *m/z(*100%) 802.13, found *m/z*(100%) 802.44.

Synthesis of porphyrin 8a

A three-neck 50 mL round bottom flask equipped with a reflux condenser was charged with porphyrin **9a** (60 mg, 75 µmol), 4-aza-18-crown-6 (90 mg, 0.34 mmol) and methanol (20 mL). The mixture was sparged with argon for 15 minutes and stirred at 60 °C, under argon for 60 hours. The mixture was cooled down to room temperature, and the solvent was evaporated. Column chromatography purification (SiO_2, elution gradient CH_2Cl_2-1% MeOH to CH_2Cl_2-7% MeOH) followed by recrystallization from CH_2Cl_2-hexannes yielded the desired. product **8a** (42.3 mg, 41 µmol, 55%, third eluted compound) as deep purple crystals.

^{1}H-NMR (500 MHz, $CDCl_3$) δ 10.20 (s, 2H), 9.34 (d, *J* = 4.4 Hz, 2H), 9.31 (d, *J* = 4.4 Hz, 2H), 9.26 (s, 1H), 8.98 (d, *J* = 4.4 Hz, 2H), 8.87 (br. s, 2H), 8.70 (d, *J* = 8.3 Hz, 1H), 7.95 – 7.87 (m, 2H), 7.86 – 7.82 (m, 2H), 7.77 (d, *J* = 7.6 Hz, 1H), 7.66 (td, *J* = 7.5, 1.5 Hz, 1H), 7.50 (td, *J* = 7.5, 1.3 Hz, 1H), 4.67 (s, 2H), 3.74 (s + br s, 3 + 2H), 3.33 (s, 3H), 2.64 (s, 2H), 2.50 – 2.29 (m, 8H), 1.88 (s, 4H), 1.22 (m, 4H), 1.01 (m, 4H).

Note: the signal of 4 protons are not visible (crown ether CH_2), due to the overlapping signal of the water at 1.38 ppm.

^{1}H-NMR (500 MHz, DMSO-d_6) δ 10.33 (s, 2H), 9.48 (d, *J* = 4.4 Hz, 2H), 9.43 (d, *J* = 4.4 Hz, 2H), 9.32 (s, 1H), 8.84 – 8.81 (m, *J* = 4.4, 2.7 Hz, 4H), 8.75 (dd, *J* = 8.4, 1.3 Hz, 1H), 8.04 (dd, *J* = 7.6, 1.3 Hz, 1H), 7.95 (td, *J* = 7.7, 1.2 Hz, 1H), 7.90 (dd, *J* = 7.4, 1.6 Hz, 1H), 7.88 – 7.80 (m, 2H), 7.76 (dd, *J* = 8.0, 1.4 Hz, 1H), 7.52 (td, *J* = 7.5, 1.3 Hz, 1H), 4.47 (s, 2H), 3.52 (s, 3H), 3.45 (s, 2H), 2.94 – 2.77 (m, 4H), 2.66 (s, 3H), 2.58 (s, 2H), 2.53 – 2.48 (m, 4H), 1.78 (br. s, 4H), 1.40 (br. s, 4H), 0.92 – 0.83 (m, 4H), 0.70 (br. s, 4H).

Note: the signal of 4 protons are not distinguished (crown ether CH_2) due to the overlapping of the residual DMSO signal at 2.50 ppm.

MS (MALDI-TOF, positive) calcd for $C_{53}H_{55}N_7O_{11}Zn$ [M^+] *m/z(*100%) 1029.33, found *m/z*(100%) 1029.66.

Partial thermal re-equilibration of the αα' atropisomer during the synthesis led to the isolation of atropisomer **8b** (6 mg, 5.8 µmol, 8%, second eluted compound) in addition to **8a**.

Synthesis of porphyrin 8b

Porphyrin **8b** was obtained following the same procedure described for **8a** with the following reagent and solvent quantities: porphyrin **9b** (50 mg, 62 µmol), 4-aza-18-crown-6 (80 mg, 0.30 mmol) and methanol (20 mL). Purification was conducted using column chromatography (SiO_2, elution gradient CH_2Cl_2-1% MeOH to CH_2Cl_2-4% MeOH) followed by recrystallization from CH_2Cl_2-hexannes. Only limited thermal re-equilibration of the staring αβ' atropisomer occurred during the reaction and yield to the isolation of traces of **8a** (1 mg, 0.97 µmol, 2% (third product eluted) in addition to the desired porphyrin **8b** (41 mg, 40 µmol, 65%, second product eluted).

^{1}H-NMR (500 MHz, $CDCl_3$) δ 10.18 (s, 2H), 9.82 (s, 1H), 9.33 (br. s, 2H), 9.32 (d, *J* = 4.4 Hz, 2H), 9.09 (br. s, 2H), 9.13 (dd, *J* = 8.6, 1.2 Hz, 1H), 8.94 (d, *J* = 4.3 Hz, 2H), 8.41 – 8.37 (m, 1H), 7.91 – 7.85 (m, 2H), 7.85 – 7.78 (m, 2H), 7.70 (dd, *J* = 7.4, 1.6 Hz, 1H), 7.39 (td, *J* = 7.4, 1.3 Hz, 1H), 4.05 (br. s, 1H), 3.29 (br. s, 1H), 3.01 (br. s, 2H), 2.66 (s, 3H), 2.63 (s, 2H), 2.06 (br. s, 8H), 1.60 (s, 3H), 1.47 (m, 4H), 1.29 – 1.05 (m, 12H).

^{1}H-NMR (500 MHz, DMSO-d_6) δ 10.32 (s, 2H), 9.45 (d, *J* = 4.4 Hz, 2H), 9.41 (d, *J* = 4.4 Hz, 2H), 8.94 (s, 1H), 8.81 – 8.75 (m, 3H), 8.74 (d, *J* = 4.4 Hz, 2H), 8.01 (dd, *J* = 7.4, 1.6 Hz, 1H), 7.95 – 7.91 (m, 2H), 7.86 – 7.79 (m, *J* = 13.4, 2H), 7.72 (dd, *J* = 8.2, 1.4 Hz, 1H), 7.53 (td, *J* = 7.5, 1.3 Hz, 1H), 4.43 (s, 2H), 3.48 (s, 3H), 3.45 (s, 2H), 2.64 (s, 3H), 2.48 – 2.43 (m, 4H), 2.40 (s, 2H), 2.21 – 2.02 (m, 4H), 1.59 – 1.41 (m, 4H), 0.66 (q, *J* = 6.7, 5.8 Hz, 8H), 0.04 – -0.02 (m, 4H).

Note: The signal of 4 protons (crown ether CH_2) is partly overlapping the residual DMSO signal

MS (MALDI-TOF, positive) calcd for $C_{53}H_{55}N_7O_{11}Zn$ [M^+] *m/z(*100%) 1029.33, found *m/z*(100%) 1029.67.

Synthesis of porphyrin 2a

Porphyrin **8a** (6.4 mg, 6.2 µmol) was dissolved in 2 mL of a 0.1 M NaOH solution (MeOH-20% H_2O). The solution was stirred at room temperature for 4 hours. TLC analysis (SiO_2, EtOAc-CH_2Cl_2-MeOH, 6-6-1) showed that all the starting material was converted. The solvent was evaporated and the crude residue was purified by column chromatography (SiO_2, elution gradient: ACN-12% H_2O to ACN-15% H_2O). The desired compound was collected as the second (main) band. Recrystallization from CH_2Cl_2-0.1%MeOH / hexanes to yield the desired porphyrin **2a** as a purple powder (5.3 mg, 5.3 µmol, 86%).

^{1}H-NMR (400 MHz, DMSO-d_6) δ 18.48 (s, 2H), 10.36 (s, 2H), 9.49 (d, *J* = 4.5 Hz, 2H), 9.46 (d, *J* = 4.4 Hz, 2H), 9.30 (s, 1H), 8.87 (d, *J* = 4.4 Hz, 2H), 8.82 – 8.76 (m, 3H), 8.04 – 7.95 (m, 1H), 7.92 – 7.82 (m, 3H), 7.81 – 7.75 (m, 2H), 7.55 – 7.49 (m, 1H), 2.79 (s, 2H), 2.69 –2.63 (m, 4H), 2.55 (s, 2H), 2.17 – 2.11 (m, 4H), 1.27 (br. s, 4H), 1.18 (br. s, 4H), 0.90 –0.78 (m, 4H), 0.49 – 0.40 (m, 4H).

MS (MALDI-TOF, positive) calcd for $C_{51}H_{51}KN_7O_{11}Zn$ [M + K^+] *m/z(*100%) 1040.26, found *m/z*(100%) 1040.43.

Note: the protons associated to the methylene groups of the diacid moieties do not lead to the observation of well defined peaks in the ^{1}H-NMR spectrum; instead a very broad signal could be observed in the baseline between 3.65 – 3.20 ppm.

Synthesis of porphyrin 2b

Porphyrin **2b** was obtained following the same procedure described for **2a** with the following reagent and solvent quantities: porphyrin **8b** (9 mg, 8.7 µmol), 0.11 M NaOH in MeOH-20% H_2O (2.5 mL). An adiitional 1 mL of THF was required to fully dissolve the material. Hydrolysis was complete after 4 hours as observed by TLC analysis (SiO_2, EtOAc-CH_2Cl_2-MeOH, 6-6-1). Column chromatography purification (SiO_2 ACN-12% H_2O, followed by recrystallization from CH_2Cl_2-0.1%MeOH / hexanes yielded the desired porphyrin **2b** as a purple powder (7.9 mg, 7.9 µmol, 94%).

^{1}H-NMR (400 MHz, DMSO-d_6) δ 18.40 (s, 2H), 10.35 (s, 2H), 9.48 (d, *J* = 4.5 Hz, 2H), 9.45 (d, *J* = 4.5 Hz, 2H), 8.93 (s, 1H), 8.84 (d, *J* = 4.4 Hz, 2H), 8.81 – 8.73 (m, 3H), 8.04 (d, *J* = 7.4 Hz, 1H), 8.01 (d, *J* = 7.4 Hz, 1H), 7.94 – 7.79 (m, 3H), 7.74 (d, *J* = 7.6 Hz, 1H), 7.56 (t, *J* = 7.5 Hz, 1H), 3.81 (br. s, 2H), 2.67 (s, 2H), 2.55 – 2.50 (m, 4H), 2.42 (s, 2H), 2.21 – 2.11 (m, 4H), 1.60 – 1.50 (m, 4H), 0.80 – 0.72 (m, 4H), 0.72 – 0.65 (m, 4H), 0.11 – 0.02 (d, *J* = 5.8 Hz, 4H).

MS (MALDI-TOF, positive) calcd for $C_{51}H_{51}KN_7O_{11}Zn$ [M + K^+] *m/z(*100%) 1040.26, found *m/z*(100%) 1040.41.

1.5 Preparation of ligands R1 and R2

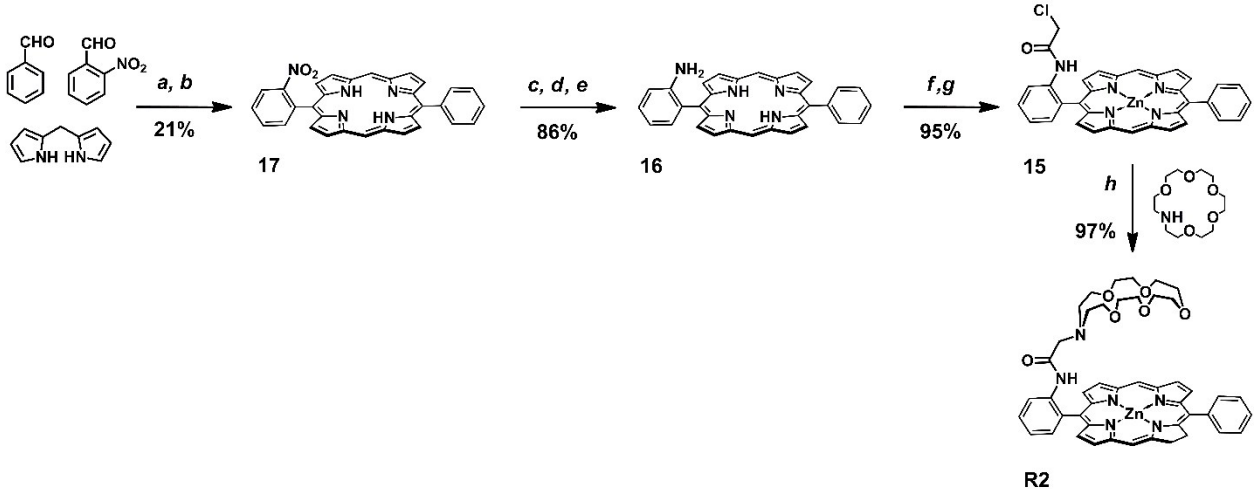

Scheme 4. Synthetic scheme for ligand **R2**. *a)* TFA, CH_3Cl, Ar, RT; *b)* DDQ, $CHCl_3$, RT; *c)* $Zn(OAc)_2$, CH_2Cl_2, MeOH, RT; *d*) Zn, AcOH, CH_2Cl_2, THF, Ar, RT; *e)* TFA, CH_2Cl_2, RT; *f)* $ClCH_2COCl$, K_2CO_3, CH_2Cl_2, Ar, O°C – RT; *g)* $Zn(OAc)_2$, DMF, 45°C; *h)* EtOH, Ar, 78°C.

Synthesis of 5-phenyl-15-(2-nitrophenyl)porphyrin 17

A two-neck 1 L round bottom flask was charged with benzaldehyde (140 mg, 1.37 mmol), 2-nitrobenzaldehyde (207 mg, 1.37 mmol) and chloroform (500 mL). The mixture was sparged with argon

for 30 minutes and dipyrrylmethane (450 mg, 2.74 mmol) was added. The mixture was further sparged with argon for 10 minutes and trifluoroacetic acid (0.8 mL, 534 mg, 4.7 mmol) was added. The mixture was stirred under argon, at room temperature, for 1 hour and 2,3-dichloro-5,6-dicyao-1,4-benzoquinone (2 g, 8.8 mmol) was added The mixture was further stirred at room temperature for 1 hour. The reaction mixture was quenched with the addition of triethylamine (1 mL) and washed with a 5% aqueous $NaHCO_3$ solution (3 x 200 mL) and water (1 x 100 mL). The organic layer was collected, dried over Na_2SO_4, filtered and the solvent was evaporated under reduced pressure. The crude residue was filtered through a silica short plug (SiO_2, CH_2Cl_2); fractions were collected until no porphyrin eluted; the solvent was evaporated under reduced pressure, and the resulting porphyrin mixture was further purified by column chromatography (SIO_2, CH_2Cl_2-hexannes 1-1) to yield the desired 5-phenyl-15-(2-nitrophenyl)porphyrin **17** (second product eluted) as purple crystals after recrystallization for CH_2Cl_2-hexannes (148 mg, 0.29 mmol, 21%).

^{1}H-NMR (400 MHz, Chloroform-*d*) δ 10.31 (s, 2H), 9.38 (d, *J* = 4.6 Hz, 4H), 9.07 (d, *J* = 4.6 Hz, 2H), 8.87 (d, *J* = 4.6 Hz, 2H), 8.56 – 8.41 (m, 1H), 8.35 – 8.28 (m, 1H), 8.28 – 8.19 (m, 1H), 8.09 – 7.91 (m, 2H), 7.88 – 7.76 (m, 3H), -3.10 (s, 2H).

MS (MALDI-TOF, positive) calcd for $C_{32}H_{21}N_5O_2$ [M^+] *m/z(*100%) 507.17, found *m/z*(100%) 507.31.

Synthesis of 5-phenyl-15-(2-aminophenyl)porphyrin 16

Metallation:

In a 100 mL round bottom flask, 5-phenyl-15-(2-nitrophenyl)porphyrin **17** (45 mg, 89 µmol) was dissolved in CH_2Cl_2-MeOH 2-1 (40 mL); zinc acetate dihydrate (250 mg, 1.1 mmol) was added and the mixture was stirred at room temperature for 10 hours. The mixture was washed with water (3 x 50 mL), the organic layer was collected, dried over Na_2SO_4, filtered and the solvent was evaporated. The resulting material was used without further purification in the following step.

Reduction of the nitro group:

A 25 mL three-neck flask equipped with a 10 mL addition funnel was charged with the zinc porphyrin, zinc powder (50 mg, 0.74 mmol) and a mixture of CH_2Cl_2-THF 1-1 (10 mL). The slurry was sparged with argon for 5 minutes before a solution of 10% acetic acid in CH_2Cl_2 (7 mL) was added dropwise over a period of 30 minutes. After the end of the addition the mixture was further stirred at room temperature under argon. The progression of the reaction was followed by TLC analysis (SIO_2, CH_2Cl_2), when no starting material remained (~ 45 minutes stirring at room temperature) the remaining zinc powder was removed by filtration and the mixture was diluted to 50 mL with CH_2Cl_2. The organic phase was extracted with a 5% aqueous $NaHCO_3$ solution (2 x 100 mL), and water (1 x 100 mL). The organic layer was collected, dried over Na_2SO_4, filtered and the solvent was evaporated under reduced pressure.

Demetallation:

Due to the poor solubility of the resulting material the crude zinc-5-phenyl-15-(2-aminophenyl)porphyrin was demetallated before purification. The crude product obtained from the precedent step was partly solubilized in CH_2Cl_2 (20 mL) and trifluoroacetic acid (0.5 mL) was added. The mixture was stirred at room temperature for 5 minutes, transferred into a separatory funnel and washed with water (1 x 50 mL), 5%

aqueous $NaHCO_3$ solution (2 x 50 mL) and again water (1 x 50 mL). The organic layer was collected, dried over Na_2SO_4, filtered and the solvent was evaporated. Column chromatography (SiO_2, CH_2Cl_2-10% hexanes) followed by recrystallization from CH_2Cl_2-1% MeOH/hexanes yielded the desired 5-phenyl-15-(2-aminophenyl)porphyrin (third compound eluted) as bright purples needles (36.6 mg, 77 µmol, 86%).

^{1}H-NMR (400 MHz, Chloroform-*d*) δ 10.30 (s, 2H), 9.39 (d, *J* = 4.6, 4H), 9.10 (d, *J* = 4.6 Hz, 2H), 9.08 (d, *J* = 4.6 Hz, 2H), 8.34 – 8.27 (m, 1H), 8.27 – 8.20 (m, 1H), 7.93 (dd, *J* = 7.4, 1.5 Hz, 1H), 7.85 – 7.76 (m, 3H), 7.64 (td, *J* = 7.8, 1.6 Hz, 1H), 7.22 (td, *J* = 7.5, 1.2 Hz, 1H), 7.17 (dd, *J* = 8.2, 1.2 Hz, 1H), 3.58 (s, 2H), -3.12 (s, 2H).

MS (MALDI-TOF, positive) calcd for $C_{32}H_{23}N_5$ [M^+] *m/z(*100%) 477.20, found *m/z*(100%) 477.40.

Synthesis of 5-phenyl-15-(2-(2-chloroacethylaminophenyl))porphyrin zinc(II) complex 15

In a 50 mL round bottom flask, 5-phenyl-15-(2-aminophenyl)porphyrin (33 mg, 70.3 µmol) was dissolved in CH_2Cl_2 (10 mL). Potassium carbonate (120 mg, 87 mmol) was added and the slurry was sparged with argon for 5 minutes. The mixture was cooled to 0 °C under argon and 2-choroacethyl chloride (9.8 µL, 13.9 mg, 0.12 mmol) was added. The mixture was stirred at 0 °C, under argon, for 5 minutes than allowed to warm up to room temperature. The progression of the reaction was followed by TLC analysis (SiO_2, CH_2Cl_2). After 30 minutes no starting material remained, the reaction mixture was diluted to 50 mL with CH_2Cl_2, and was transferred to a separatory funnel. It was washed with 5% aqueous $NaHCO_3$ (2 x 50 mL) and water (1 x 50 mL) the organic layer was collected, dried over Na_2SO_4, filtered and the solvent was evaporated under reduced pressure. The crude residue was filtered through a silica short plug (SIO_2, CH_2Cl_2) the eluted product was recrystallized from CH_2Cl_2-hexanes to yield the desired 5-phenyl-15-(2-(2-chloroacethyl)aminophenyl)porphyrin as deep purple crystals (37 mg, 67 µmol, 95 %). This compound was metallated before further characterization.

Metallation:

The porphyrin (37 mg, 67 µmol) was dissolved in DMF (10 mL) and zinc acetate (44 mg, 0.2 mmol) was added. The mixture was stirred at 45 °C for 1 hour after which time no starting material remained according to TLC analysis (SiO_2, CH_2Cl_2-1% MeOH). The mixture was poured into 100 mL of water and the solid filtered. It was further washed with water (100 mL) then dissolved in CH_2Cl_2-1% MeOH (50 mL). The solution was extracted with water (3 x 50 mL), dried over Na_2SO_4, filtered and the solvent was evaporated. The crude solid was filtered over a silica short plug (SiO2, CH_2Cl_2-1% MeOH) CH_2Cl_2 1% MeOH -hexanes to yield the desired porphyrin as bright purple crystals (38 mg, 62 µmol, 92 %).

^{1}H-NMR (500 MHz, Chloroform-*d*) δ 10.35 (s, 2H), 9.48 – 9.44 (m, 4H), 9.16 (d, *J* = 4.4 Hz, 2H), 9.02 (d, *J* = 4.4 Hz, 2H), 8.67 (dd, *J* = 8.5, 1.2 Hz, 1H), 8.30 – 8.26 (m, 1H), 8.26 – 8.20 (m, 1H), 8.13 (dd, *J* = 7.5, 1.6 Hz, 1H), 8.12 (br. s, 1H), 7.87 (ddd, *J* = 8.7, 7.7, 1.6 Hz, 1H), 7.85 – 7.74 (m, 3H), 7.61 (td, *J* = 7.5, 1.3 Hz, 1H), 3.27 (s, 2H).

MS (MALDI-TOF, positive) calcd for $C_{34}H_{22}ClN_5OZn$ [M^+] *m/z(*100%) 615.08, found *m/z*(100%) 615.38.

Synthesis of R2

A three-neck 50 mL round bottom flask equipped with a reflux condenser was charged with 5-phenyl-15-(2-(2-chloroacethyl)aminophenyl)porphyrin (37 mg, 67 µmol), 4-aza-18-crown-6 (106 mg, 0.40 mmol) and ethanol (20 mL). The mixture was sparged with argon for 10 minutes and then stirred under argon, under vigorous reflux. The progression of the reaction was followed by analytical TLC (SiO_2, CH_2Cl_2-10% acetone). After 48 hours only trace amount of starting material remained, the reaction mixture was cooled down to room temperature and the solvent evaporated under reduced pressure. The crude residue was dissolved in CH_2Cl_2 (50 mL) and extracted with water (3 x 100 mL). The organic layer was collected, dried over Na_2SO_4, filtered and the solvent was evaporated under reduced pressure. Column chromatography (SiO_2, eluting gradient: CH_2Cl_2-10% acetone to CH_2Cl_2-30% acetone 0.5% triethylamine). The compound was obtained in several fraction of increasing polarity. ^{1}H NMR analysis indicated the presence of increasing amounts of triethylammonoium salts in the fractions. The combined fractions were treated with 0.5% aqueous citric acid solution (1 x 100 mL), EDTA aqueous solution (pH 9) (1 x 100 mL) and water (2 x 100 mL). The organic layer was collected dried over Na_2SO_4, filtered and the solvent was evaporated. Recrystallization from CH_2Cl_2-hexanes yielded the desired compound as small violet needles (55 mg, 65 µmol, 97%).

^{1}H-NMR (500 MHz, DMSO-d_6) δ 10.40 (s, 2H), 9.51 (dd, *J* = 4.4, 4.0 Hz, 2H), 9.02 – 8.88 (m, 3H), 8.86 – 8.76 (m, 3H), 8.35 – 8.25 (m, 1H), 8.16 – 8.10 (m, 1H), 8.06 (dd, *J* = 7.4, 1.5 Hz, 1H), 7.92 – 7.82 (m, *4*H), 7.56 (td, *J* = 7.5, 1.3 Hz, 1H), 2.48– 2.44 (m, 4H), 2.43 (s, 2H), 2.19 – 2.06 (m, 4H), 1.58 – 1.48 (m, 4H), 0.76 – 0.70 (m, 4H), 0.68 (t, *J* = 5.9 Hz, 4H), 0.05 (t, *J* = 5.8 Hz, 4H).

MS (MALDI-TOF, positive) calcd for $C_{46}H_{46}N_6O_6Zn$ [M^+] *m/z(*100%) 842.28, found *m/z*(100%) 842.62.

HRMS (ESI-TOF, positive) calcd for $C_{46}H_{47}N_6O_6Zn$ [M + H^+] *m/z(*100%) 843.2849, found *m/z*(100%) 843.3881.

Synthesis of R1

In a 25 mL round bottom flask, porphyrin **11a** (15 mg, 19.8 µmol) was dissolved in tetrahydrofuran-20 % methanol mixture (5 mL) and the solution was sparged with argon for 15 minutes. Aqueous potassium hydroxide (1 M solution in MeOH-H_2O 1-1, 1 mL) was added and the mixture was stirred at room temperature under argon. The progression of the reaction was followed by TLC analysis (SiO2, EtOAc-Acetone-H_2O 10-9-1); after 1 hour at room temperature the hydrolysis was complete. The reaction mixture was poured into saturated aqueous NH_4Cl solution (50 mL) and the aqueous layer was extracted with EtOAc-10% MeOH, until most of the porphyrin was recovered (5 x 25 mL). The combined organic layer was died over Na_2SO_4 filtered and the solvent was evaporated to yield the desired **R1** as a purple powder (7.8 mg, 10.7 µmol, 54%).

Note due to the high water-solubility of the target compound and the small quantity of the starting material used losses during the work up of the reaction explain the low yield of material isolated after saponification. The compound was particularly insoluble in most organic solvent and required the addition of a base to reach an acceptable concentration for ^{1}H-NMR studies.

^{1}H-NMR (400 MHz, Methanol-d_4 - 5% Pyridine-d_5) δ 10.20 (s, 2H), 9.38 (d, *J* = 4.5 Hz, 4H), 8.98 (d, *J* = 4.4 Hz, 2H), 8.89 (d, *J* = 4.4 Hz, 2H), 8.50 (d, *J* = 8.6 Hz, 1H), 8.35 – 8.28 (m, 1H), 8.28 – 8.21 (m, 1H), 8.13 – 8.03 (m, 2H), 7.98 (d, *J* = 7.3 Hz, 1H), 7.96 – 7.84 (m, 2H), 2.95 (s, 2H).

Note: the signals of the CH_2 – carboxylic acids are missing probably due to slow exchange. The acidic protons are not expected to be observed in these conditions.

^{1}H-NMR (500 MHz, DMSO-d_6 - 5% Pyridine-d_5) δ 10.31 (s, 2H), 9.48 (d, *J* = 4.4 Hz, 2H), 9.44 (d, *J* = 4.4 Hz, 2H), 8.85 (d, *J* = 4.4 Hz, 2H), 8.82 (d, *J* = 4.4 Hz, 2H), 8.55 – 8.50 (m, 1H), 8.45 – 8.38 (m, 1H), 8.19 (d, *J* = 7.4, 1H), 8.18 – 8.12 (m, 2H), 7.92 (td, *J* = 7.8, 1.3 Hz, 1H), 7.86 (td, *J* = 7.5, 1.5 Hz, 1H), 7.82 – 7.76 (m, 1H), 3.99 (br. s, 2H), 2.79 (s, 2H).

2 ^{1}H NMR analysis

2.1 Determination of the ratio of 1a-OMe/1b-OMe

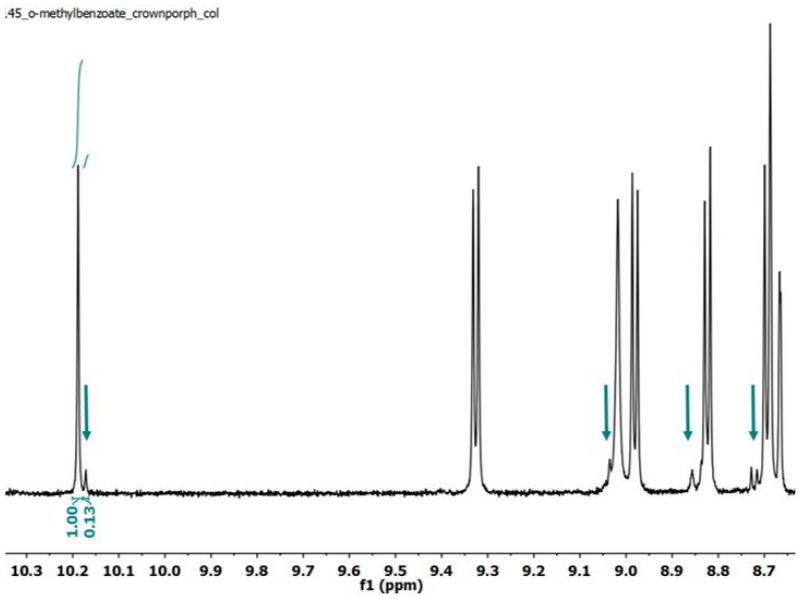

Figure S1. Selected area of the 1HNMR spectra of the mixture of the atropisomers **1a-OMe** and **1b-OMe** obtained directly after the Suzuki coupling reaction. The arrow indicates the signals corresponding to the minor isomer (**1a-OMe**). A ratio of 1/8 was estimated from the integration of the *meso*-signals of porphyrin rings (left most signals). Spectra recorded in $CDCl_3$, at 295 K, on a 400 MHz spectrometer.

2.2 Comparison of the ^{1}H NMR spectra of 1a isolated after hydrolysis of 1a-OMe/1b-OMe mixture and of 1a obtained after thermal equilibration of 1b in presence of $NaBPh_4$

A)

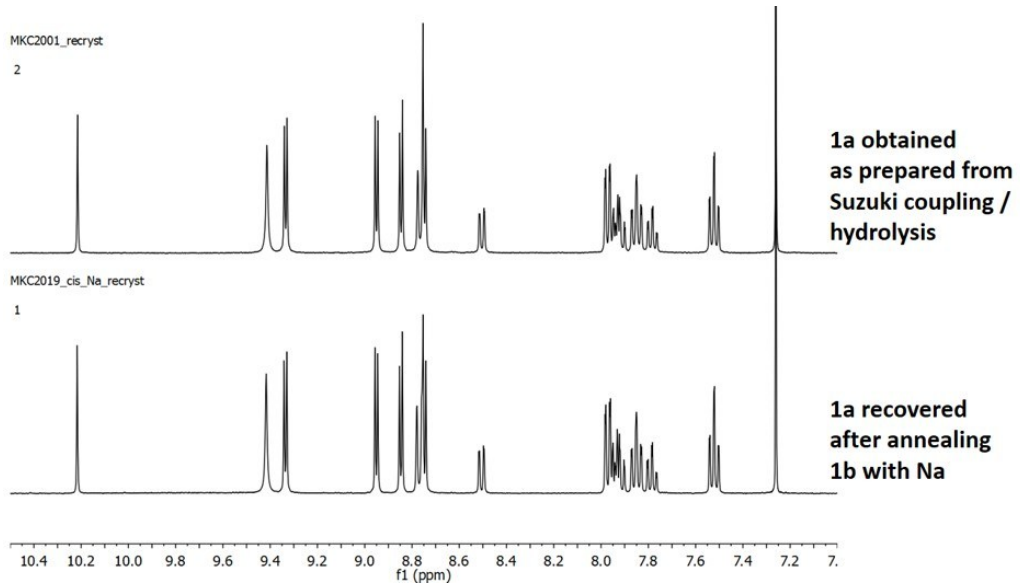

B)

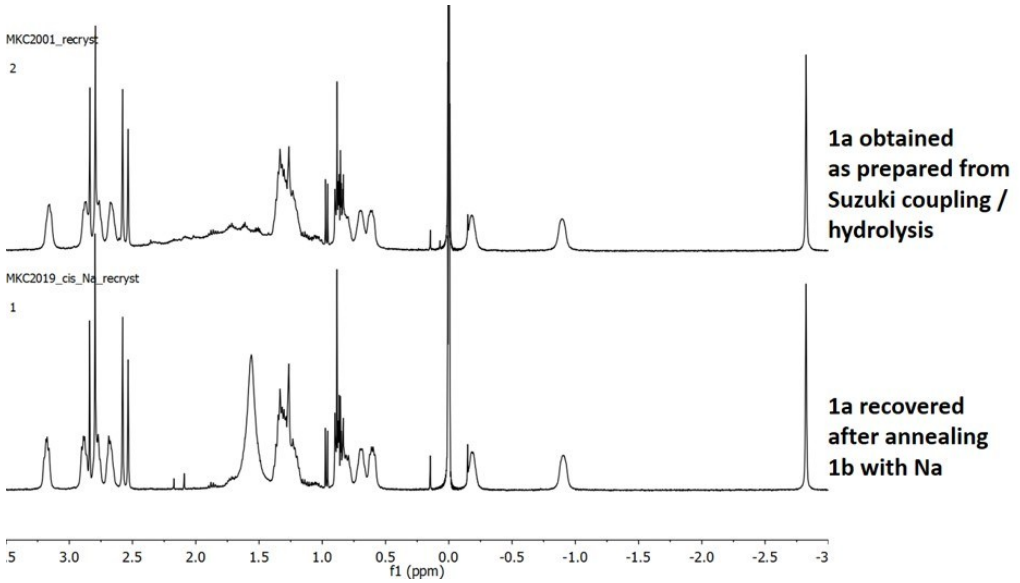

Figure S2. Qualitative comparison of the ^{1}H NMR spectra of ligand **1a** obtained after hydrolysis and purification of the methyl ester precursors mixture (**1a-OMe** and **1b-OMe** 1/8 mixture, top), and of the product obtained after annealing **1b** in pyridine at 90 °C in the presence of sodium tetraphenylborate (bottom). Spectra recorded in $CDCl_3$, at 295 K, on a 400 MHz spectrometer. Note the perfect matching between the spectra. Aromatic region (A) and aliphatic region (B).

2.3 Assignments of the conformations of ligands 1a and 1b

As shown in the following the ^{1}H-NMR spectra of ligands **1a** and **1b** in deuterated chloroform ($CDCl_3$) are distinct, both in the aromatic and the aliphatic regions (see Figures S4 and S5). The most striking differences are observed for the signals associated with the crown ether moieties (HCr) and with the protons of the methylene groups (CH2/CH2') which link the crown ether to the porphyrin macrocycle. In the case of ligand **1a** the signals associated with the crown ether substituent form a well resolved series of peaks spread over a large range of chemical shifts (between -1 ppm and 4 ppm). The signals of the methylene bridges appear as two doublets centered at 2.6 ppm and 2.8 ppm. In contrast, for **1b** the signals of the crown ether moiety form a broad massif that extends over a narrower range of chemical shifts (from ca. 0 ppm to 2 ppm) and presents only two major features, centered at 1.6 ppm and 1.4 ppm. Moreover, the signals associated with the methylene bridges appear as a sharp singlet centered at 2.6 ppm. These observations led us to the assignment of **1b** to the *trans* atropisomer and **1a** to the *cis* atropisomer. For the latter, the orientation of the carboxylic acid towards the crown ether strap permits the development of an internal hydrogen bond and locks the structure into a well-defined conformation. On the contrary, in the case of the *trans* atropisomer, the orientation of the carboxylic acid towards the opposite face of the porphyrin does not permit stabilization of any specific conformation of the strap and thus results in the observation of a much less resolved set of signals. The formation of an internal hydrogen bond in **1a** is supported by the observation that the addition of deuterated methanol (MeOD) leads to the partial loss of the strongly unsymmetrical signal pattern observed in pure $CDCl_3$ and to the coalescence of the strap signals into broad massifs reminiscent of the signals observed for **1b** (*cf.* section 2.4).

Assignment of the ^{1}H NMR signals for 1a

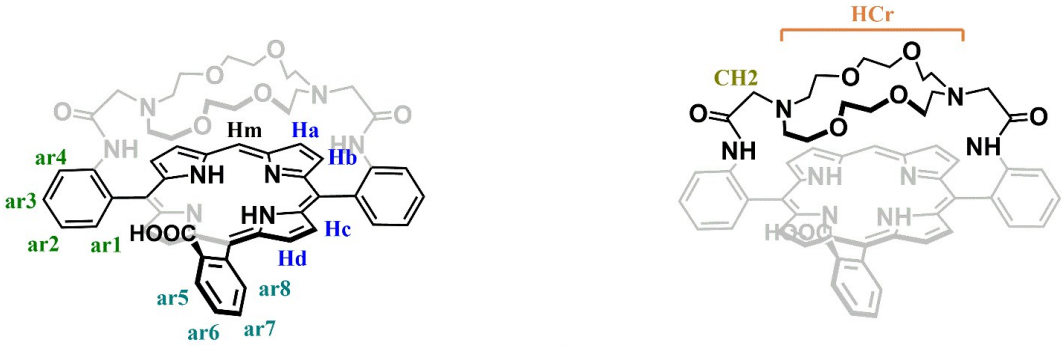

1a

Scheme 5. Schematic representation of **1a** and protons numbering

^{1}H NMR (500 MHz, Chloroform-*d*) δ 10.21 (s, 1H, Hm), 9.41 (s, 2H, NH), 9.33 (d, *J* = 4.6 Hz, 2H, Ha), 8.95 (d, *J* = 4.6 Hz, 2H, Hb), 8.85 (d, *J* = 4.7 Hz, 2H, Hc), 8.77 (d, *J* = 8.0 Hz, 2H, ar4), 8.75 (d, *J* = 4.7 Hz, 2H, Hd), 8.50 (d, *J* = 8.0 Hz, 1H, ar5), 7.97 (d, *J* = 8.0 Hz, 2H, ar1), 7.96 – 7.89 (m, 2H, ar6,8), 7.86 – 7.84 (m, 2H, ar3), 7.79 – 7.77 (m, 1H, ar7), 7.53 – 7.51 (m, 2H, ar2), 3.23 – 3.04 (m, 2H, HCr), 2.89 – 2.85 (m, 2H, HCr), 2.81 (d, *J* = 17.4 Hz, 2H, CH2), 2.80 – 2.74 (m, 2H, HCr), 2.68 – 2.64 (m, 2H, HCr), 2.55 (d, *J* = 17.4 Hz, 2H, CH2), 1.37 – 1.32 (m, 4H, HCr), 1.28 – 1.21 (m, 2H, HCr), 0.86 – 0.76 (m, 2H, HCr), 0.70 – 0.65 (m, 2H, HCr), 0.63 – 0.58 (m, 2H, HCr), -0.21 – 0.17 (m, 2H, HCr), -0.92 – -0.87 (m, 2H, HCr), -2.82 (s, 2H, NHPor).

Note: the aromatic protons could be assigned using the careful analysis of COSY and ROESY spectra; chemical exchange and weak NOE signals impeded the full attribution of the aliphatic signals (crown-ether)

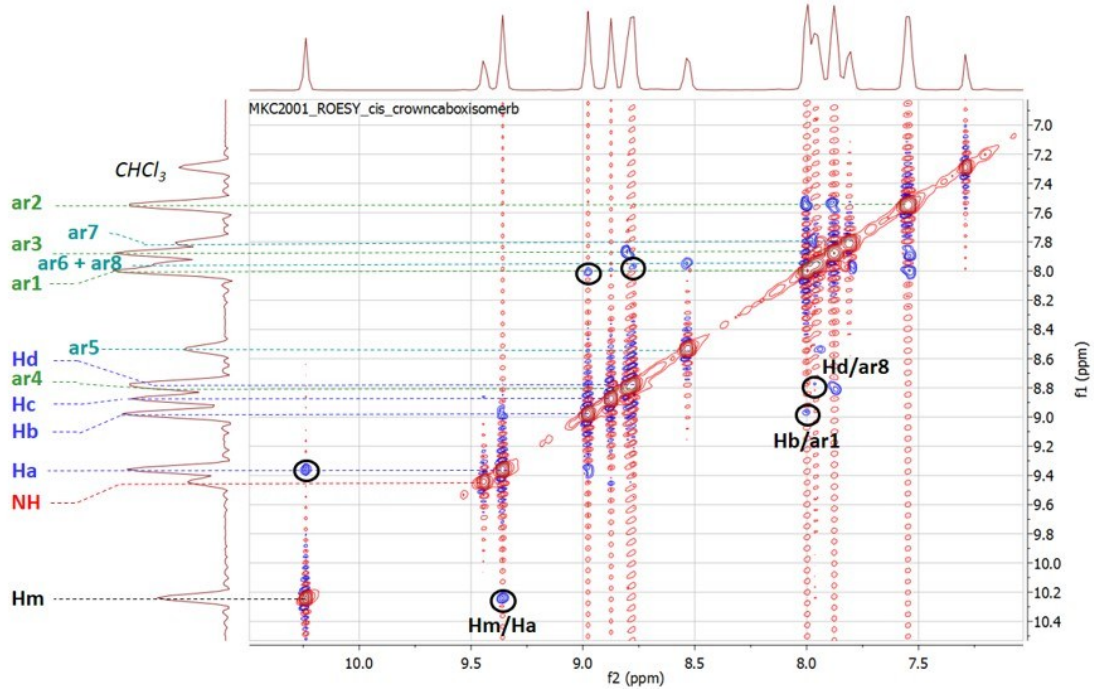

Figure S3. Principal Nuclear Overhauser Effect (NOE) contacts observed for ligand **1a** (aromatic region).

Assignment of ^{1}H NMR signals for 1b

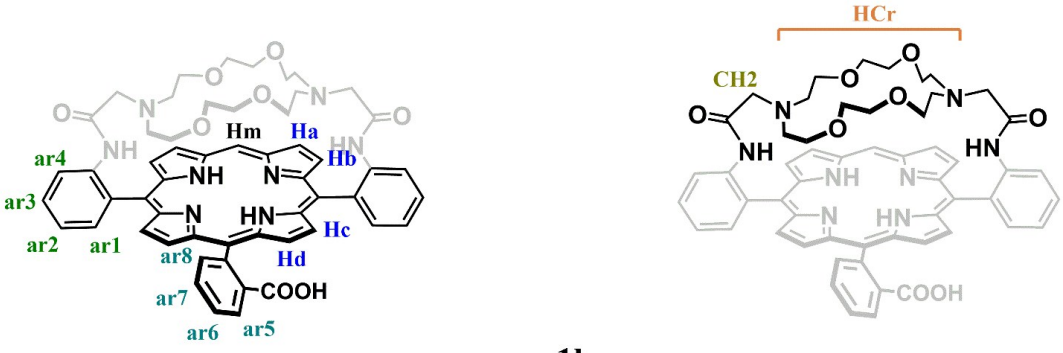

1b

Scheme 6. Schematic representation of **1a** and protons numbering

^{1}H NMR (400 MHz, Chloroform-*d*) δ 10.14 (s, 1H, Hm), 9.28 (d, *J* = 4.7 Hz, 2H, Ha), 8.97 – 8.92 (m, 3H, Hb, NH), 8.78 (d, *J* = 4.8 Hz, 2H, Hc), 8.69 – 8.57 (m, 4H. Hd, ar4), 8.28 (m, 2H, ar5, ar8), 7.99 (d, *J* = 7.4 Hz, 2H, ar1), 7.90 –7.80 (m, 4H, ar6, ar7, ar3), 7.54 – 7.49 (m, 2H, ar2), 2.58 (s, 4H, CH2), 2.04 – 0.4 (br.m, 24H, HCr), -2.86 (s, 2H, NHPor).

-due to the overlapping signals the full attribution of the aromatic protons could not be conducted; the attribution is proposed based on the analysis of the spectra of **1a** and assuming minor shifting of the aromatic peaks between the two atropisomers-

Comparison of the ^{1}H NMR spectra of compounds 1a and 1b in CDCl3

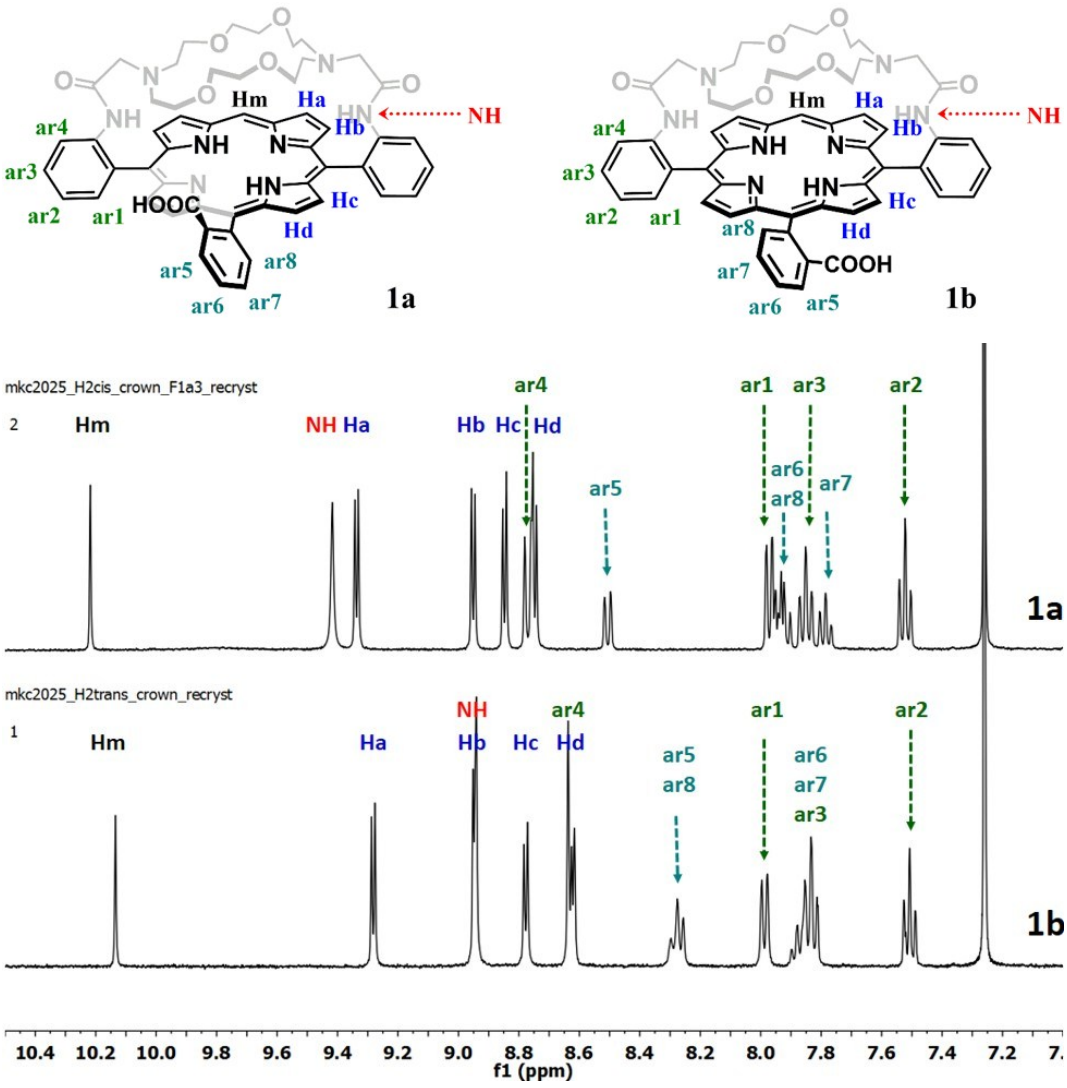

Figure S4. Comparison of the aromatic protons signals of the ligands **1a** (top) and **1b** (bottom) in $CDCl_3$, at 295 K. ^{1}H NMR spectra recorded on a 400 MHz spectrometer. Due to the overlapping signals the full attribution of the aromatic protons of the spectra of **1b** could not be conducted; the attribution is proposed based on the analysis of the spectra of **1a**, assuming minor shifting of the signals. Differences in the spectra are however evident.

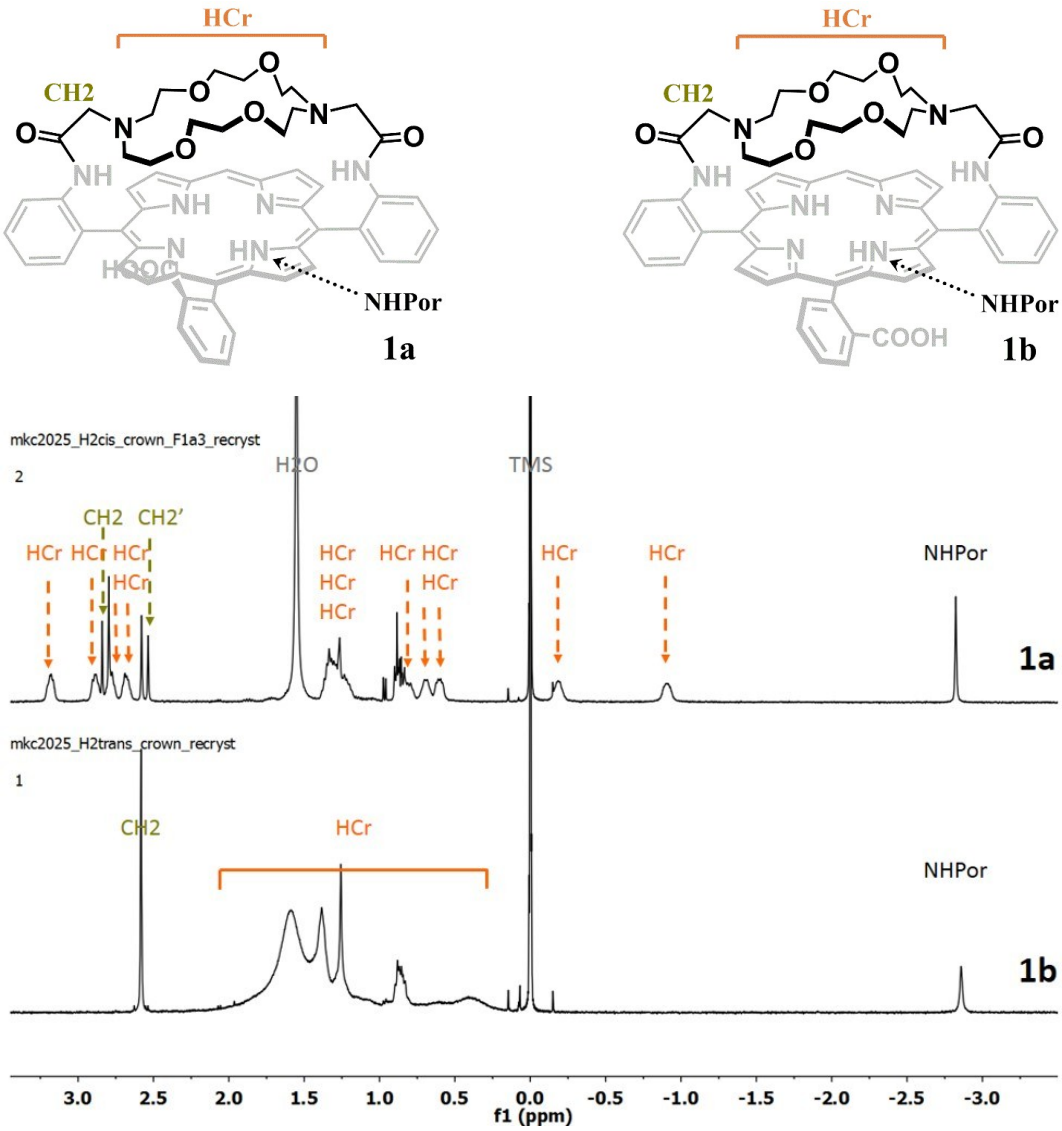

Figure S5. Comparison of the aliphatic protons signals of ligands **1a** (top) and **1b** (bottom) in $CDCl_3$, at 295 K. ^1H NMR spectra recorded on a 400 MHz spectrometer. Due to the broadness of the crown ether signals only weak NOE contacts could be observed in the ROESY spectra. The analysis was further complicated by chemical exchange between the crown ether signals and thus, did not permit the unambiguous assignment of all crown ether signals in the case of **1a**. However the presence of a well-defined set of signals as compared to the wide massif observed for **1b** points towards a much slower dynamical exchange of the crown ether protons, *ie*. a more rigid structure of **1a** in solution.

2.4 Effect of the addition of MeOD on the ^{1}H NMR spectra of 1a

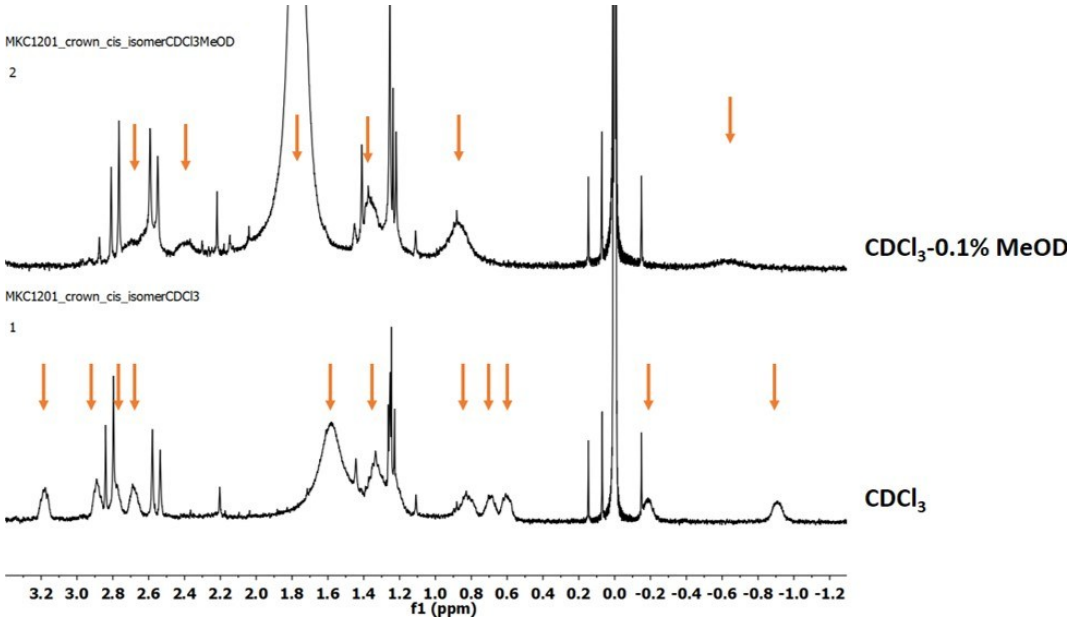

Figure S6. Comparison the ^{1}H NMR spectra (aliphatic region) of ligand **1a** recorded in the presence (top) or absence (bottom) of MeOD, in $CDCl_3$, at 295 K. Spectra recorded on a 400 MHz spectrometer. Signals belonging to the crown ether moiety are indicated with orange arrows. Note the coalescence of the individual signals of the crown ether into broad massifs upon addition of methanol.

2.5 Assignments of the conformations of ligands 2a and 2b

The assignments of the conformations of ligands **2a** and **2b** were supported by a careful analysis of their respective ^{1}H-NMR spectra in deuterated dimethylsulfoxide (DMSO-d_6). As shown in the following, both the aromatic and the aliphatic regions of the spectra exhibit distinct patterns for the two ligands (Figures S17 and S18). More specifically, in the aliphatic region, the signals of the crown ether (HCr1-HCr6) are generally shifted more up-field for **2b** than for **2a**, suggesting a stronger influence of the ring-current of the porphyrin macrocycle, *i.e.,* a generally closer proximity of the crown ether to the porphyrin plane for **2b** than for **2a**. In the absence of notable differences observed for the signals of the protons of the carboxylic acids functionalities of **2a** and **2b** (*Figure S17*), the differences noticed for the chemical shifts of the protons belonging to the crown ether moiety can be simply attributed to the steric effects associated with the orientation of the substituents with respect to each other; we thus can attribute **2b** to the *trans* atropisomer and **2a** to the *cis* atropisomer. To further support this attribution, we note the presence of an identical pattern for the crown ether signals in the ^{1}H-NMR spectrum of **2b** and that of the reference ligand **R2**. The latter does not bear the carboxylic acid functionalities and thus the crown ether moiety experiences minimal steric crowding as expected for the *trans*-atropisomer (*cf.* section 2.6). Furthermore, the observation of a clear nuclear Overhauser effect (NOE) indicating contacts between the crown ether and the opposite phenyl substituent in the case of **2b** (Figure S16), as well as weak NOE effects indicating contacts between the crown ether substituent and a methyl group of the di-carboxylic acid substituent in the case of ligand **2a** (Figure S10), confirm our assignments.

Assignment of the ^{1}H NMR spectrum of 2a

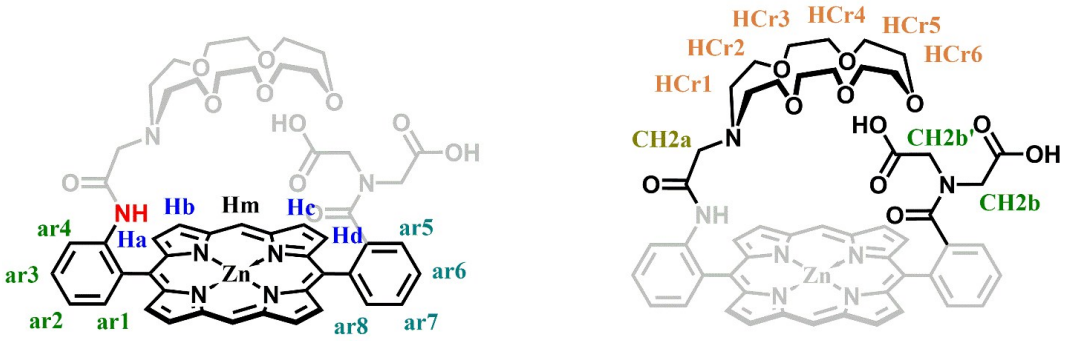

2a

Scheme 7. Schematic representation of **2a** and protons numbering.

1H NMR (500 MHz, DMSO-d6 1% Pyridine-d_5) δ 18.1 (br s, 2H, COOH)10.31 (s, 2H, Hm), 9.46 (d, *J* = 4.4 Hz, 2H, Hb), 9.43 (d, *J* = 4.4 Hz, 2H, Hc), 9.18 (s, 1H, NH), 8.86 (d, *J* = 4.4 Hz, 2H, Hd), 8.79 (d, *J* = 4.5 Hz, 2H, Ha), 8.66 (d, *J* = 8.4 Hz, 1H, ar4), 8.02 (d, *J* = 7.4 Hz, 1H, ar8), 7.95 (d, *J* = 7.4, 1H, ar1), 7.92 – 7.86 (m, 1H, ar6), 7.87 –7.83 (m, 1H, ar3), 7.83 – 7.77 (m, 1H, ar7), 7.76 (d, *J* = 7.8 Hz, 1H, ar5), 7.56 –7.52 (m, 1H, ar2), 2.83 (br s, 4H, HCr6), 2.73 (br s, 2H, CH2b/b'), 2.48 (s, 2H, CH2a), 2.40 (br s, 4H, HCr5), 1.66 (br s, 4H, HCr4), 1.52 (br s, 4H, HCr3), 1.02 (br s, 4H, HCr1), 0.88 (br s, 4H, HCr2)

The spectra were recorded in DMSO-d_6 containing 1% of deuterated pyridine, with presaturation of the water signal at 1 db. The addition of pyridine permits to reach a higher concentration of the ligand, which was required for ROESY experiments. The presence of pyridine lead to noticeable shifts of the proton signal of the ligands (see below) due to coordination to the zinc. It led to a better resolved spectra (slightly less overlapping signals). See below for the comparison of the spectra of **2a** in presence or absence of pyridine. Importantly the assignemt obtained in the presence of pyridine could be used to assign the spectra of **2a** in pure DMSO as well.

Note: the signature of 2 CH_2 protons associated with the carboxylic arms (CH_2b/b') are not visible on the spectra, as mentioned in the experimental part, these signals associated with these protons experience important broadening effects probably to restricted structural relaxation of the system.

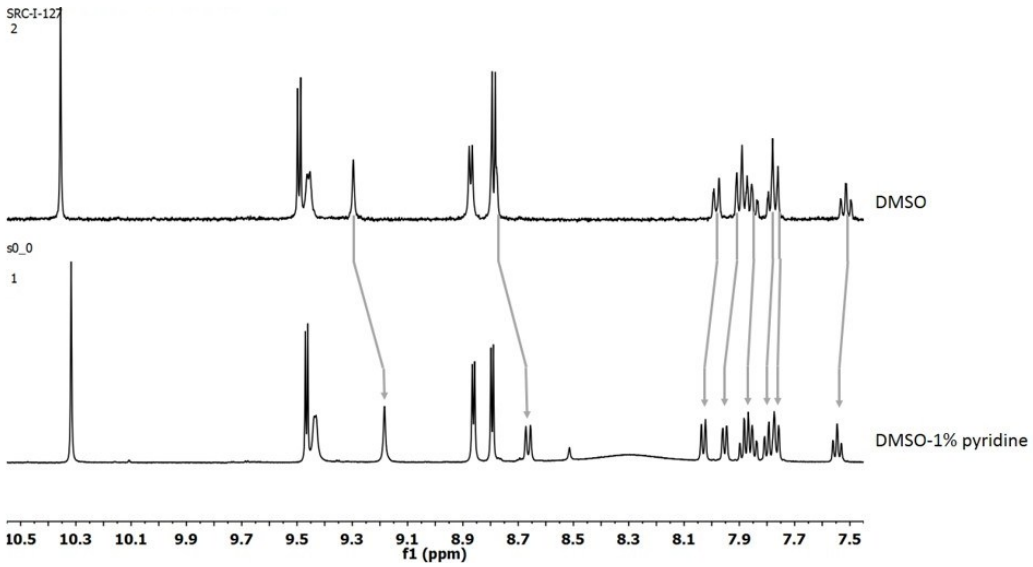

Figure S7. Shifting of the aromatic signals of the ^{1}HNMR spectrum of ligand **2a** upon addition of pyridine.

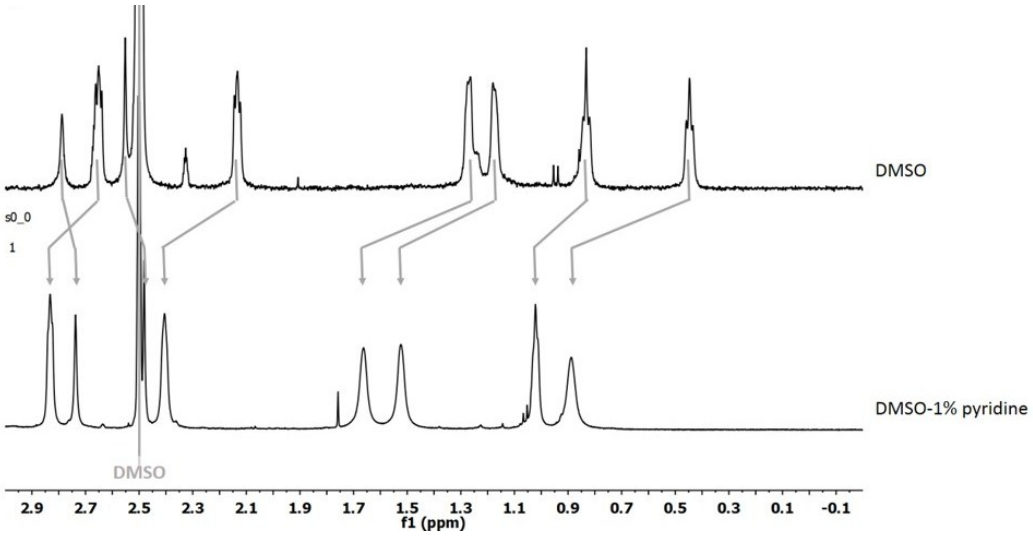

Figure S8. Shifting of the aliphatic signals of the ^{1}HNMR spectrum of ligand **2a** upon addition of pyridine.

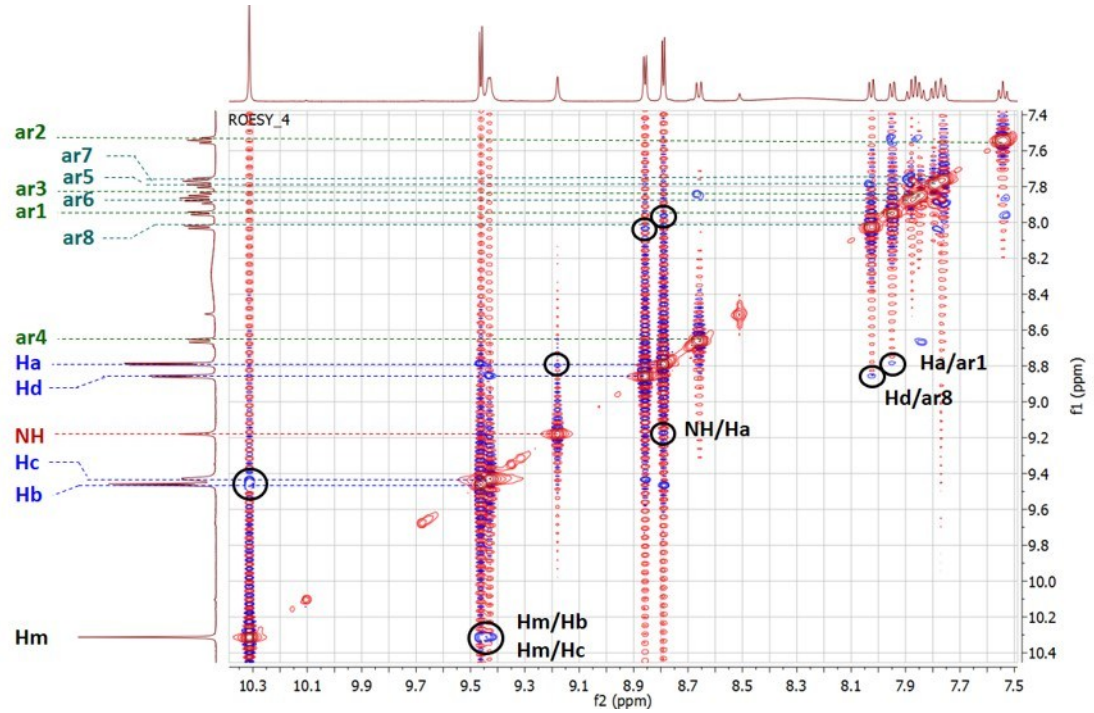

Figure S9. Principal NOE contacts obsereved in the aromatic region of the ^{1}HNMR spectrum of ligand **2a**, recorded in DMSO-d_6 – 1% pyridine-d_5.

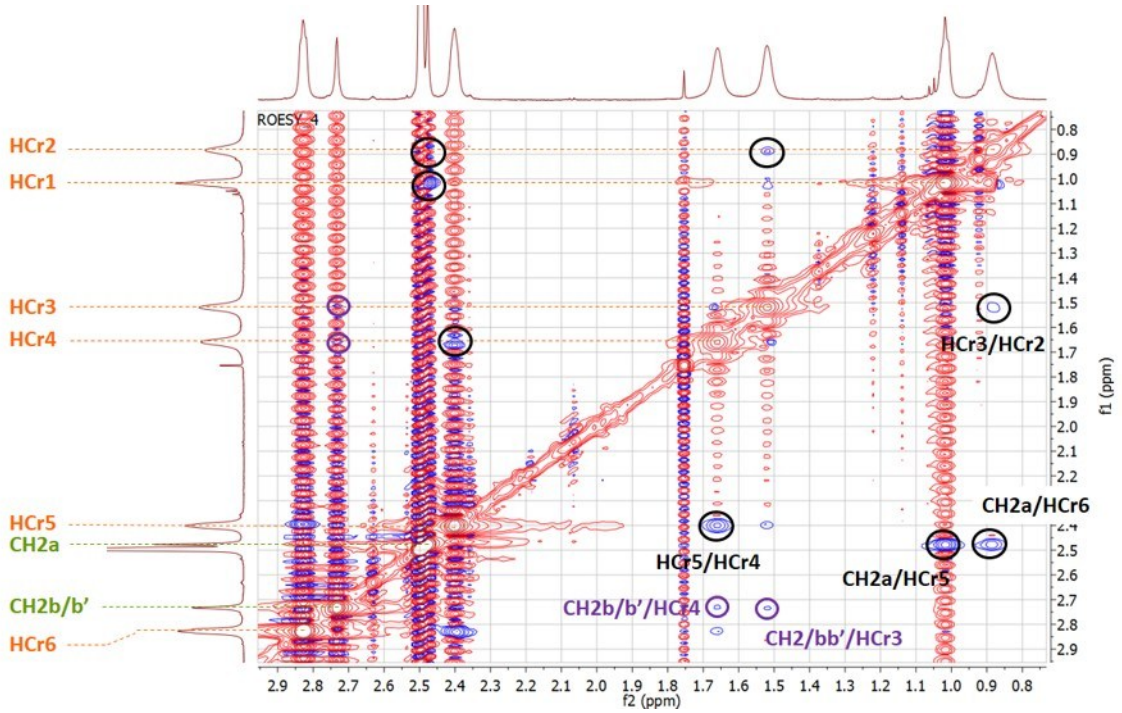

Figure S10. Principal NOE contacts obsereved in the aliphatic region the ^{1}HNMR spectrum of ligand **2a**, recorded in DMSO-d_6 – 1% pyridine-d_5.

Note the weak NOE contacts observed between CH2b' (carboxylic acid arms) and HCr4/3 (crown ether substituent) confirming the attribution of this atropisomer to the cis-isomer (purple circles).

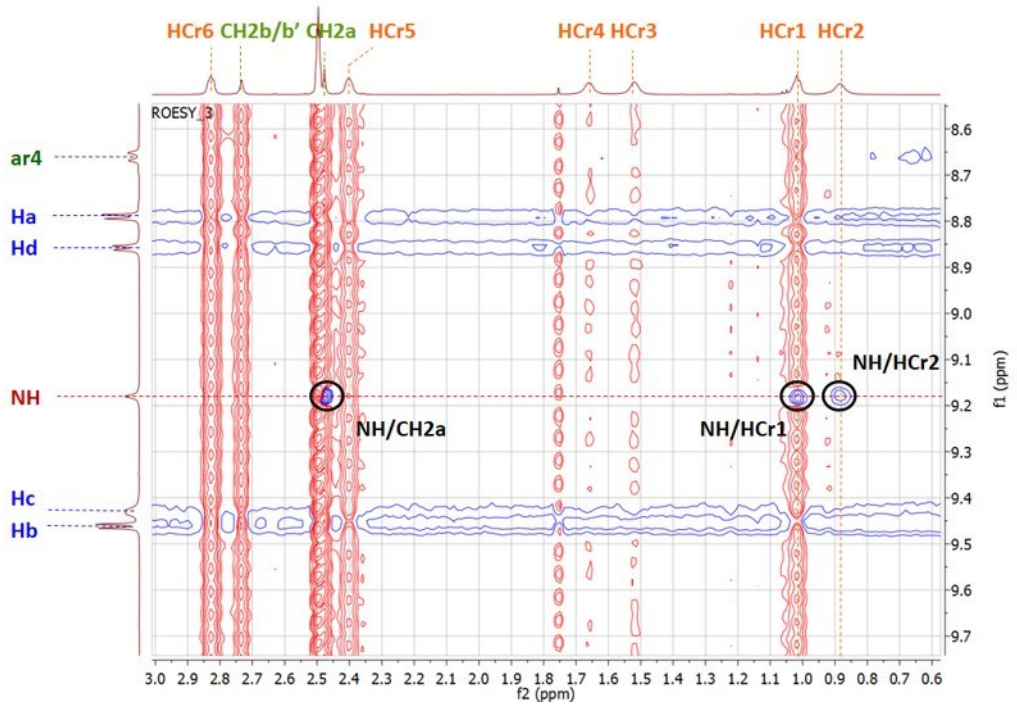

Figure S11. Aliphatic-aromatic NOE contacts obsereved in the ^{1}HNMR spectrum of ligand **2a**, recorded in DMSO-d_6 – 1% pyridine-d_5.

Assignment of the ^{1}H NMR spectrum of 2b

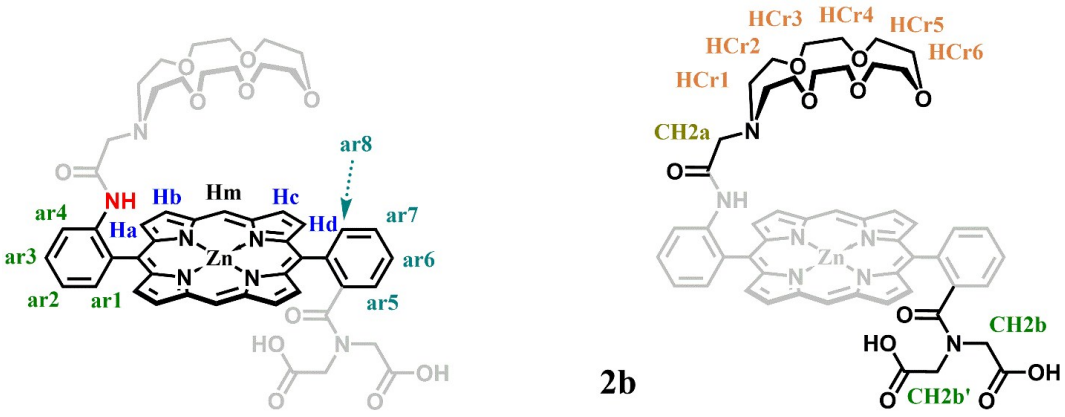

2b

Scheme 8. Schematic representation of **2b** and protons numbering.

^{1}H NMR (500 MHz, DMSO-d_6) δ 18.3 (br s, 2H, COOH),10.34 (s, 2H, Hm), 9.47 (d, *J* = 4.4 Hz, 2H, Hb), 9.44 (d, *J* = 4.4 Hz, 2H, Hc), 8.92 (s, 1H, NH), 8.84 (d, *J* = 4.4 Hz, 2H, Hd), 8.78 ─8.75 (m, 1H, ar4), 8.76 (d, *J* = 4.6 Hz, 2H, Ha), 8.04 (dd, *J* = 7.5, 1.6 Hz, 1H, ar1), 8.00 (d, *J* = 7.4 Hz, 1H, ar8), 7.90 ─ 7.87 (m, 1H, ar6), 7.87 ─ 7.84 (m, 1H, ar3), 7.83 ─7.80 (m, 1H, ar7), 7.73 (d, *J* = 7.8 Hz, 1H, ar5), 7.57 ─7.53 (m, 1H, ar2), 3.80 (br s, 2H, CH2b/CH2b'), 2.66 (s, 2H, CH2b/CH2b'), 2.52 ─ 2.50 (m, 4H, HCr6), 2.41 (s, 2H, CH2a), 2.18 ─ 2.16 (b, 4H, HCr5), 1.56 ─ 1.55 (m, 4H, HCr4), 0.75 (br s, 4H, HCr3), 0.69 (br s, 4H, HCr1), 0.07 (br s, 4H, HCr2).

The spectra were recorded in DMSO-d_6 containing 1% of deuterated pyridine, with presaturation of the water signal at 1 db. The addition of pyridine permits to reach a higher concentration for the ligand, which was beneficial for ROESY experiments. At the concentration used, the presence of pyridine did not lead to major shifts in the ^{1}H NMR spectrum (see below).

Note: the signature of 2 CH_2 protons associated with the carboxylic arms (CH_2b/b') are not visible on the spectra, as mentioned in the experimental part, these signals associated with these protons experience important broadening effects probably to restricted structural relaxation of the system.

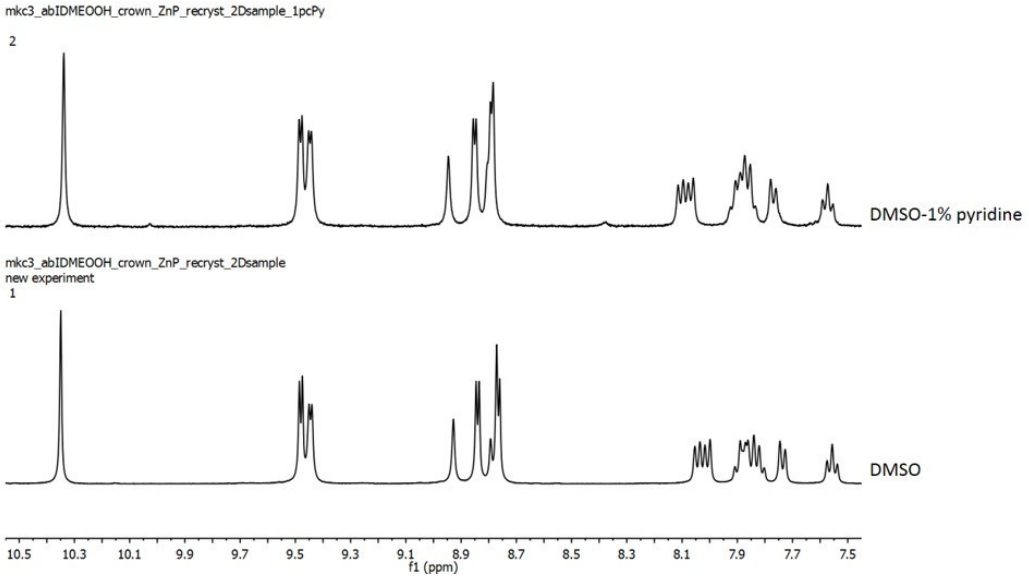

Figure S12. Comparison between the aromatic region of the ^{1}HNMR spectrum of ligand **2b** in presence (top) or absance (bottom) of pyridine-d_5 in DMSO-d_6.

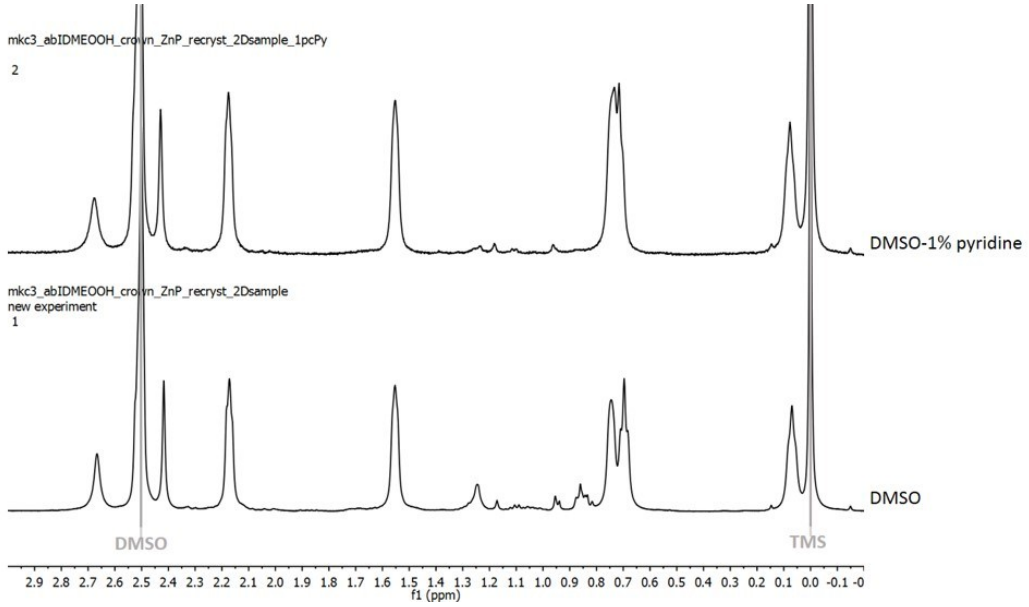

Figure S13. Comparison between the aliphatic region of the ^{1}HNMR spectrum of ligand **2b** in presence (top) or absance (bottom) of pyridine-d_5 in DMSO-d_6.

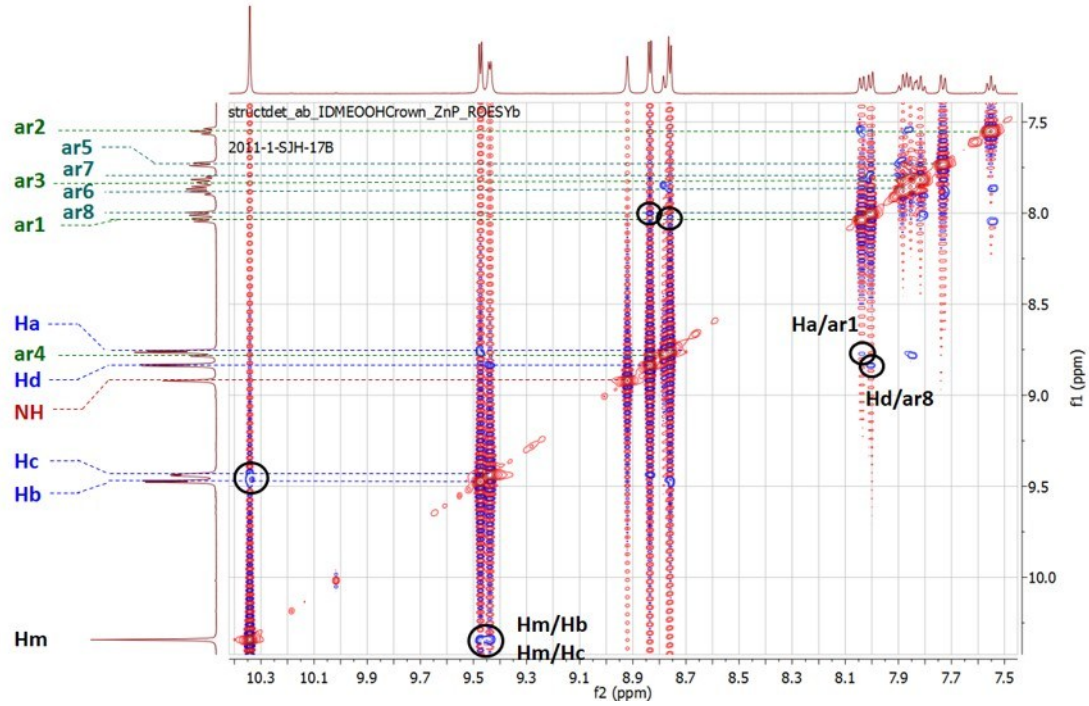

Figure S14. Principal NOE contacts obsereved in the aromatic region of the ^{1}HNMR spectrum of ligand **2b**.

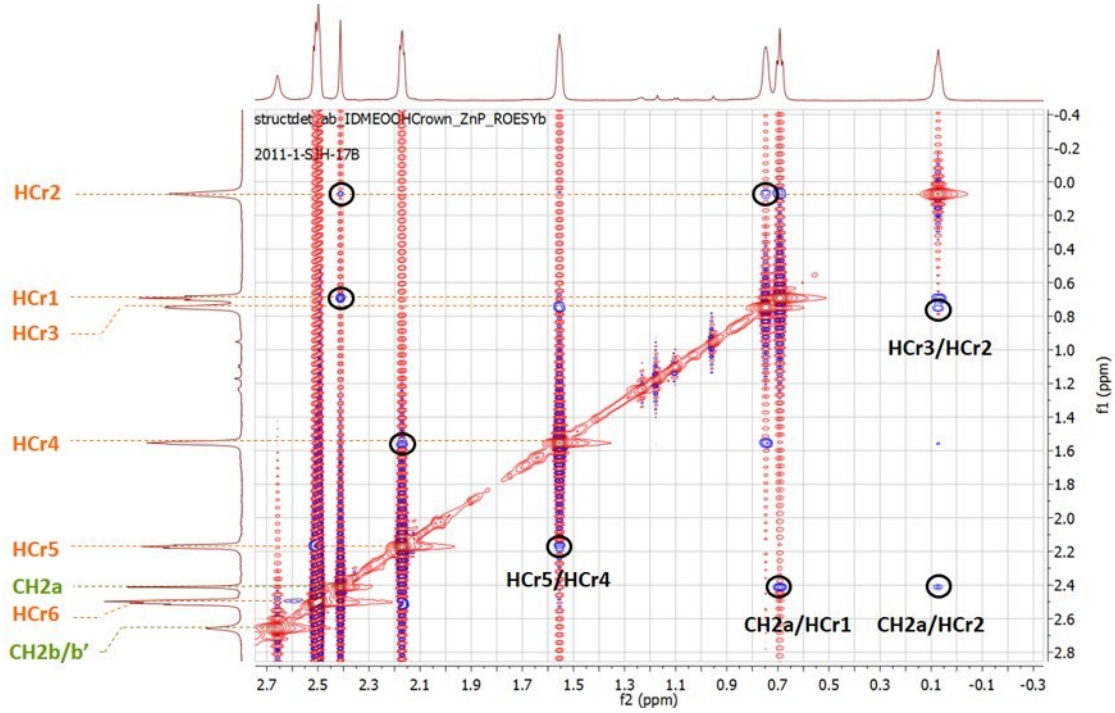

Figure S15. Principal NOE contacts obsereved in the aaliphatic region of the ^{1}HNMR spectrum of ligand **2b**.

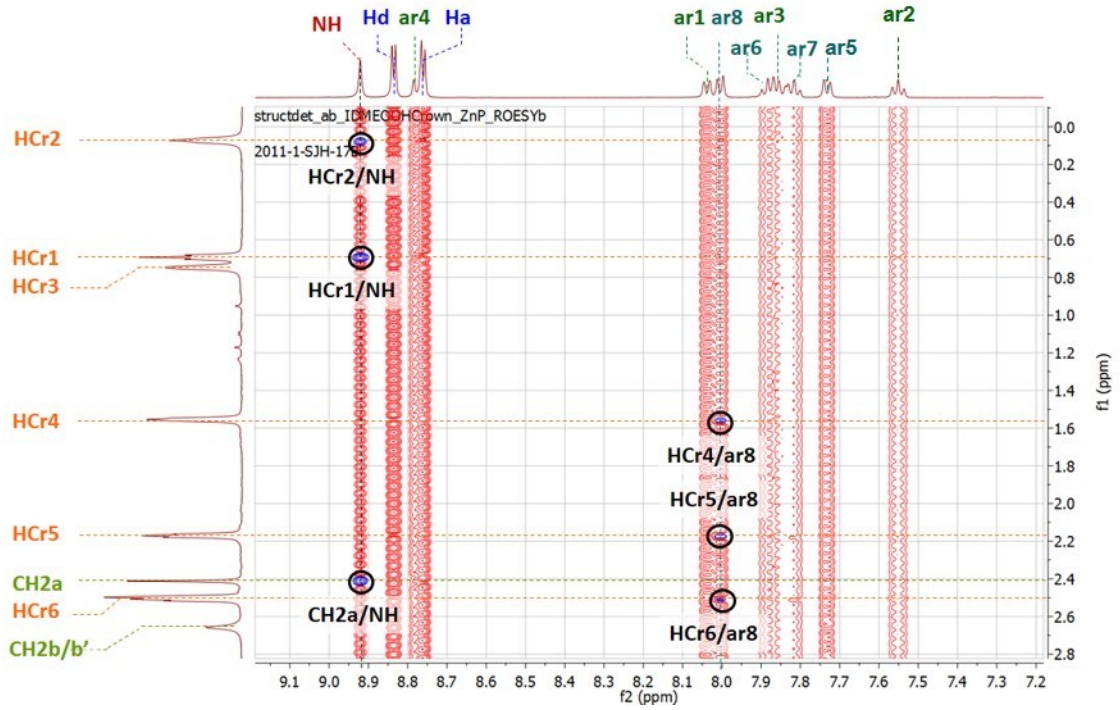

Figure S16. Aliphatic-aromatic NOE contacts obsereved in the ^{1}HNMR spectrum of ligand **2b**.

Comparison between the ^{1}H NMR spectra of compounds 2a and 2b in DMSO-d6

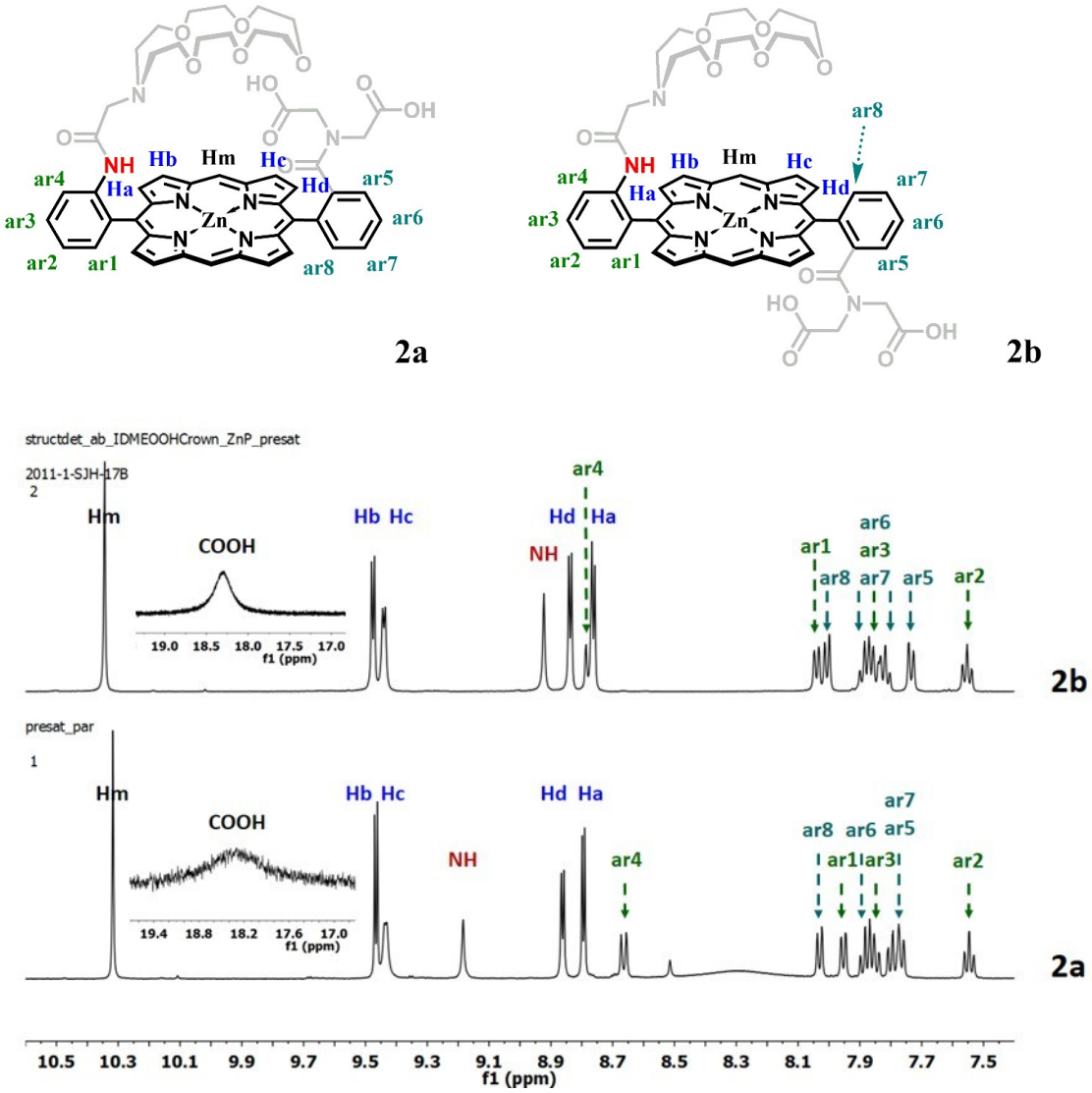

Figure S17. Comparison between the aromatic regions of the ^{1}H NMR spectra of ligands **2a** (top) and **2b** (bottom) in DMSO-d_6, at 295 K. Spectra recorded on a 500 MHz spectrometer.

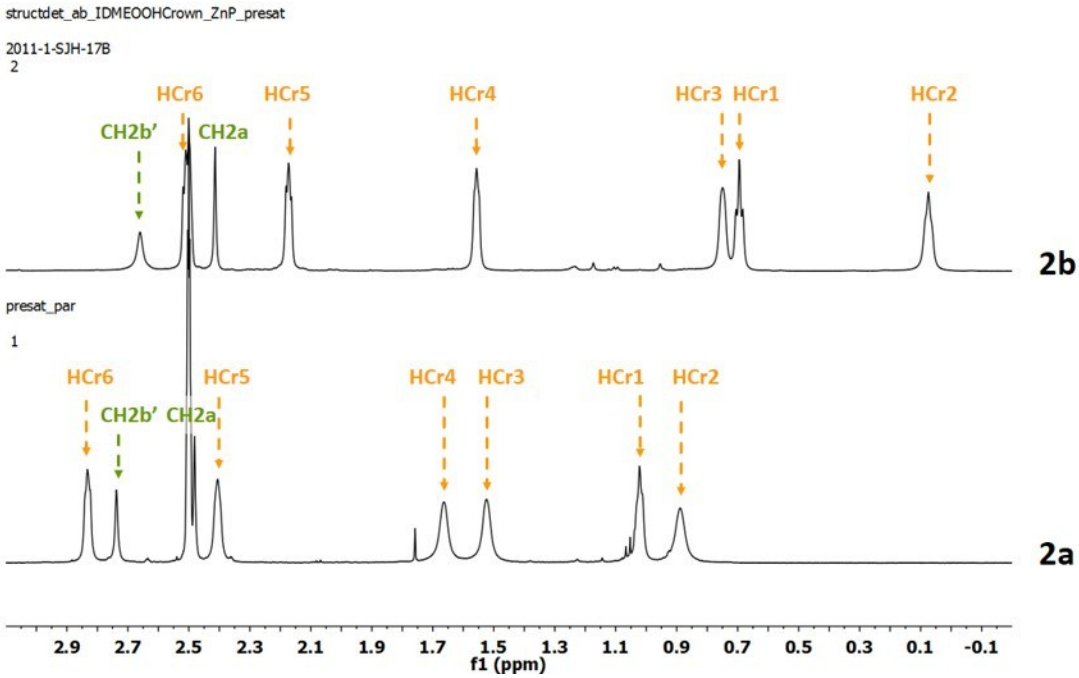

Figure S18. Comparison between the aliphatic regions of the ^{1}H NMR spectra of ligands **2a** (top) and **2b** (bottom) in DMSO-d_6, at 295 K. Spectra recorded on a 500 MHz spectrometer.

2.6 ^{1}H NMR spectra of 2a, 2b, and R2 in DMSO-d_6

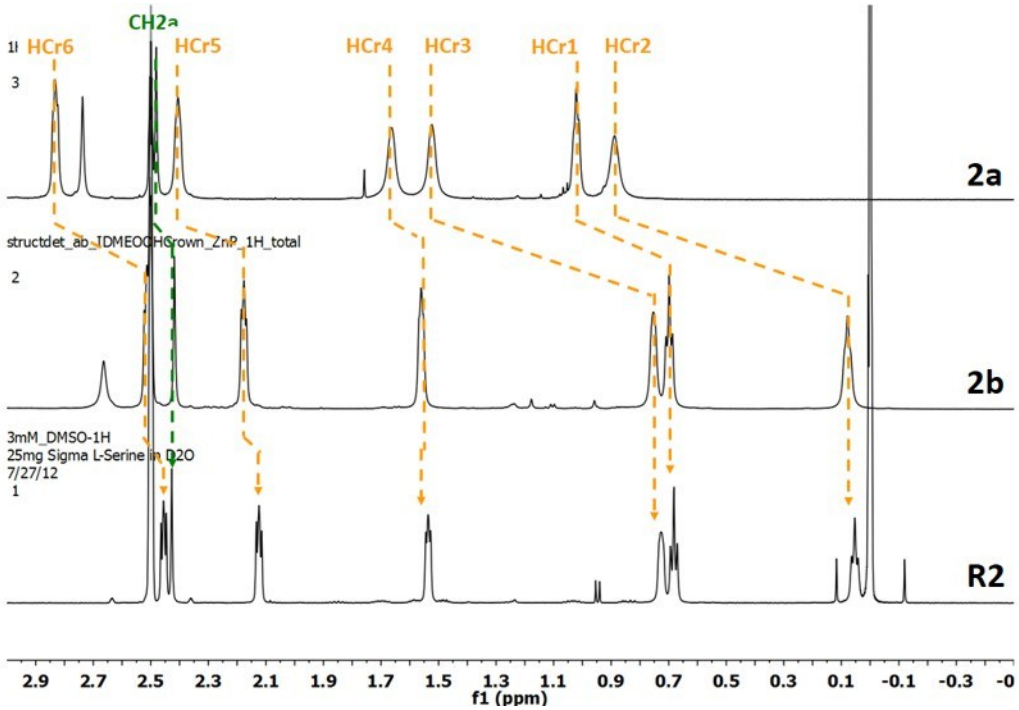

Figure S19. Selected area of the ^{1}H NMR spectra of ligands **2a** (top) and **2b** (middle) and **R2** (bottom) in DMSO-d_6, at 295 K. Spectra recorded on a 500 MHz spectrometer. The attribution of the crown ether signals is proposed based on the analysis of 2D ^{1}HNMR GCOSY and ROESY spectra of the ligands. Note the close matching between the chemical shifting of the signals of the crown ether substituents of ligand **2b** and **R2**.

2.7 Titration of ligand 1a with Ca^{2+}

Spectra recorded for 2 mM solutions of the ligands in DMSO-d_6 - 5% pyridine-d_5 at 298 K. Bottom spectra: free ligand (2 mM), subsequent spectra recorded after the addition of 1 to 50 equivalents of $CaCl_2$. Note the slight broadening and shifting of the signals at high calcium concentration but generally minor effect of the salts at low concentration. The starred signals correspond to protons belonging to the pyridine.

Aromatic region

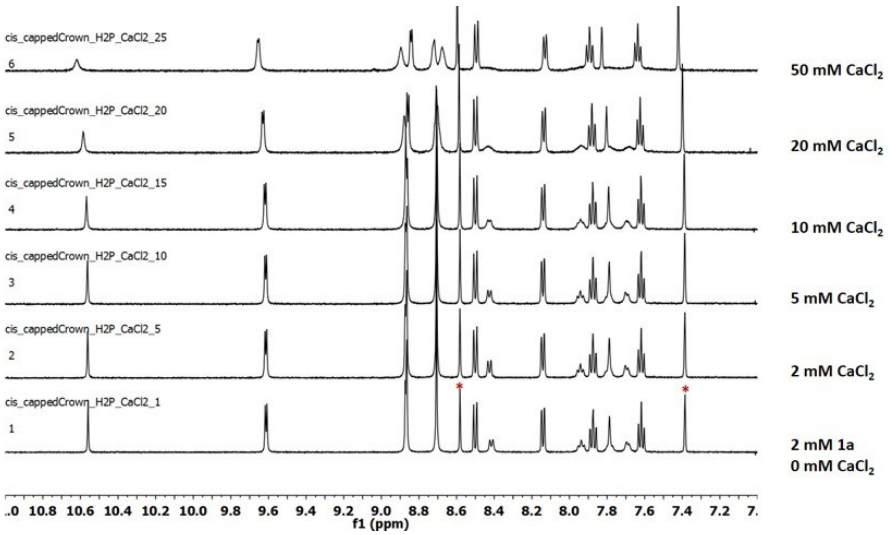

Figure S20. Evolution of the aromatic signals of the ^{1}H NMR spectra of **1a** upon addition of Ca^{2+} .

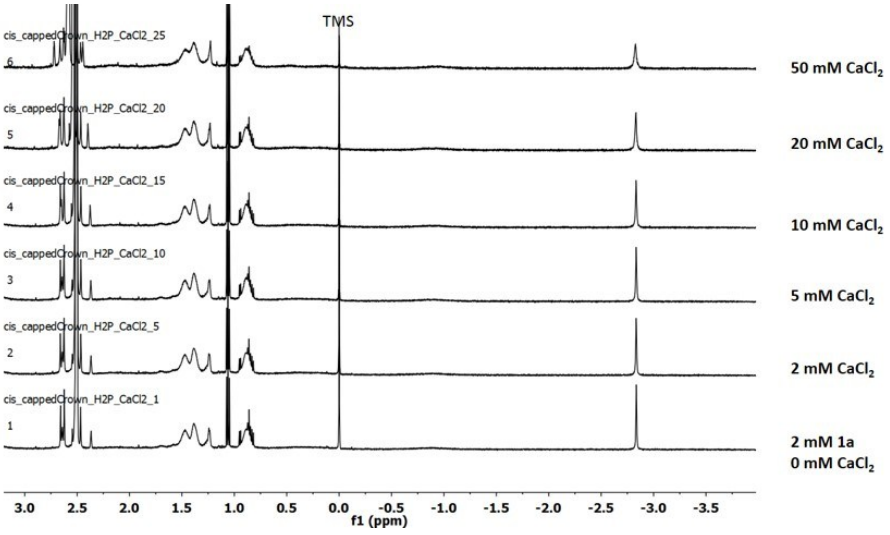

Figure S21. Evolution of the aliphatic signals of the ^{1}H NMR spectra of **1a** upon addition of Ca^{2+}.

2.8 Titration of ligand 2a with Ca^{2+}

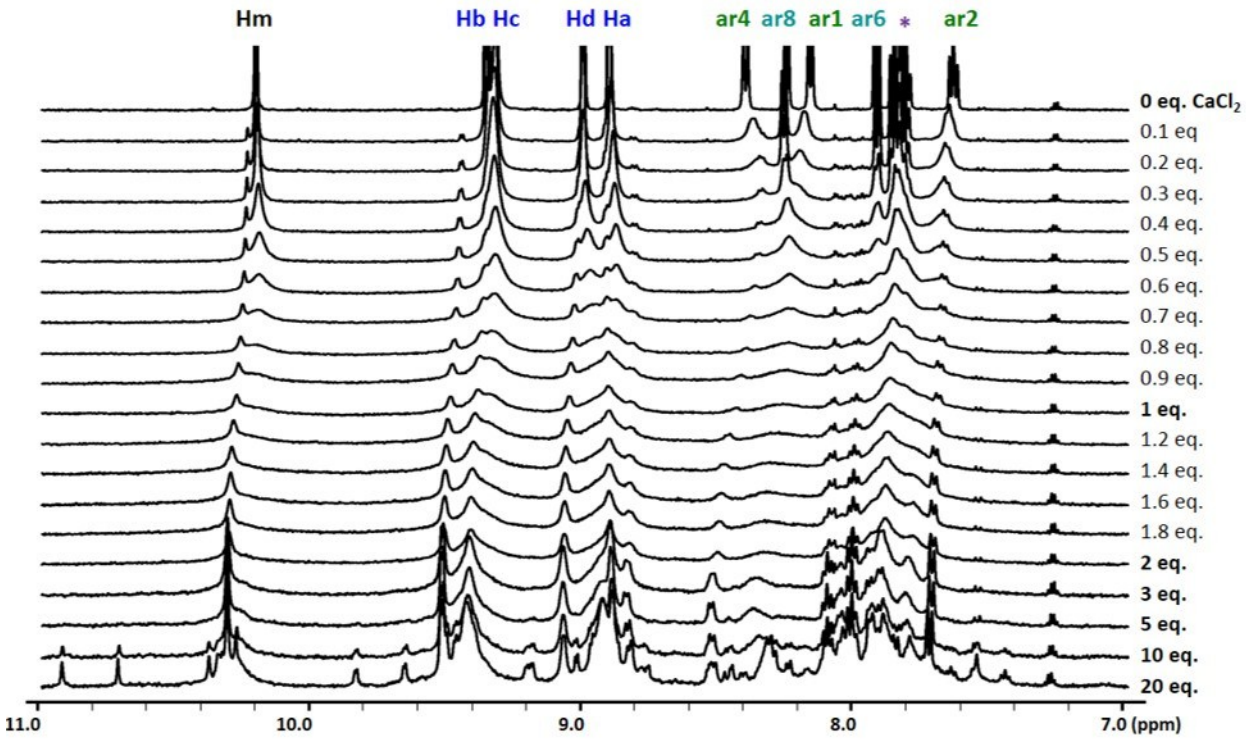

Figure S22. Effect of the addition of Ca^{2+} on the ^{1}H NMR spectra of **2a**. Spectra recorded for 2 mM solutions of the ligand in MeOD - 5% diisopropylamine (DIPEA) at 298 K. Top spectra: free ligand (2 mM), subsequent spectra recorded after the addition of 0.1 to 20 equivalents of $CaCl_2$. Note the gradual broadening and shifting of the signals upon addition of calcium. The aliphatic area is not shown for simplicity. The attribution of the signals was done with the help of GCOSY and ROESY correlations obtained for the free ligand. The starred massif of peaks correspond to the overlay of ar3, ar5 and ar7 signals (see above for numbering of the signals).

2.9 Titration of ligand 2b with Ca^{2+}

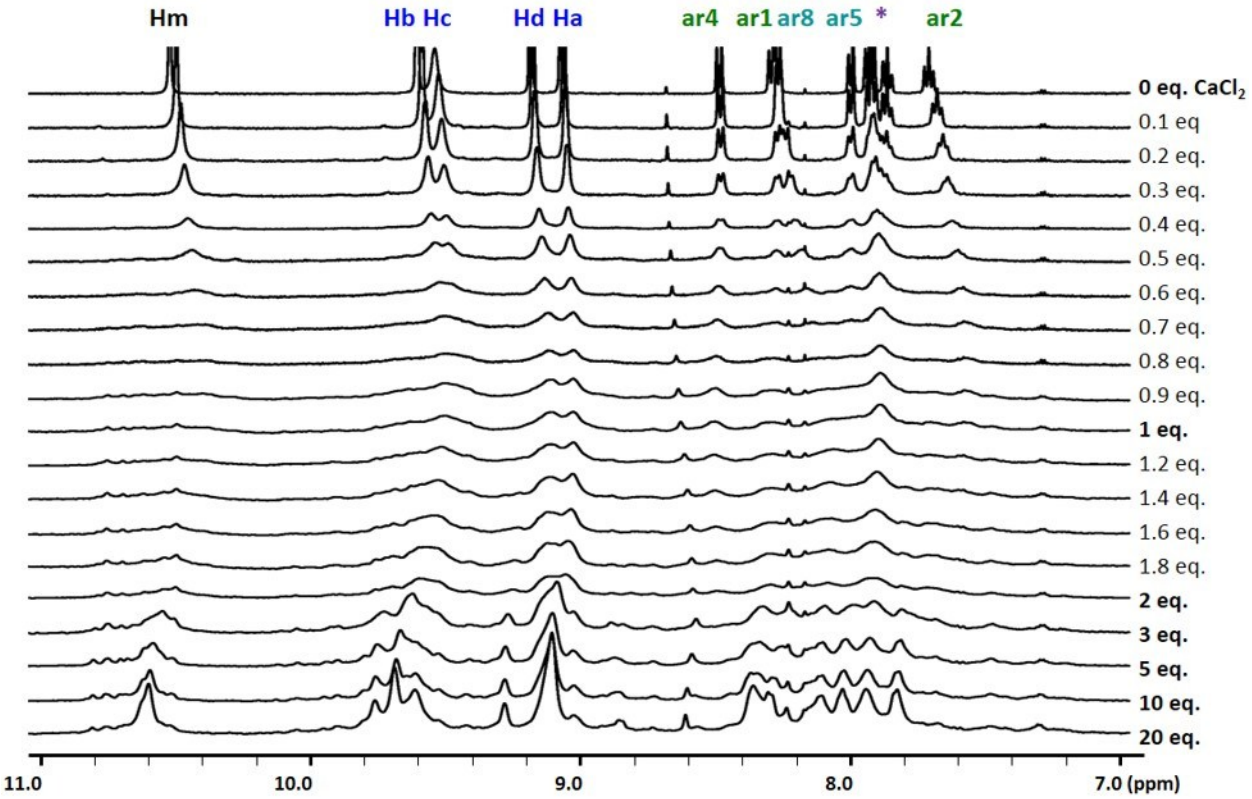

Figure S23. Effect of the addition of Ca^{2+} on the ^{1}H NMR spectra of **2b**. Spectra recorded for 2 mM solutions of the ligand in MeOD - 5% diisopropylamine (DIPEA) at 298 K. Top spectra: free ligand (2 mM), subsequent spectra recorded after the addition of 0.1 to 20 equivalents of $CaCl_2$. Note the rapid broadening of the signals upon addition of calcium and refining of the spectra at high calcium concentration. The aliphatic area is not shown for simplicity. The attribution of the signals was done with the help of GCOSY and ROESY correlations obtained for the free ligand. The starred massif of peaks correspond to the overlay of ar3, ar6 and ar7 signals (see above for numbering of the signals).

2.10 ^{1}H COSY spectrum of 2a in the presence of excess Ca^{2+}

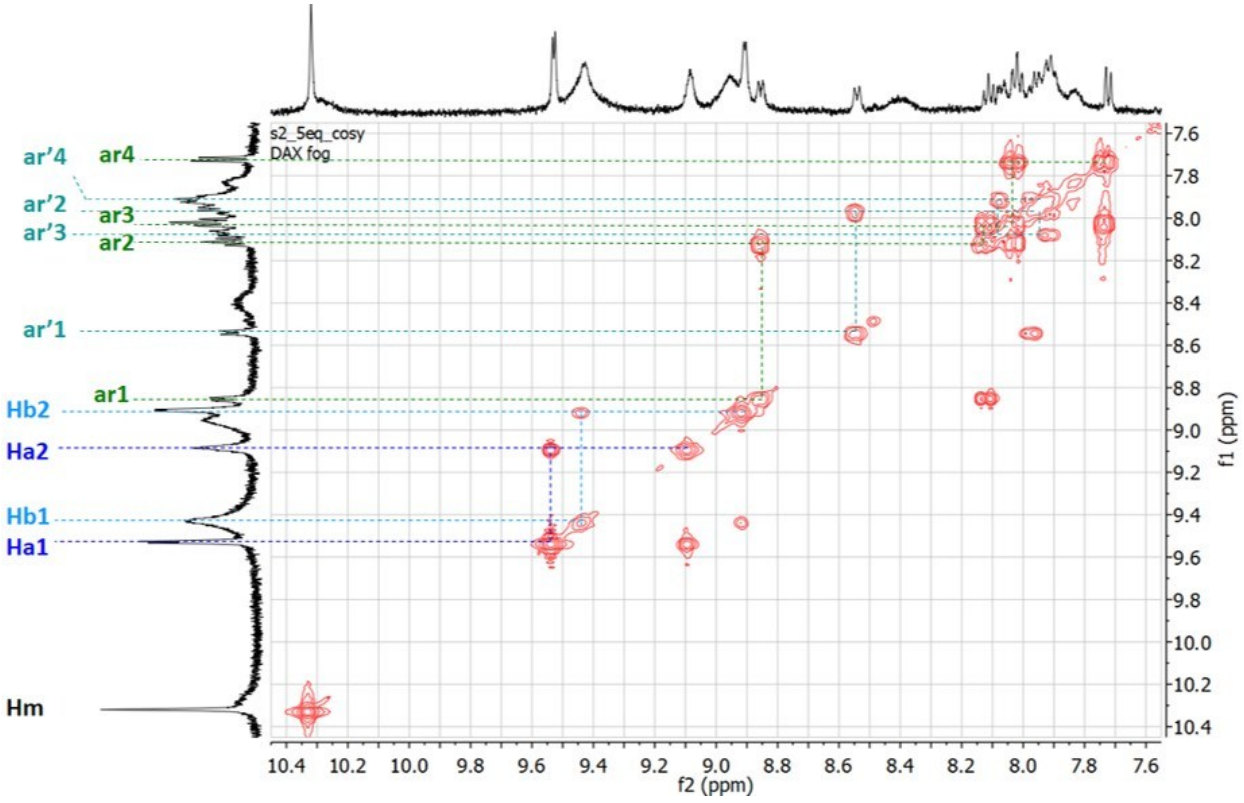

Figure S24. GCOSY correlation spectrum of **2a** in the presence of 5 equivalents of Ca^{2+}Selected region of the GCOSY spectra of a solution of ligand **2a** (2 mM) in MeOD–5% DIPEA, in the presence of 5 equivalents of $CaCl_2$ (A). The clear J-J coupling pattern observed points towards the presence of a well-defined species in solution. Protons belonging to the same spin systems are indicated by the same color. Consecutives protons of each spin system are indicated by following indices.

2.11 ^{1}H NMR spectra of [2a⊂Ca^{2+}] complexes: effect of the concentration

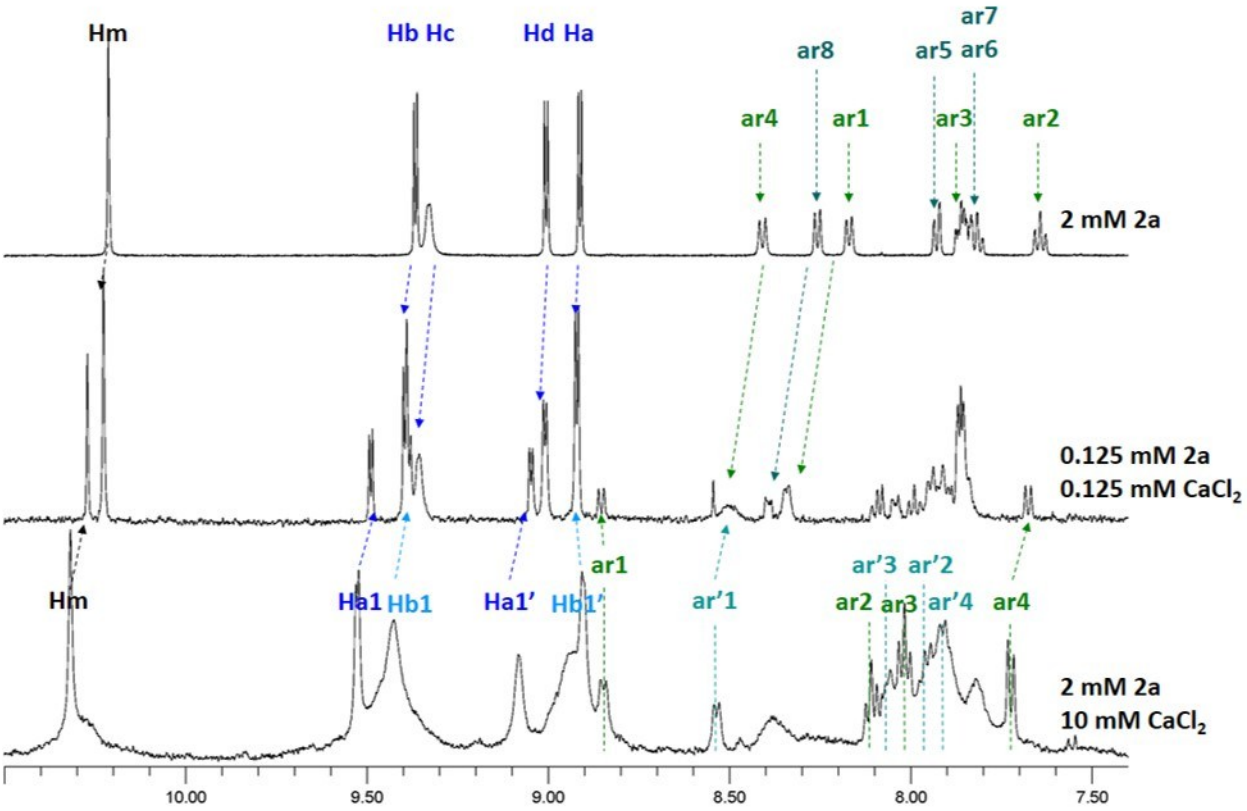

Figure S25. Selected region of the 1H NMR spectra of a 2 mM solution of **2a** in MeOD-5% DIPEA in absence (top) or presence of 5 equivalents of $CaCl_2$ (bottom). The middle spectrum was obtained from dilute solution of **2a** (0.125 mM) in MeOD-5% DIPEA, in the presence of 1 equivalent of $CaCl_2$. Note the sharpness of the signals at lower concentration suggesting no or limited oligomerization of the ligand in these conditions. The presence of two well-defined *meso* signals and, corresponding sets of beta and aromatic protons, suggests the presence of two major species in slow equilibrium in these conditions. The shifting of all signals as compared to the free ligand (see arrow) suggests the presence complexed [**2a⊂Ca**] species only in these conditions. The two sets of signals are thus tentatively attributed to two distinct modes of calcium binding by the ligand. Using the integration of the *meso* signals, the ratio between the two forms of complexed [**2a⊂Ca**] species is estimated to be [**2a⊂Ca**]/[**2a⊂Ca**]' ~ 2/3. Further studies are required to fully characterize the two possible mode of calcium complexation within the ligands.

3 Fluorescence anisotropy decay analysis

3.1 General:

Time resolved fluorescence anisotropy measurements were performed with a time-correlated single photon counting (TC-SPC) system. The excitation source was a fiber supercontinuum laser based on a passive mode-locked fiber laser and a high-nonlinearity photonic crystal fiber supercontinuum generator (Fianium SC450). The laser provides 6 ps pulses at a repetition rate variable between 0.1 and 40 MHz. The laser output was sent through an Acousto-Optical Tunable Filter (Fianium AOTF) to obtain excitation pulses at the desired wavelength. Fluorescence emission was collected at 90° and detected using a double-grating monochromator (Jobin- Yvon, Gemini-180) and a microchannel plate photomultiplier tube (Hamamatsu R3809U-50). The polarization of the emission was horizontal or vertical relative to that of the excitation. Data acquisition was done using a single photon counting card (Becker-Hickl, SPC-830). The IRF had a FWHM of ~50 ps, measured from the scattering of sample at the excitation wavelength. The data was globally fitted as a sum of exponential decays including IRF deconvolution using locally written software (ASUFIT) developed in a MATLAB environment (Mathworks Inc.).

Time resolved fluorescence anisotropy were calculated as described elsewere [6]. Setting a polarizer to obtain vertical polarization of the incident light, the fluorescence time resolved was recorded with a vertical or horizontal polarizer in front of the detector. Same procedure was realized with horizontal polarization of incident light. The anisotropy decay was calculated from the following equation [4b]:

$$r(t) = \frac{I_{II}(t) - G \times I_{\perp}(t)}{I_{II}(t) + 2G \times I_{\perp}(t)} \qquad \textbf{Equation S1}$$

where $I_{\parallel}$ (or $I_{\perp}$) is the fluorescence decay when the excitation light is vertically polarized and only the vertical (or horizontal) polarization component of the emission light is detected, respectively. The G factor is defined by $I_{\parallel}(t)/I_{\perp}(t)$ which is equal to the ration of the sensitivities of the detection system for vertical and horizontal polarizations. It was determined for each set of measurements and was 1.04 ± 0.01 in our experimental setup.

The obtained anisotropy decay were then fitted using build-in Origin 8.5 fitting equation for single or multi-exponential decays using the following equation:

$$r(t) = \sum_{i=1}^{i} r_i(0) \times \exp\left(\frac{-t_i}{\theta_i}\right) \qquad \textbf{Equation S2}$$

Rotational correlation times θ and the anisotropy at time zero r_o were determined. The time of Brownian rotation of a molecule, θ, gives information on the hydrodynamic radius (R) by the Stokes–Einstein–Debye relation [7]:

$\theta^{-1} = 6kT/(8\pi\eta R^3)$ **Equation S3**

where *k* is the Boltzmann constant, T the absolute temperature, and η the viscosity. On the other hand, r_o is related to the relative orientation of the excited- and fundamental state dipole moments of the particles.

3.2 Fluorescence anisotropy decay of the free ligand 2a

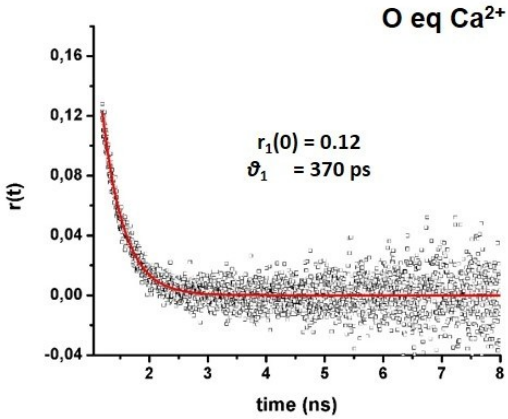

Figure S26. Fluorescence anisotropy decay of a 2 mM solution of ligand **2a** in MeOH-5% DIPEA, observed at 298 K, in the absence of Ca^{2+}. The sample was excited at 590 nm and the emission was collected at 680 nm. Experimental data (open squares) and fitting curves (red lines). The parameters obtained from the fitting procedure are reported on the graph. A single-exponential decay was best describing the evolution of the fluorescence anisotropy decay.

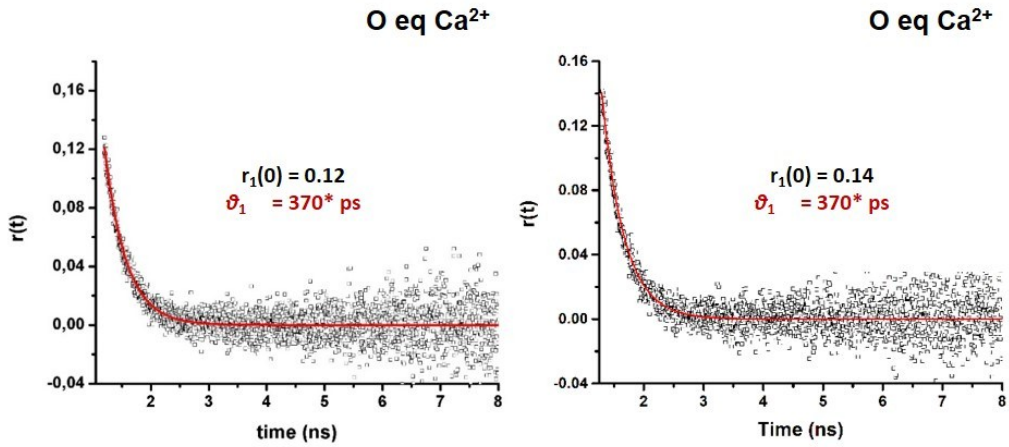

* Fixed value.

Figure S27. Fluorescence anisotropy decays of 2 mM and 0.1 mM solutions of ligand **2a** in MeOH-5% DIPEA, observed at 298 K in the absence of $CaCl_2$ (left and right panel, respectively). The samples were excited at 590 nm and the emission was collected at 680 nm. The fits were obtained using a fixed life-time value of 370 ps. Experimental data (open squares) and fitting curves (red lines). The parameters obtained from the fitting procedure are reported on the graphs. A single-exponential decay was best describing the evolution of the fluorescence anisotropy decay in each case.

3.3 Fluorescence anisotropy decay of the free ligand 2b

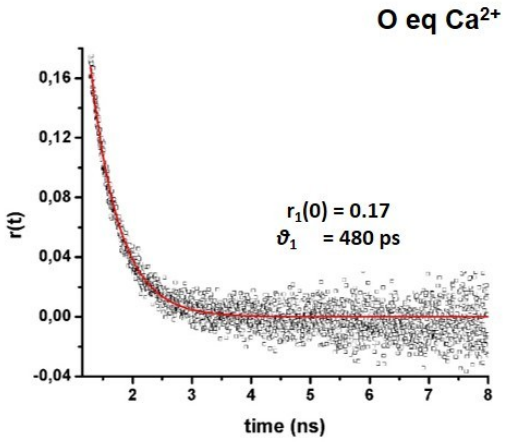

Figure S28. Fluorescence anisotropy decays of a 2 mM solution of ligand **2b** in MeOH-5% DIPEA, observed at 298 K, in the absence of $CaCl_2$. The sample was excited at 590 nm and the emission was collected at 680 nm. Experimental data (open squares) and fitting curves (red lines). The parameters obtained from the fitting procedure are reported on the graph. A single-exponential decay was best describing the evolution of the fluorescence anisotropy decay.

3.4 Fluorescence anisotropy decays of ligand 2a in the presence of Ca^{2+}

0 to 0.1 equivalents

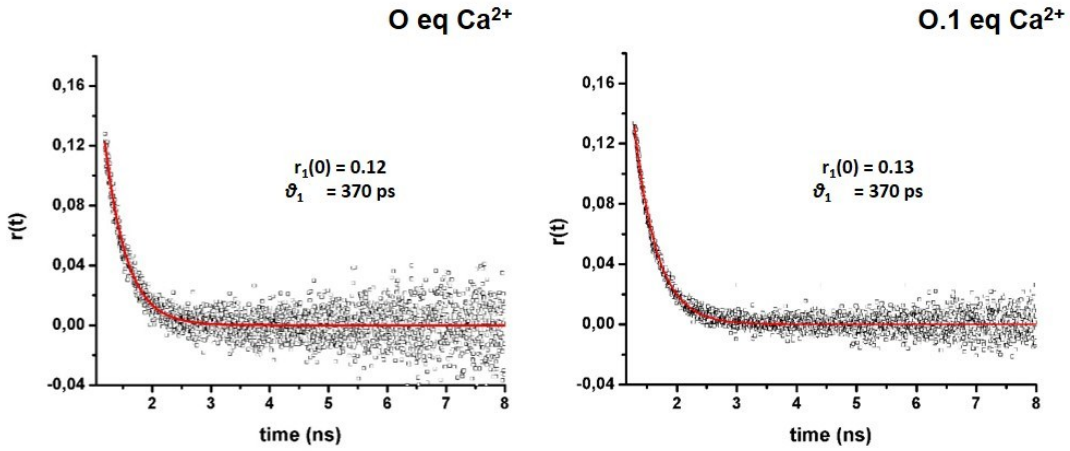

Figure S29. Fluorescence anisotropy decays of a 2 mM solution of ligand **2a** in MeOH-5% DIPEA, observed at 298 K, in the presence of 0 and 0.1 equivalents of $CaCl_2$ (left and right panel, respectively). The sample was excited at 590 nm and the emission was collected at 680 nm. Experimental data (open squares) and fitting curves (red lines). The parameters obtained from the fitting procedure are reported on the graphs. A single-exponential decay was the best fitting describing the evolution of the fluorescence anisotropy decay in each case.

0.2 to 0.4 equivalents

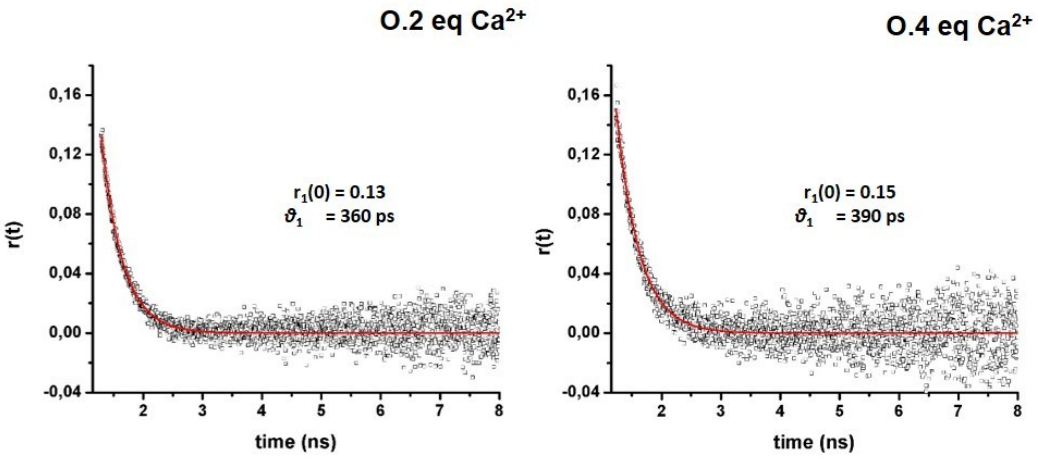

Figure S30. Fluorescence anisotropy decays of a 2 mM solution of ligand **2a** in MeOH-5% DIPEA, observed at 298 K, in presence of 0.2 and 0.4 equivalents of $CaCl_2$ (left and right panel, respectively). Experimental data (open squares) and fitting curves (red lines). The sample was excited at 590 nm and the emission was collected at 680 nm. The parameters obtained from the fitting procedure are reported on the graphs. A single-exponential decay was the best fitting describing the evolution of the fluorescence anisotropy decay in each case.

1 to 5 equivalents

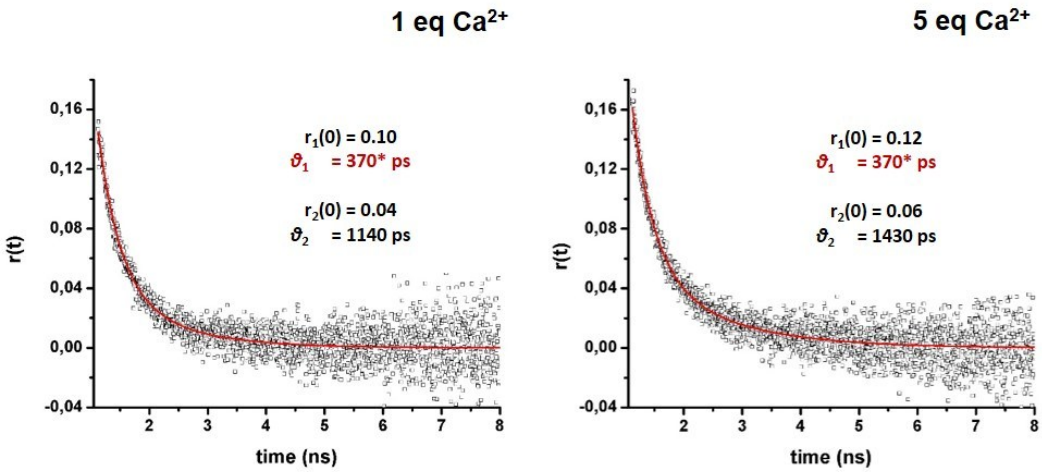

* Fixed value.

Figure S31. Fluorescence anisotropy decays of a 2 mM solution of ligand **2a** in MeOH-5% DIPEA, observed at 298 K, in presence of 1 and 5 equivalents of $CaCl_2$ (left and right panel, respectively). The sample was excited at 590 nm and the emission was collected at 680 nm. Experimental data (open squares) and fitting curves (red lines). The parameters obtained from the fitting procedure are reported on the graphs. A bi-exponential decay was the best fitting describing the evolution of the fluorescence anisotropy decay in each case. The shortest component was fixed to 370 ps to account for the presence of monomeric porphyrin species in solution (see main text).

0 to 1 equivalents in diluted conditions

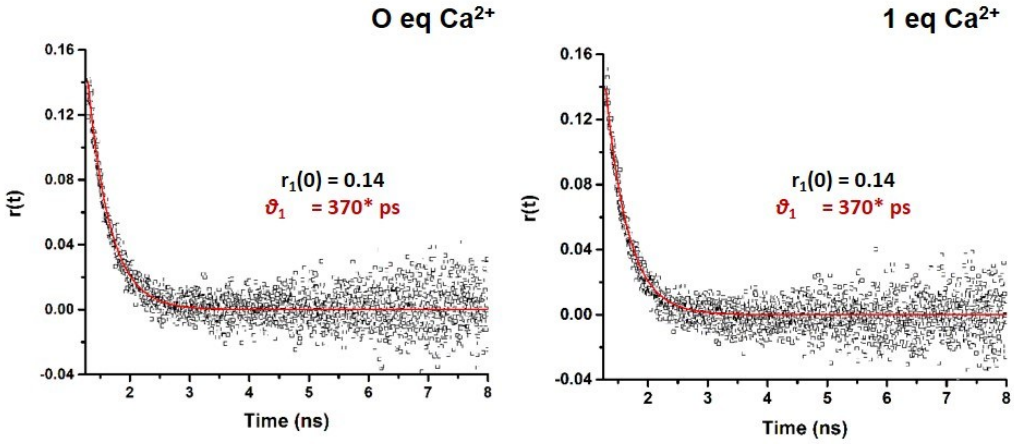

* Fixed value.

Figure S32. Fluorescence anisotropy decays of a 0.1 mM solution of ligand **2a** in MeOH-5% DIPEA, observed at 298 K, in presence of 0 and 1 equivalents of $CaCl_2$ (left and right panels respectively). The sample was excited at 590 nm and the emission was collected at 680 nm. Experimental data (open squares) and fitting curves (red lines). The parameters obtained from the fitting procedure are reported on the graphs. A single-exponential decay was the best fitting describing the evolution of the fluorescence anisotropy decay in each case. A life-time of 370 ps described accurately each decay (see main text, footnote §).

3.5 Fluorescence anisotropy decays of ligand 2b in the presence of Ca^{2+}

1 to 20 equivalents

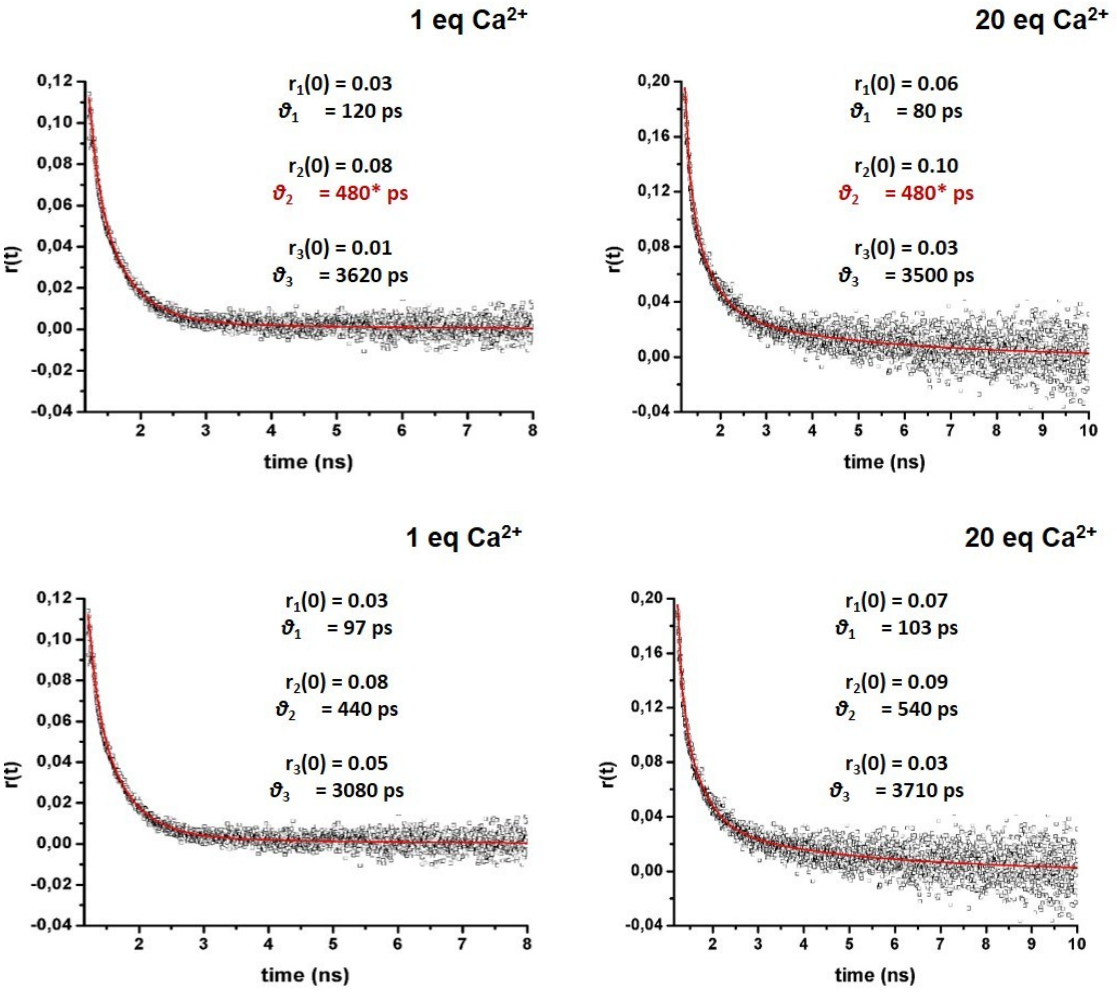

* Fixed value.

Figure S33. Fluorescence anisotropy decays of a 2m M solution of ligand **2b** in MeOH-5% DIPEA, observed at 298 K, in presence of 1 and 20 equivalents of $CaCl_2$ (left and right panel, respectively). The sample was excited at 590 nm and the emission was collected at 680 nm. Experimental data (open squares) and fitting curves (red lines). The parameters obtained from the fitting procedure are reported on the graphs. A tri-exponential decay was best describing the evolution of the fluorescence anisotropy decay in each case. Top panels: one component was fixed to 480 ps to account for the presence of monomeric porphyrin species in solution (see main text). Bottom panels: fitting obtained while letting all the parameters freely floating. Note the good agreement between the values of the components observed by constraining one component to 480 ps and by letting all the components floating during the fitting process.

4 Uv-visible spectroscopy

4.1 General

UV–Visible spectroscopy was performed using a Shimadzu UV-2550 UV–Visible spectrophotometer, using quartz cuvettes with an optical path of 1 cm. The solvents used were of spectroscopic grade and used as received. During the titrations the concentration of the porphyrin ligands was kept constant by the addition of concentrated $CaCl_2$ aliquots containing the ligand in the appropriate concentration. During the titration, the cell was kept in its original position, without removing it from the cell holder. The concentrated calcium aliquots were added with the use of glass micro-syringe and the solution mechanically stirred to permit complete equilibration of the systems before measurement were taken. All the titrations were conducted in a mixture of methanol containing 5 % (v/v) of diisopropylethylamine, at 298 K. The spectral resolution of the spectrophotometer was set-up to 0.1 nm; standard deviation on the wavelength values is ± 0.1nm (manufacturer specifications).

The association constants were estimated using a global fitting procedure using the build-in equation solving module of Origin 8.5.

In all cases we suppose the establishment of a 1:1 equilibrium in solution during the titration (see main text):

$[L] + [Ca] \leftrightarrow [L \subset Ca]$ **Equation S4**

From this assumption and we can derive the classical expression to fit the evolution of the spectra at any given wavelength:

$$Abs([Ca]_T) = \frac{A_i - A_f}{2 \times [L]_0} \times \left([L]_0 - [Ca]_T - \frac{1}{Ka}\right) + \sqrt{\left([Ca]_T - [L]_0 + \frac{1}{Ka}\right)^2 + 4 \times \frac{[L]_0}{Ka}} + A_f$$ **Equation S5**

where $Abs([Ca]_T)$ is the experimentally measured absorbance after adding the desired calcium concentration, $[Ca]_T$ the total concentration of calcium added, A_i the initial absorbance of the porphyrin solution at the wavelength considered, A_f the final absorbance of the porphyrin solution at the wavelength considered, $[L]_0$ the total concentration of the porphyrin ligand, and Ka the association constant of the equilibrium considered, with:

$$Ka = \frac{[L \subset Ca]}{[L][Ca]}$$ **Equation S6**

Where $[L \subset Ca]$ represents the concentration of the complexed species in solution, [Ca], the concentration of the remaining free calcium in solution and [L] the concentration of the remaining free ligand in solution.

4.2 Titration of ligand 2a with Ca^{2+}

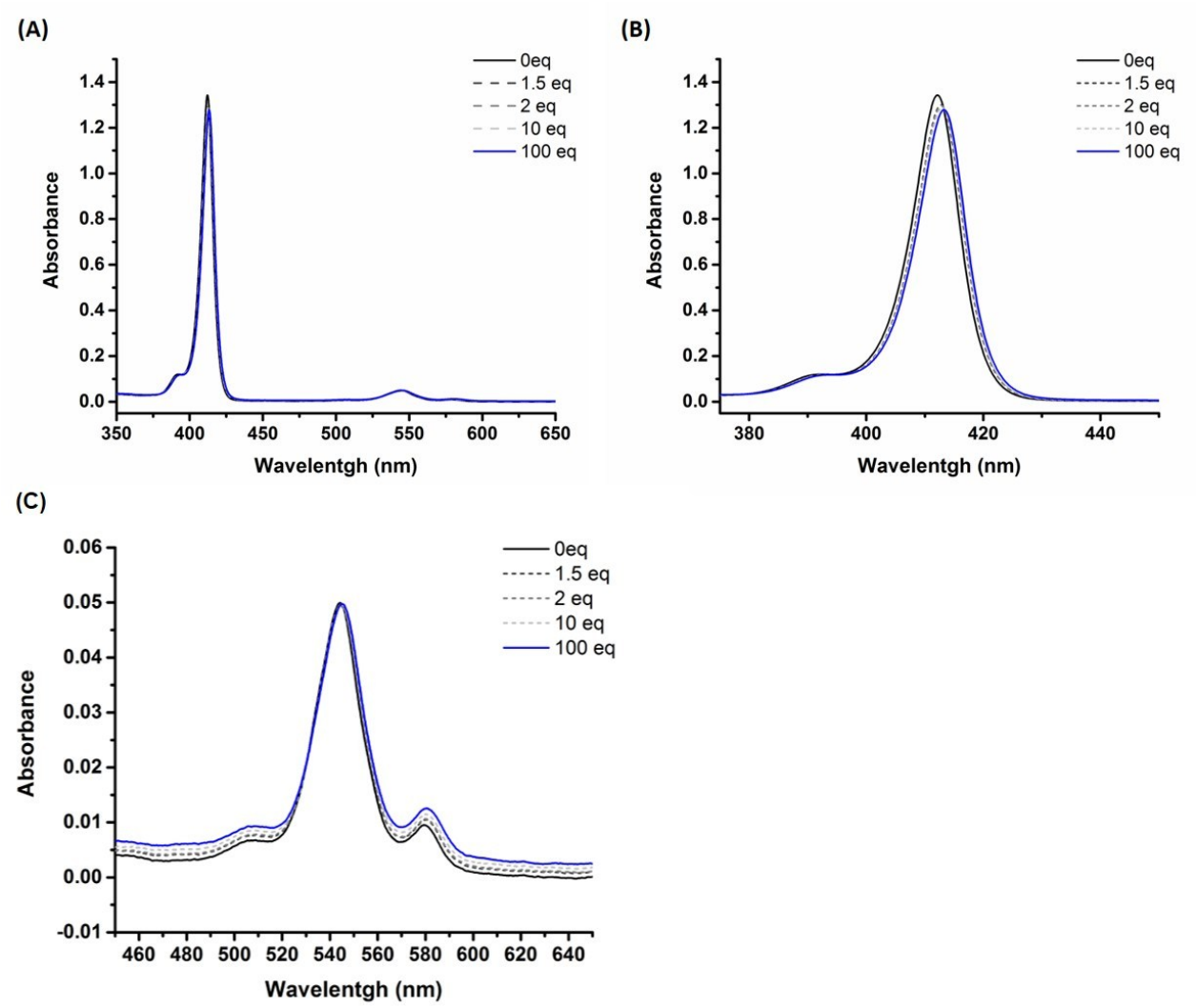

High concentration

Figure S34. Evolution of the UV- Visible absorption spectra of 2a upon addition of $CaCl_2$. Solution of **2a** at 5 µM in MeOH-5% DPEA. Addition of 0 to 100 equivalents of Ca^{2+}. Full range spectra (A), details of the Soret band (B) and of the Q bands evolution (C) upon addition of 0 to 100eq of Ca^{2+}.

Low concentration

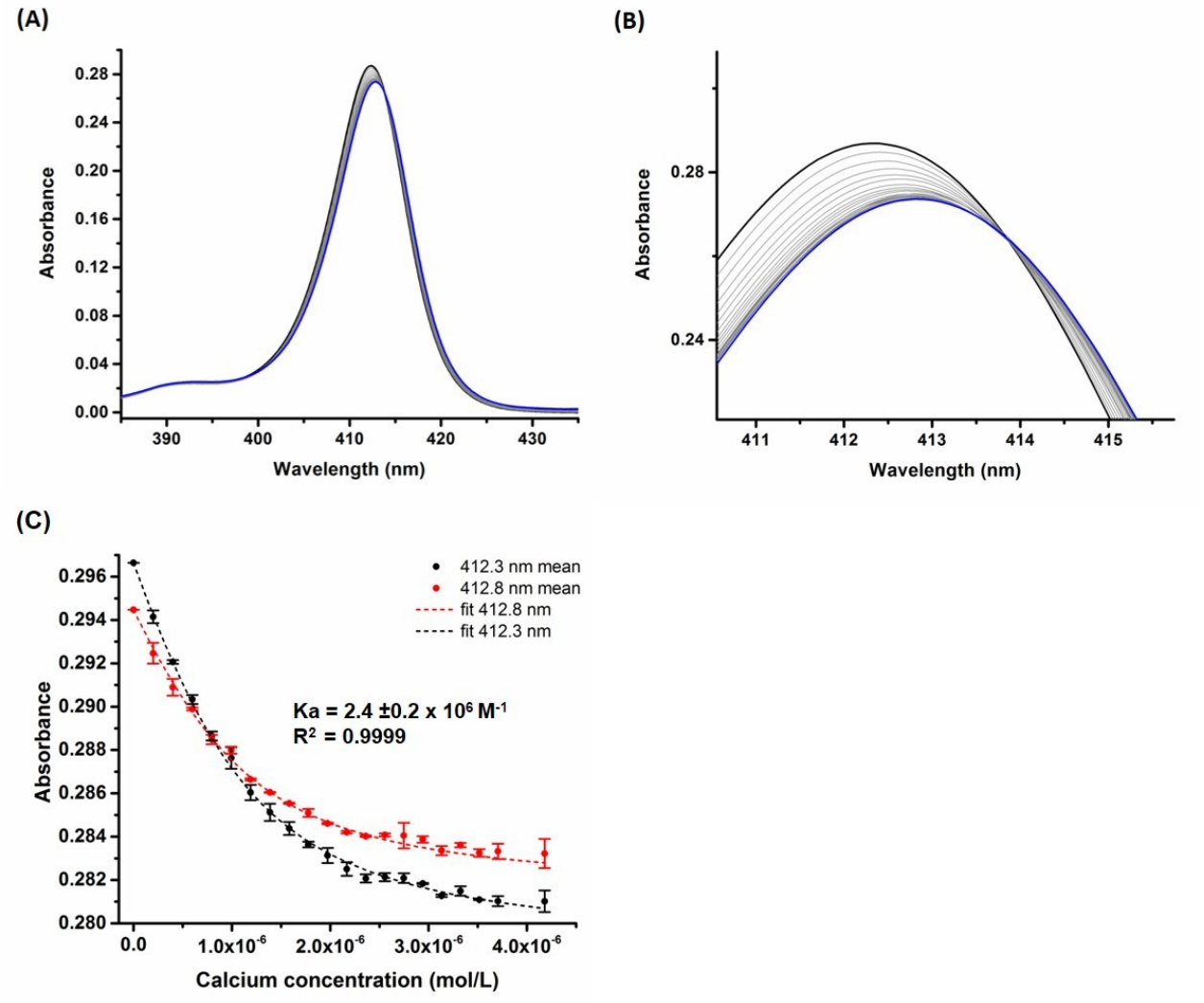

Figure S35. Evolution of the UV- Visible absorption spectrum of ligand **2a** (1 µM) upon the addition of 0 to 4.5 equivalents of $CaCl_2$; between 0 (black line) and 4 equivalents of $CaCl_2$ (blue line), every step correspond to the addition of 0.2 equivalents of $CaCl_2$. General evolution (A), detailed view (B) note the presence of a clear isobestic point. To determine the association constant Ka of the equilibrium, the evolution of the absorption of **2a** (1 µM) upon titration with 0 to 4.5 equivalents of $CaCl_2$ was followed at 412.3 nm (black circles) and 412.8 nm (red circles). The graph (C) shows the mean values of the absorbance obtained from 2 distinct measurements; the respective standard deviation are indicated by the vertical bars. Using Equation S4 and applying a global fitting procedure permitted to estimate Ka.

4.3 Titration of ligand R1 with Ca^{2+}

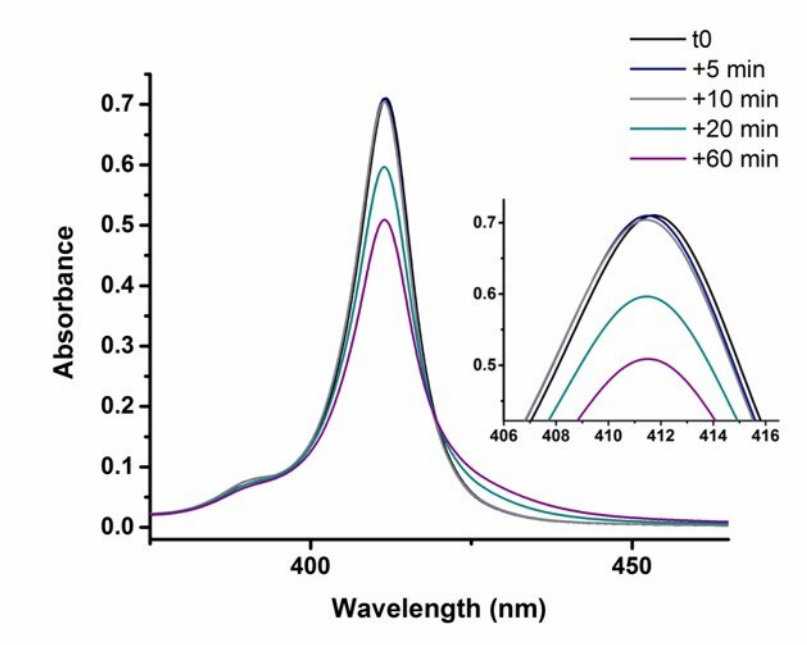

Figure S36. Evolution of the UV- Visible absorption spectrum of **R1** (2.5 µM) over time after the addition of 15 equivalents of Calcium. Spectra taken directly after the addition of calcium (black) then after five (blue), ten (grey), twenty (green) and sixty minutes (purple). Note the gradual decrease and broadening of the absorption spectra over time. The evolution of the spectra over time is most likely due to the calcium-induced aggregation of the ligand.

4.4 Titration of ligand R2 with Ca^{2+}

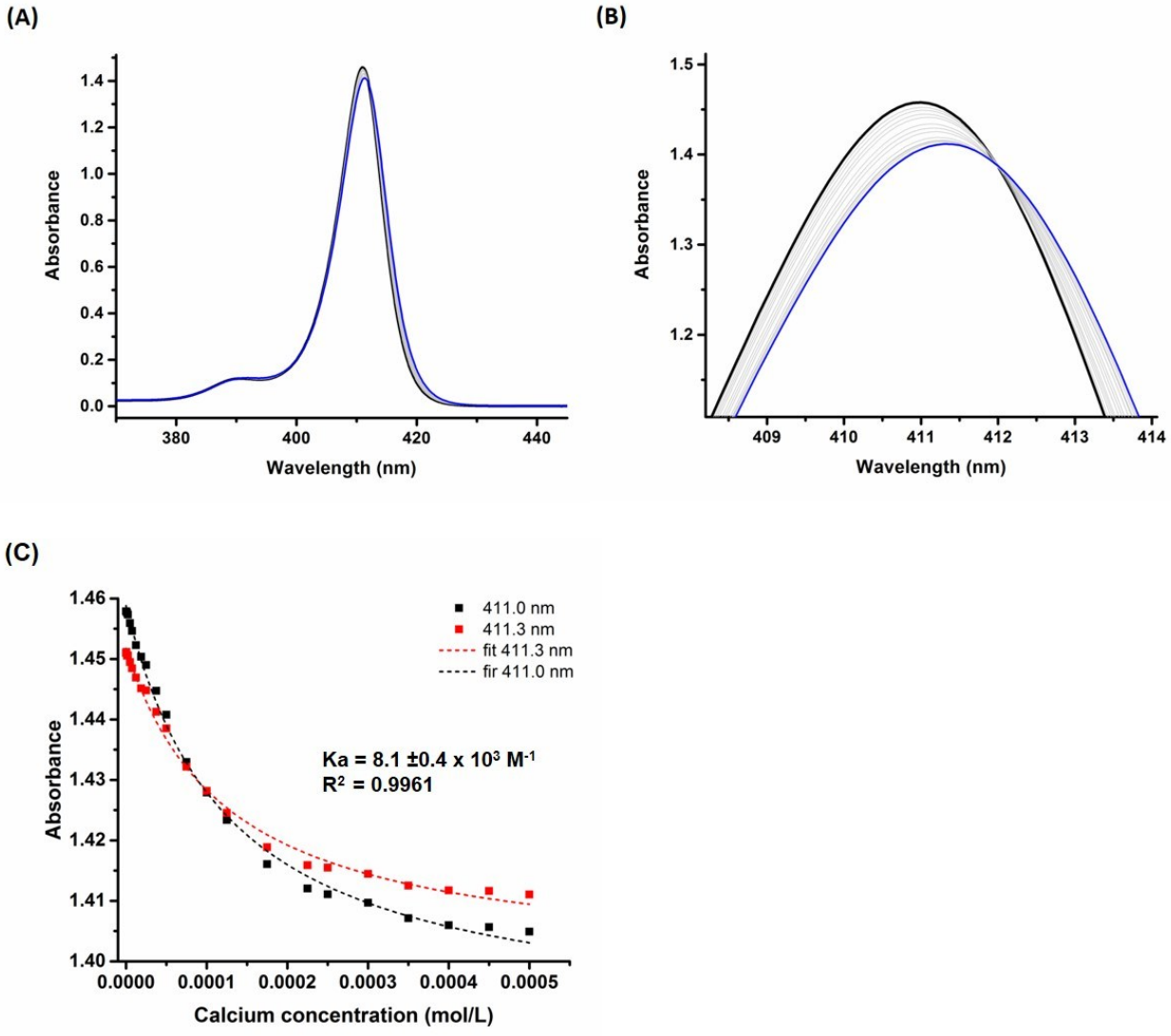

Figure S37. Evolution of the UV-Visible absorption spectra of **R2 (**2.5 µM) upon addition of $CaCl_2$. Addition of 0 (black line) to 180 eq of $CaCl_2$ (blue line). Soret band (A), details of the spectra highlighting the presence of an isobestic point (B). To determine the association constant Ka of the equilibrium, the absorption of **R2** (2.5 µM) upon titration with 0 to 180 equivalents of $CaCl_2$ was followed at 411.0 nm (black squares) and 411.3 nm (red squares) (C). The association constant was estimated using a global fitting procedure and Equation S4. We suppose the establishment of a 1:1 equilibrium in solution during the titration (see main text).

4.5 Titration of ligand 8b with Ca^{2+}

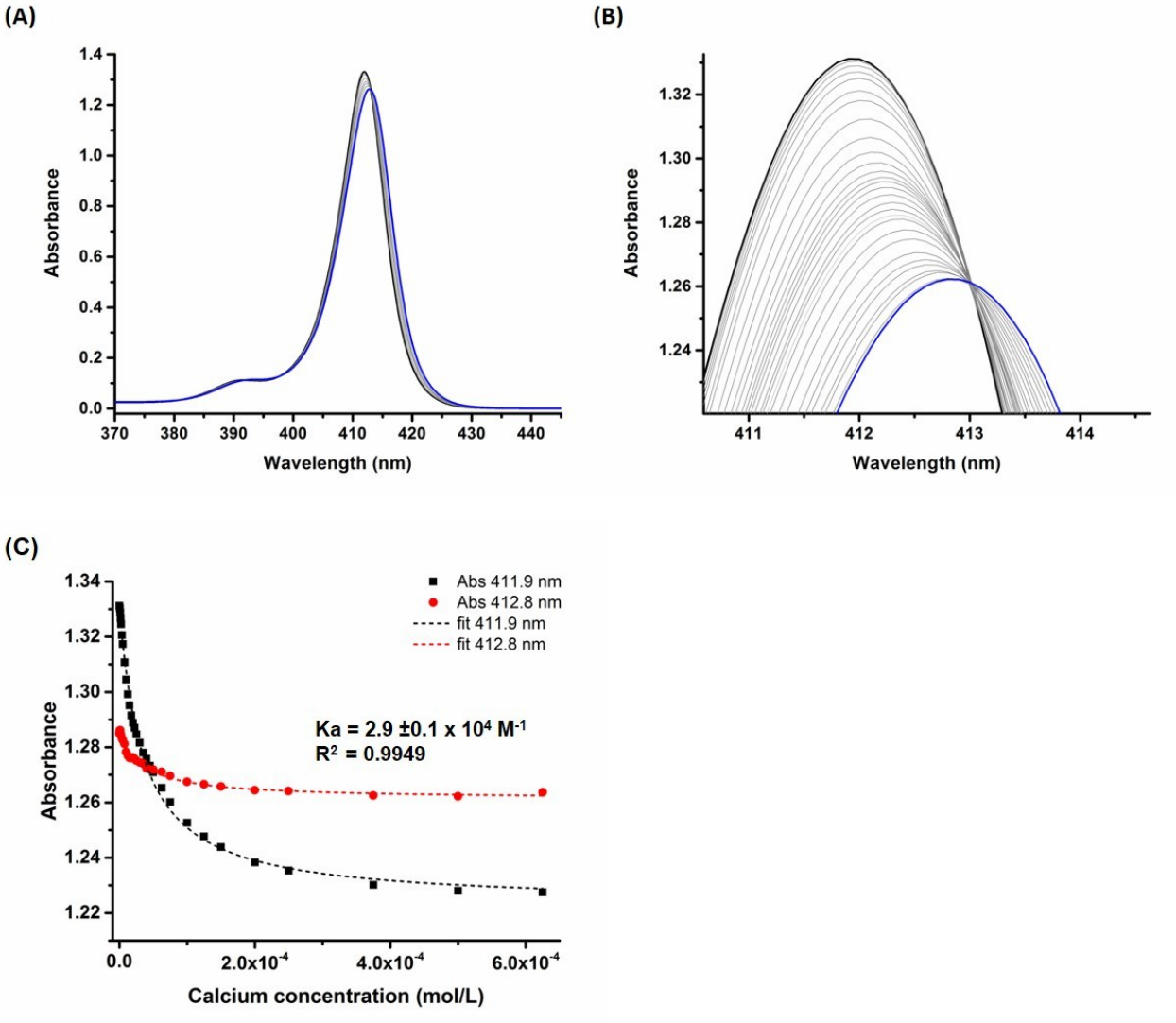

Figure S38. Evolution of the UV-Visible absorption spectra of **8a (**2.5 µM) upon addition of $CaCl_2$. Addition of 0 (black line) to 250 eq of $CaCl_2$ (blue line). Soret band (A), details of the spectra highlighting the presence of an isobestic point (B). To determine the association constant Ka of the equilibrium, the absorption of **R2** (2.5 µM) upon titration with the addition of 0 to 250 equivalents of $CaCl_2$ followed at 411.9 nm (black squares) and 411.8 nm (red squares). (C). The association constant was estimated using a global fitting procedure and Equation S4. We suppose the establishment of a 1:1 equilibrium in solution during the titration (see main text).

5 ^{1}H NMR spectra

5.1 ^{1}H NMR spectra of 5,15-bis-(2-nitrophenyl)porphyrin mixture in $CDCl_3$

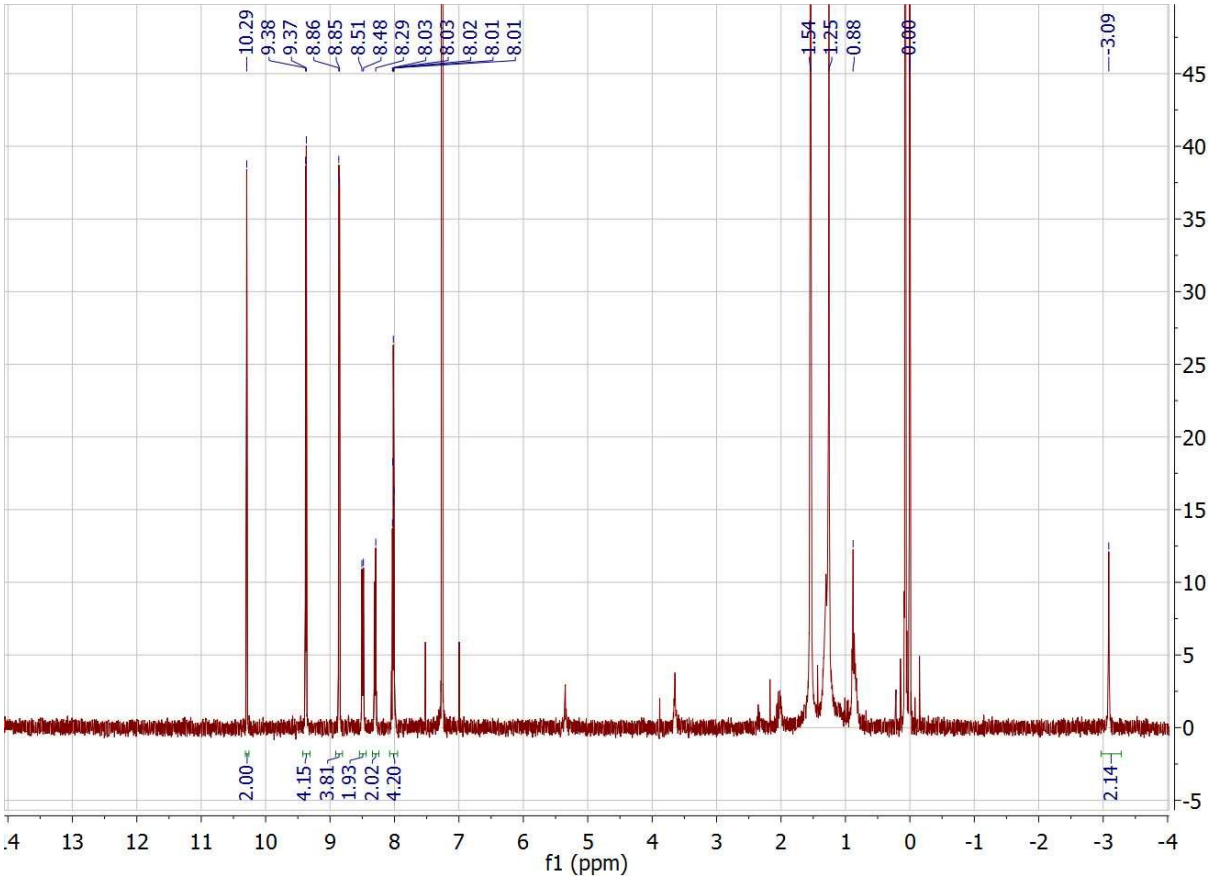

Residual signals: residual $CHCl_3$ (7.26 ppm); residual H_2O (1.54); adventitious aliphatic grease (1.25, 0.88)

5.2 ^{1}H NMR spectra of αβ-5,15-bis-(2-aminophenyl)porphyrin in $CDCl_3$

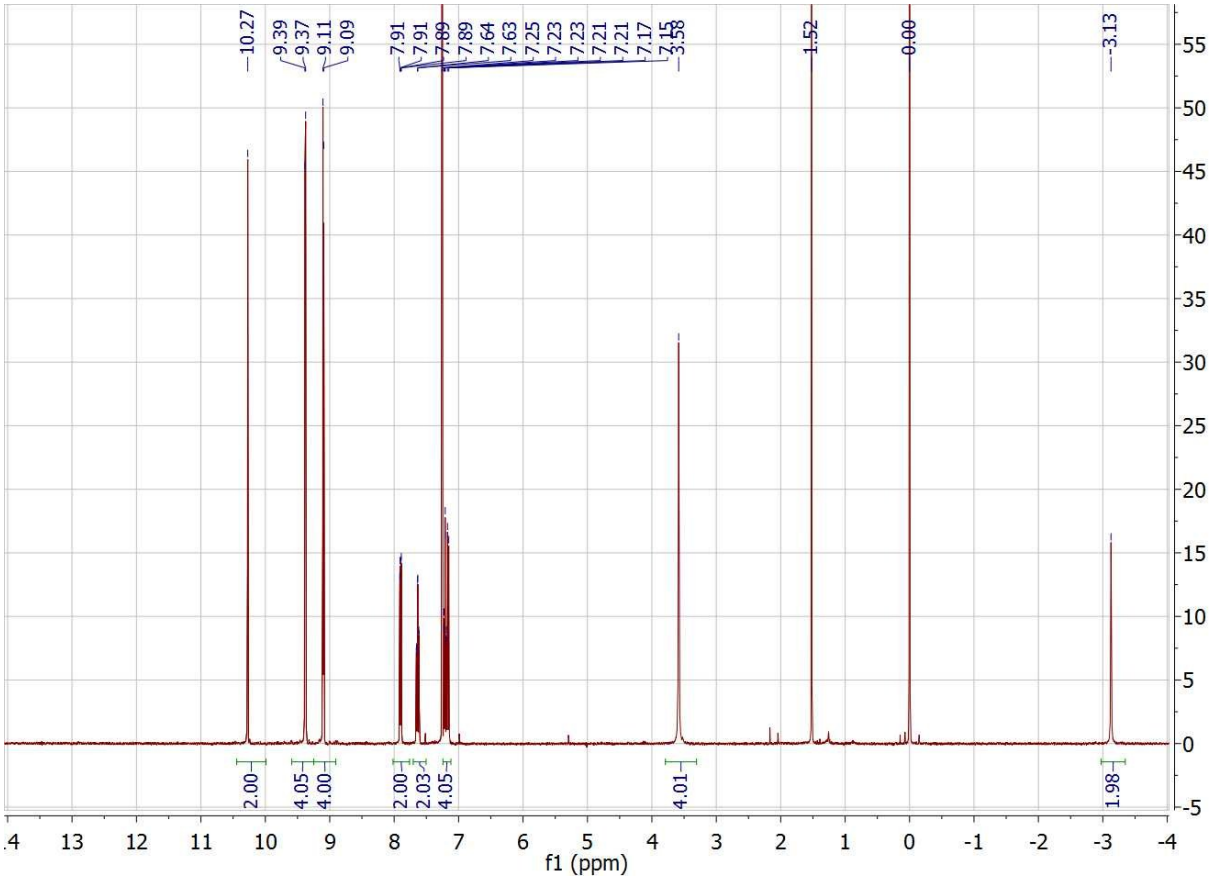

Residual signals: residual $CHCl_3$ (7.26 ppm); residual H_2O (1.52)

5.3 ^{1}H NMR spectra of αα-5,15-bis-(2-aminophenyl)porphyrin in $CDCl_3$

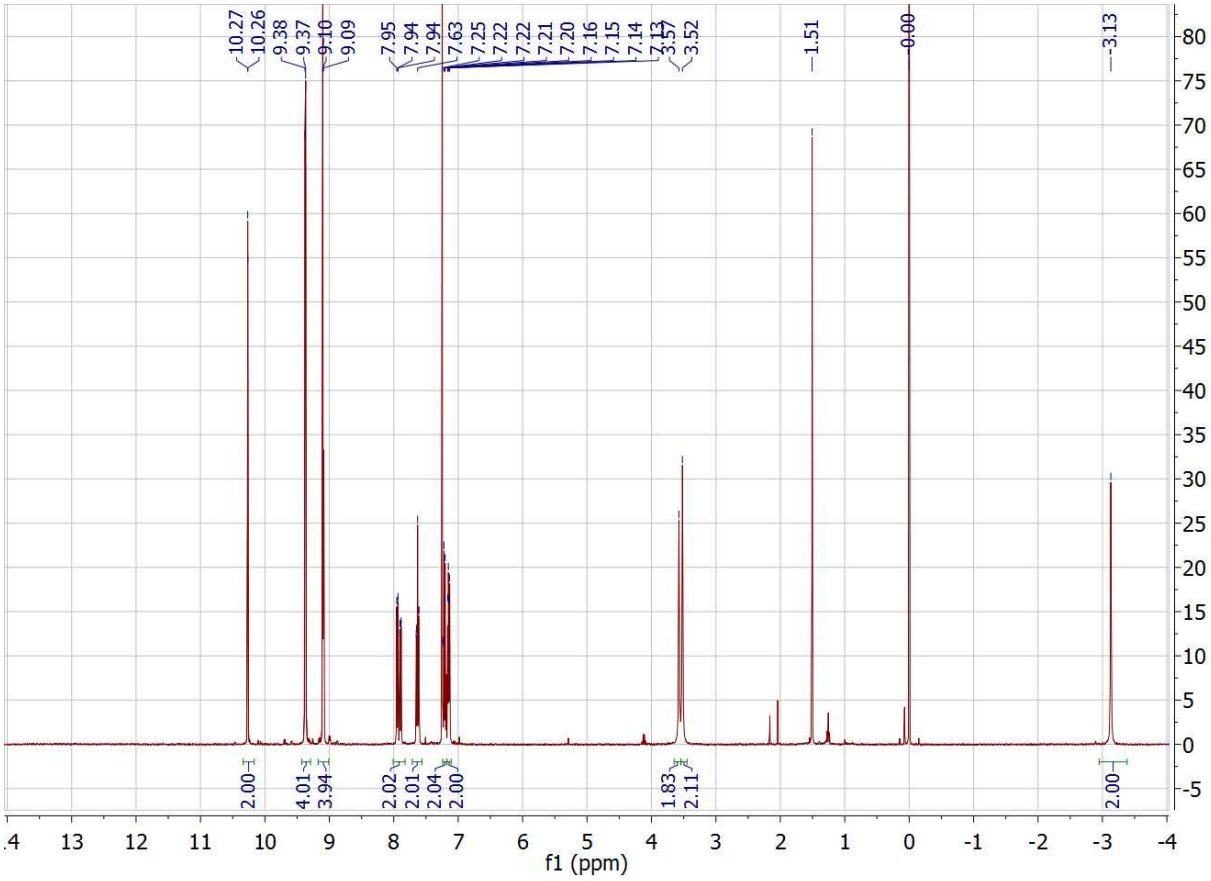

Residual signals: residual $CHCl_3$ (7.26 ppm); residual H_2O (1.51)

5.4 ^{1}H NMR spectra of αα-5,15-bis-(2-(2-chloroacethyl)aminophenyl)porphyrin in $CDCl_3$

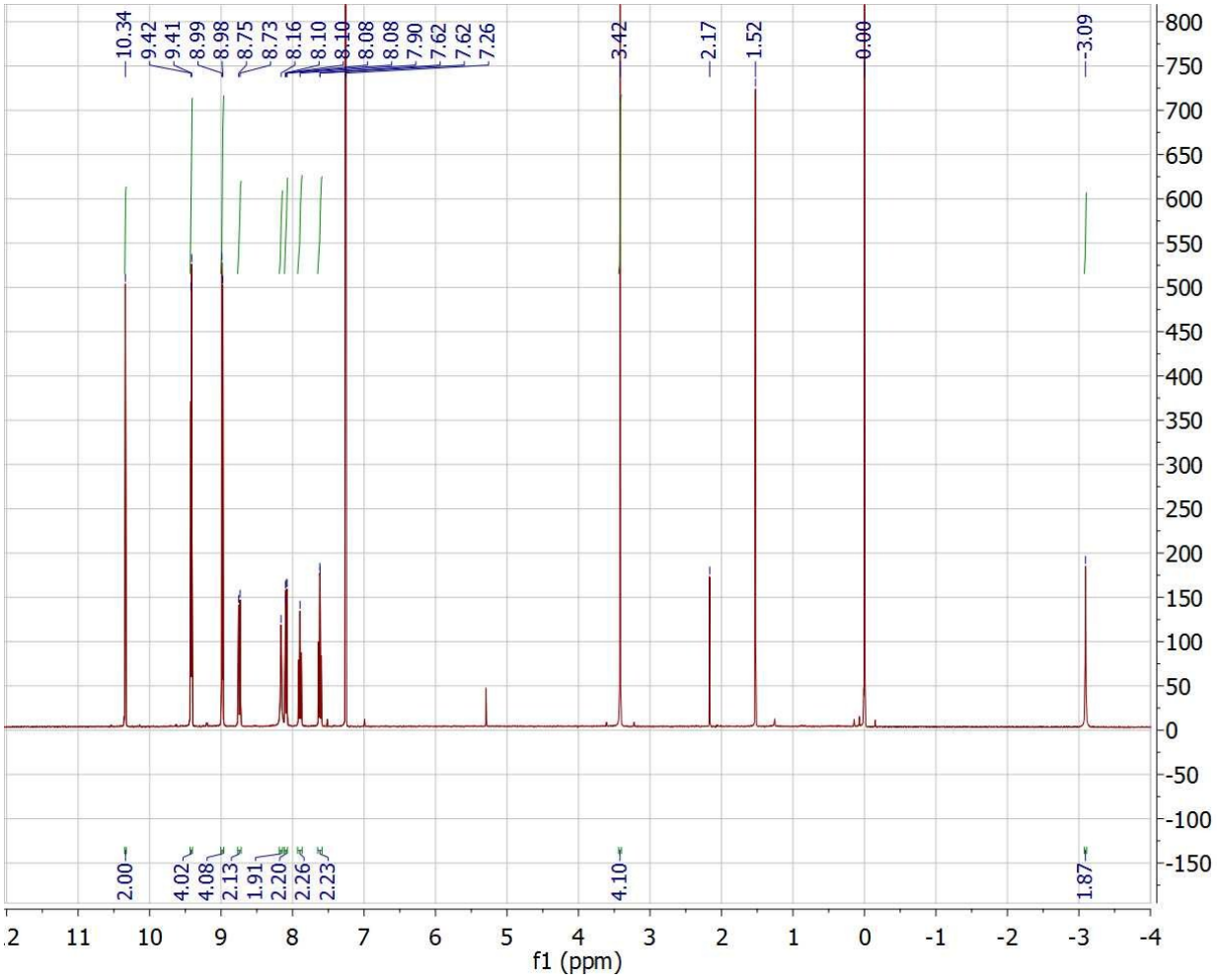

Residual signals: residual $CHCl_3$ (7.26 ppm); residual acetone (2.17 ppm); residual H_2O (1.52)

5.5 ^{1}H NMR spectra of αα-5,15-bis-(2-(2-chloroacethyl)aminophenyl)-10-bromoporphyrin 4 in $CDCl_3$

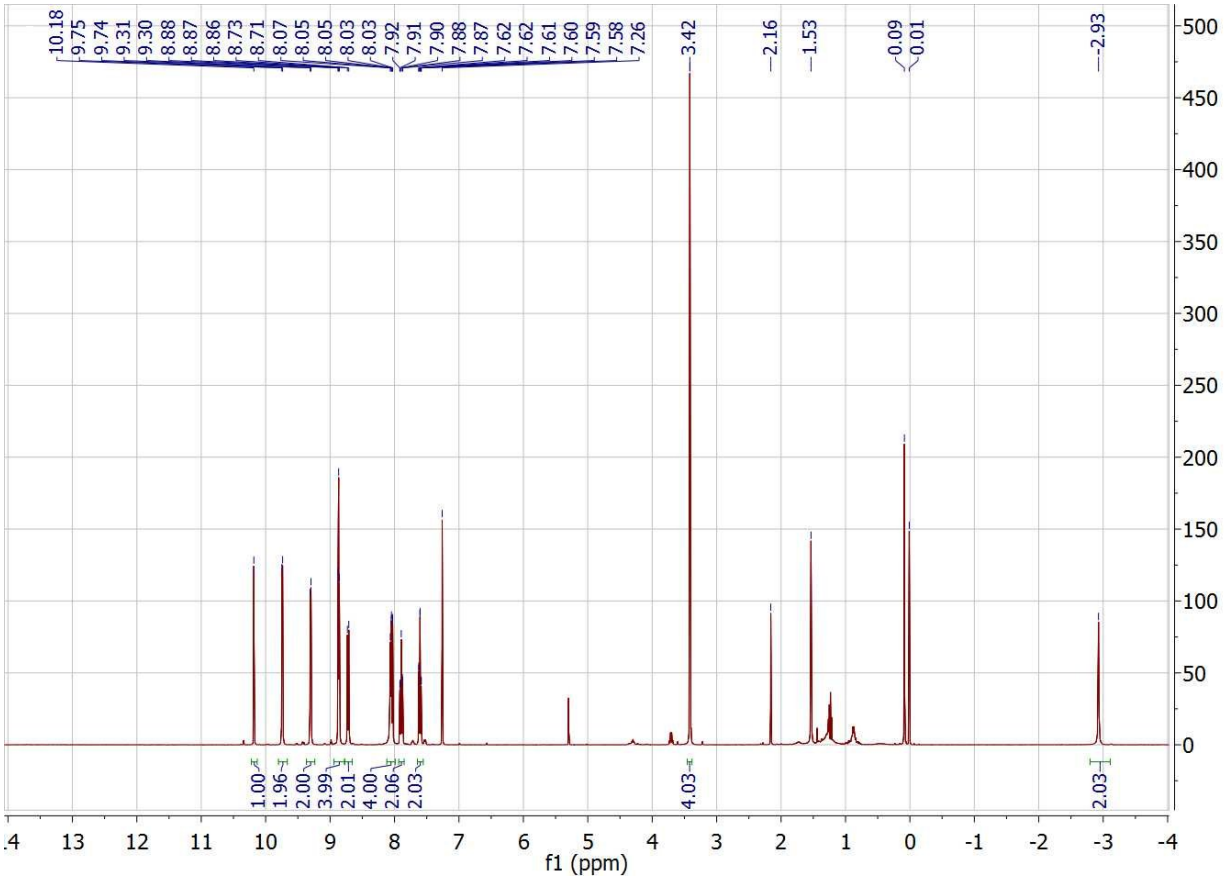

Residual signals: residual $CHCl_3$ (7.26 ppm); residual CH_2Cl_2 (5.30 ppm); residual acetone (2.17 ppm); residual H_2O (1.51); adventitious aliphatic grease (1.25, 0.88); residual silicon grease (0.09 ppm)

5.6 ^{1}H NMR spectra of strapped porphyrin 3 in $CDCl_3$

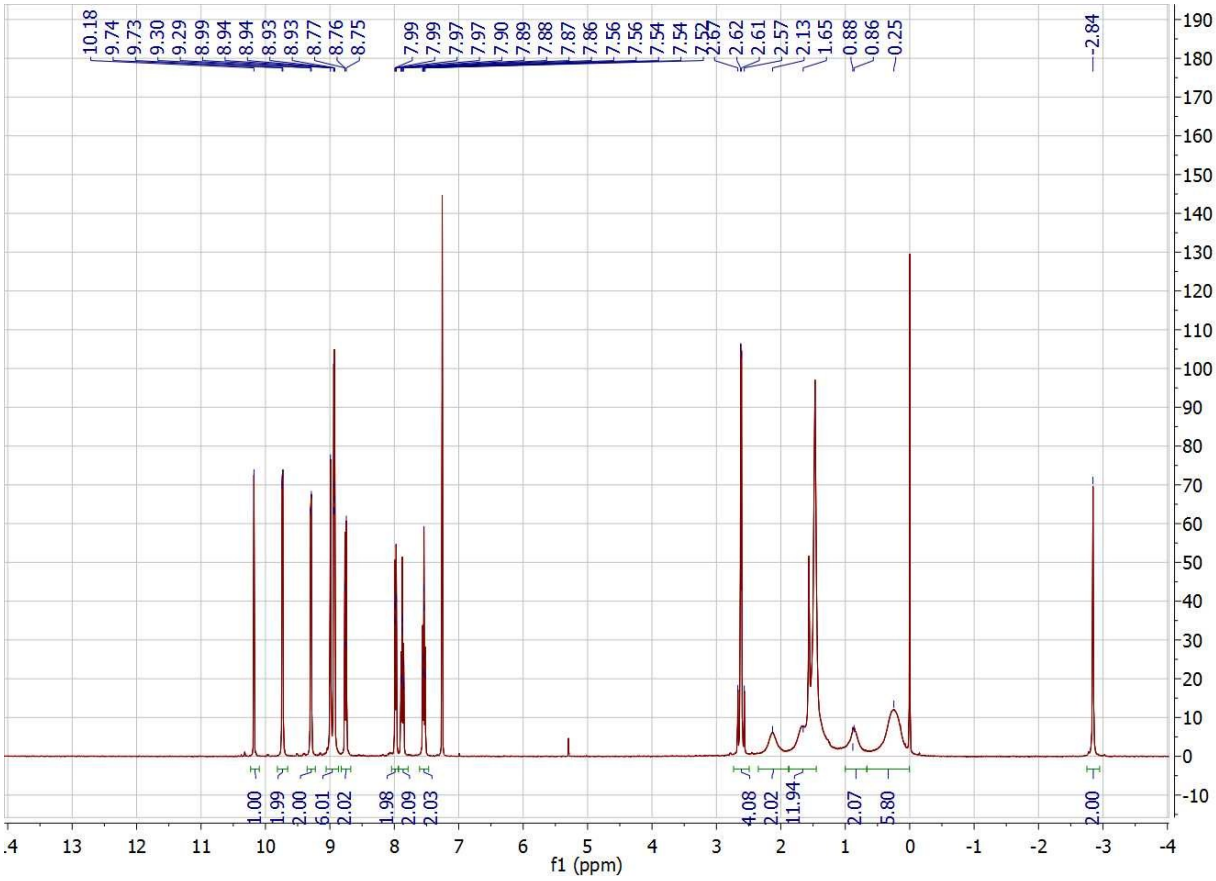

Residual signals: residual $CHCl_3$ (7.26 ppm); residual CH_2Cl_2 (5.31 ppm); residual H_2O (1.59)

5.7 ^{1}H NMR spectra of the mixture of strapped porphyrins 1a-OMe and 1b-OMe in $CDCl_3$

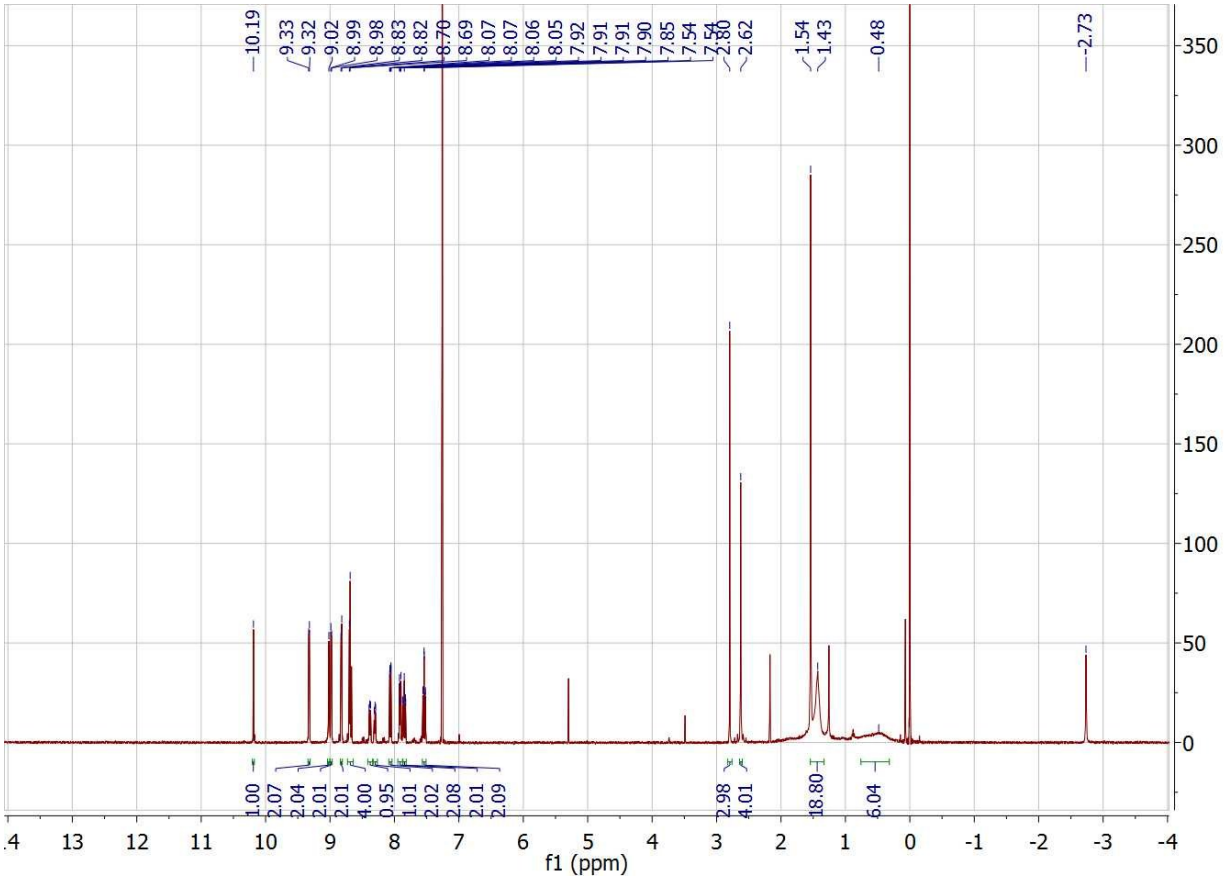

Residual signals: residual $CHCl_3$ (7.26 ppm); residual CH_2Cl_2 (5.29 ppm); residual acetone (2.16 ppm); residual H_2O (1.54); adventitious aliphatic grease (1.25, 0.88); residual silicon grease (0.09 ppm)

5.8 ^{1}H NMR spectra of atropisomer 1a-OH in $CDCl_3$

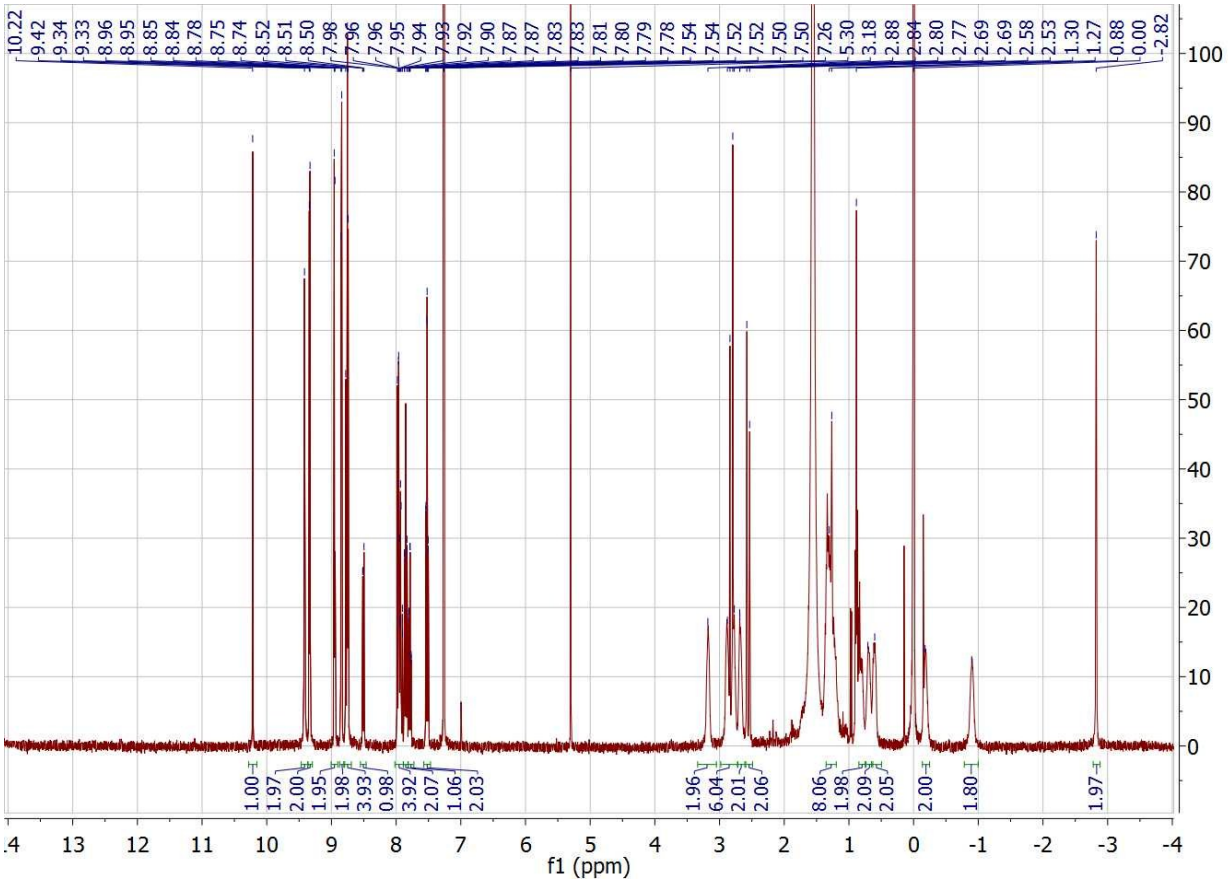

Residual signals: residual $CHCl_3$ (7.26 ppm); residual CH_2Cl_2 (5.29 ppm); residual H_2O (1.54); adventitious aliphatic grease (1.25, 0.88); residual silicon grease (0.09 ppm)

5.9 ^{1}H NMR spectra of methyl-2-carboxyphenyldioxolane 14 in $CDCl_3$

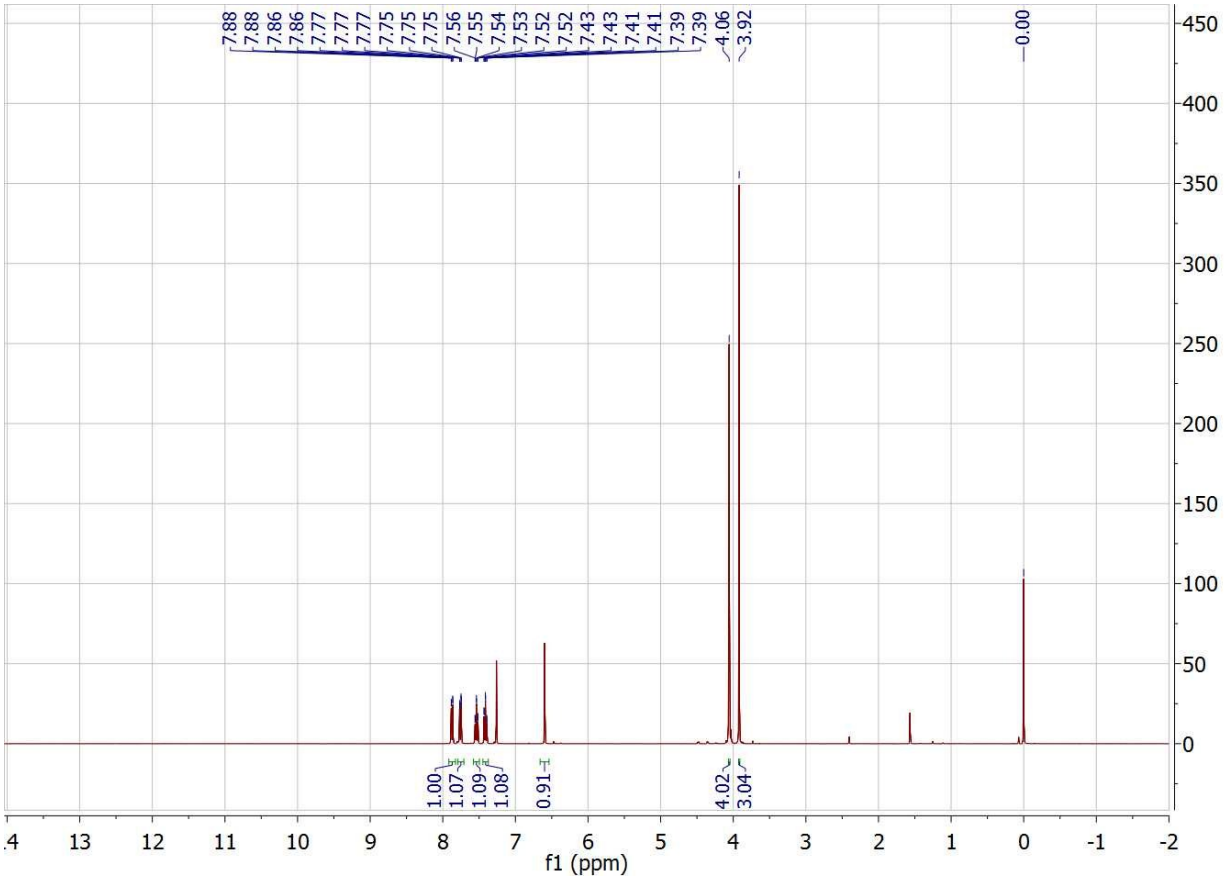

Residual signals: residual $CHCl_3$ (7.26 ppm); residual H_2O (1.54)

5.10 ^{1}H NMR spectra of 2-N,N-bis(2-methoxyacetonyl)amidophenyldioxolane 12 in $CDCl_3$

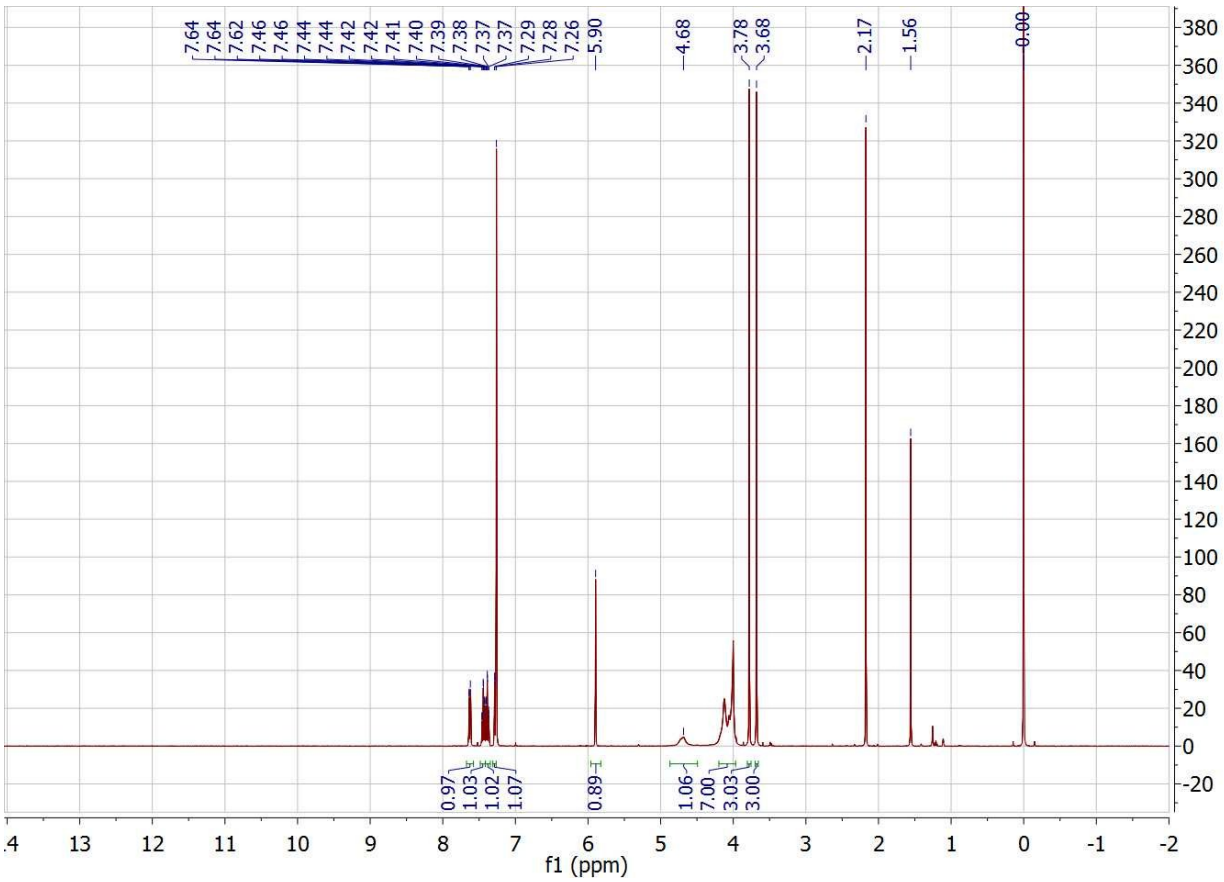

Residual signals: residual $CHCl_3$ (7.26 ppm); residual acetone (2.17 ppm); residual H_2O (1.56); adventitious aliphatic grease (1.25, 0.88)

5.11 ^{1}H NMR spectra of αα'-5-(2-nitrophenyl)-15-(2-N,N-(bis-2-methoxyacethyl)amidophenyl)porphyrins 11a in $CDCl_3$

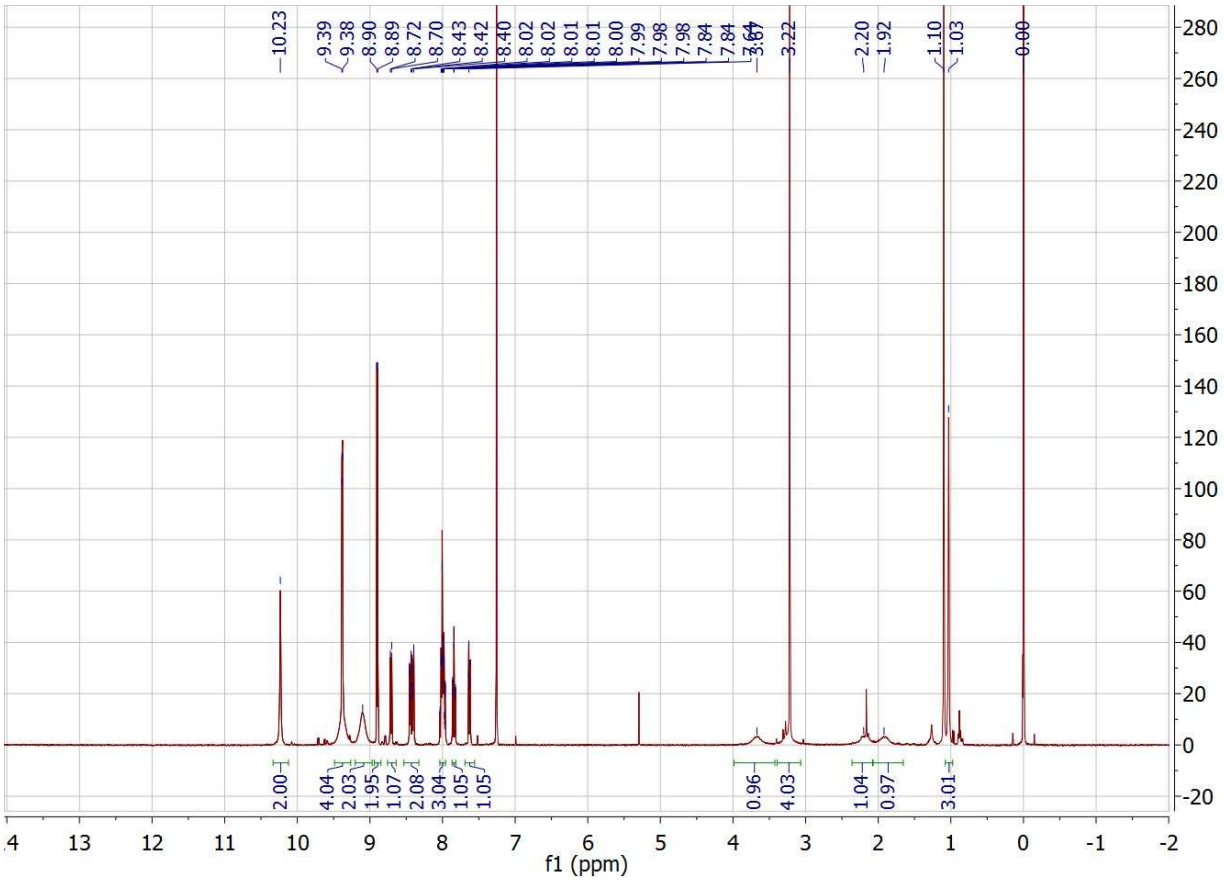

Residual signals: residual $CHCl_3$ (7.26 ppm); residual CH_2Cl_2 (5.29 ppm); residual acetone (2.16 ppm)

5.12 ^{1}H NMR spectra of αα'-5-(2-aminophenyl)-15-(2-N,N-(bis-2-methoxyacethyl)amidophenyl)-zinc-porphyrin 10a in $CDCl_3$-MeOD 4-1

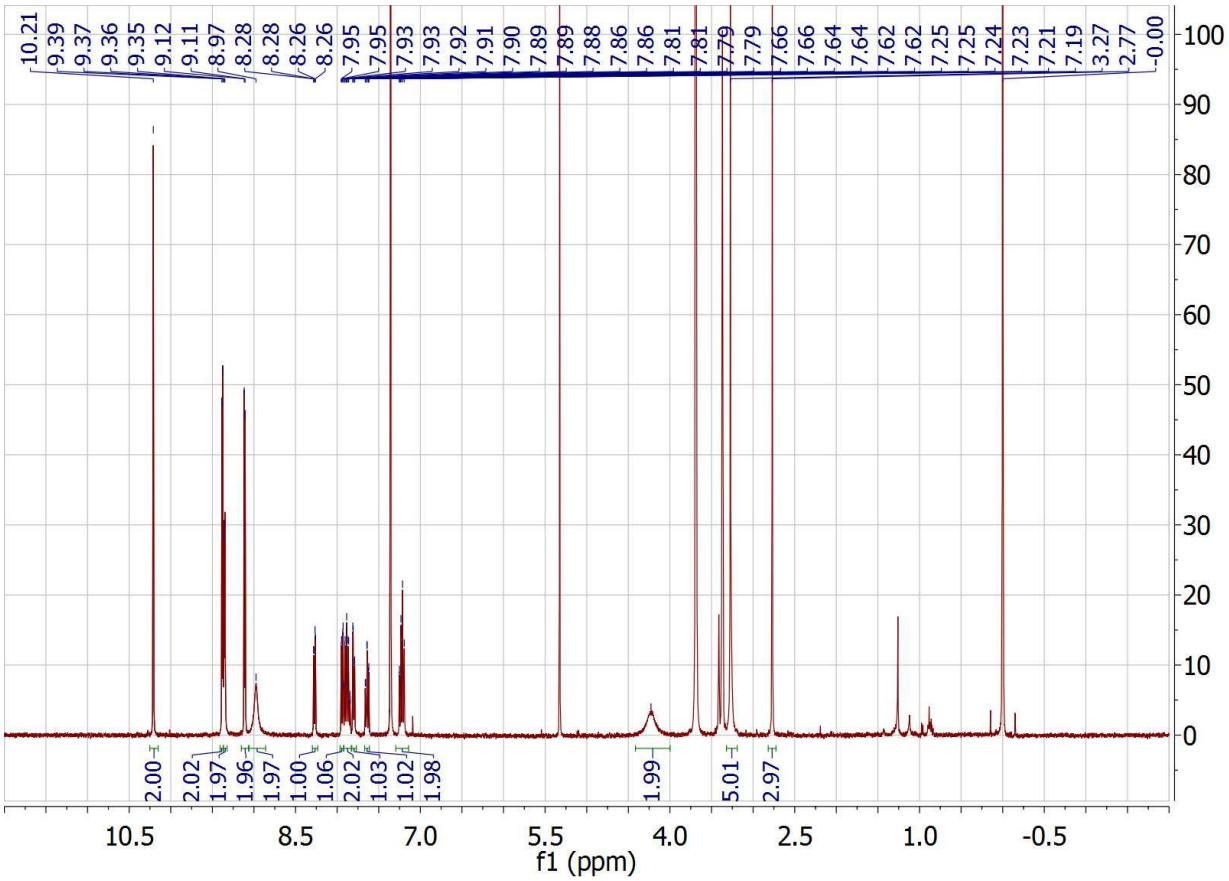

Residual signals: residual $CHCl_3$ (7.36 ppm); residual CH_2Cl_2 (5.3 ppm); residual H_2O (3.69 ppm); residual MeOH (3.37 ppm); adventitious aliphatic grease (1.25, 0.88)

5.13 ^{1}H NMR spectra of αβ'-5-(2-aminophenyl)-15-(2-N,N-(bis-2-methoxyacethyl)amidophenyl)-zinc-porphyrin 10b in $CDCl_3$

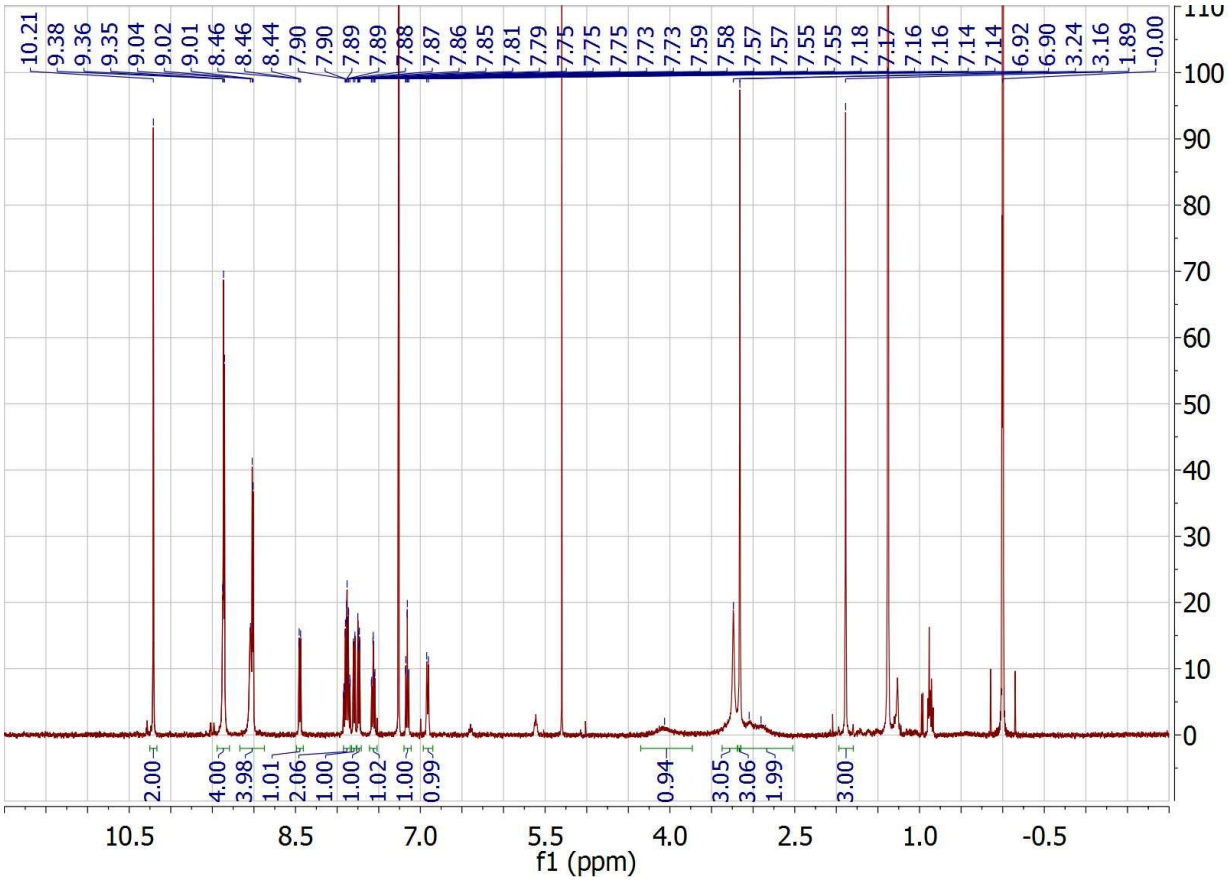

Residual signals: residual $CHCl_3$ (7.26 ppm); residual CH_2Cl_2 (5.29 ppm); adventitious aliphatic grease (1.25, 0.88)

5.14 ^{1}H NMR spectra of αα'-5-(2-(2-chloroactyl)aminophenyl)-15-(2-N,N-(bis-2-methoxyacethyl)amidophenyl)-zinc-porphyrin 9a in $CDCl_3$

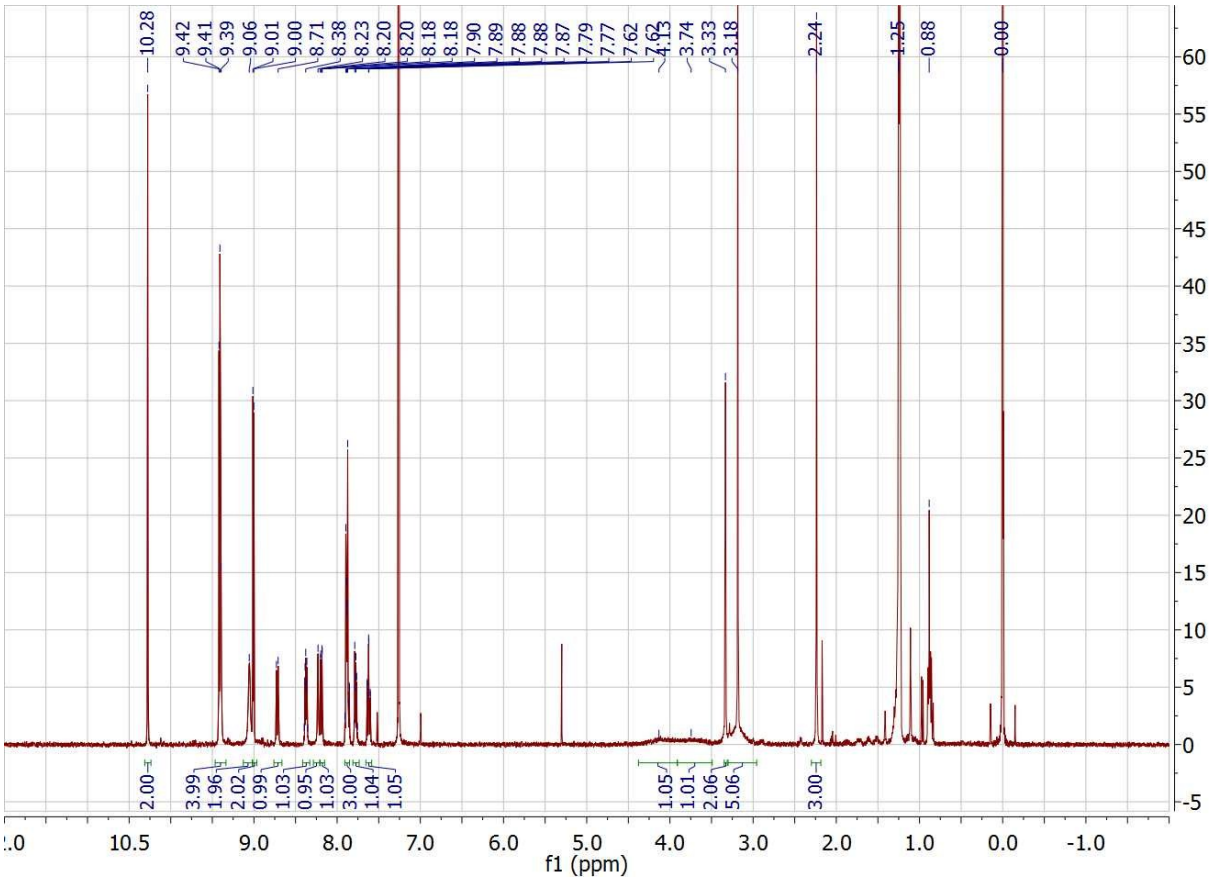

Residual signals: residual $CHCl_3$ (7.26 ppm); residual CH_2Cl_2 (5.30 ppm); residual acetone (2.17 ppm); adventitious aliphatic grease (1.25, 0.88)

5.15 ^{1}H NMR spectra of αβ'-5-(2-(2-chloroactyl)aminophenyl)-15-(2-N,N-(bis-2-methoxyacethyl)amidophenyl)-zinc-porphyrin 9b in $CDCl_3$

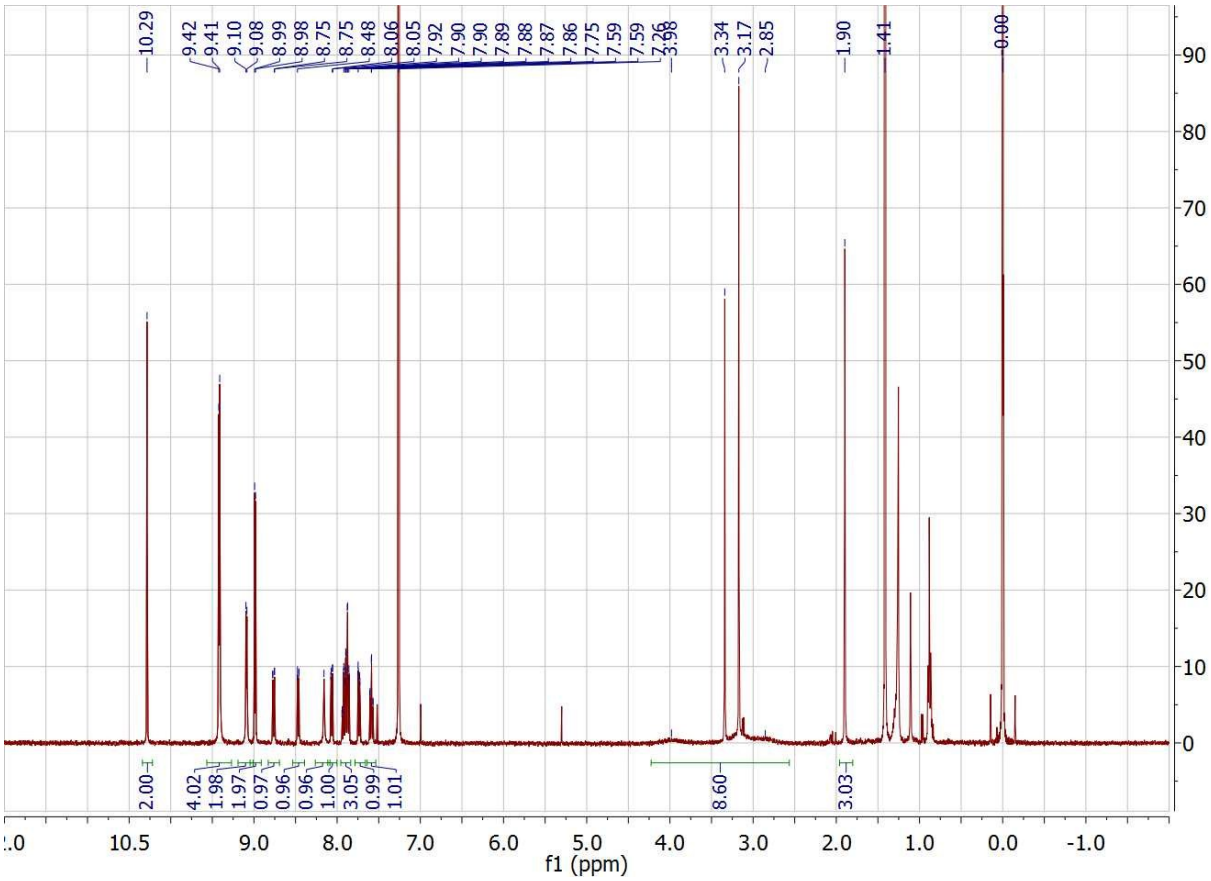

Residual signals: residual $CHCl_3$ (7.26 ppm); residual CH_2Cl_2 (5.31 ppm); residual H_2O (1.41 ppm); adventitious aliphatic grease (1.25, 0.88)

5.16 ^{1}H NMR spectra of porphyrin 8a in $CDCl_3$

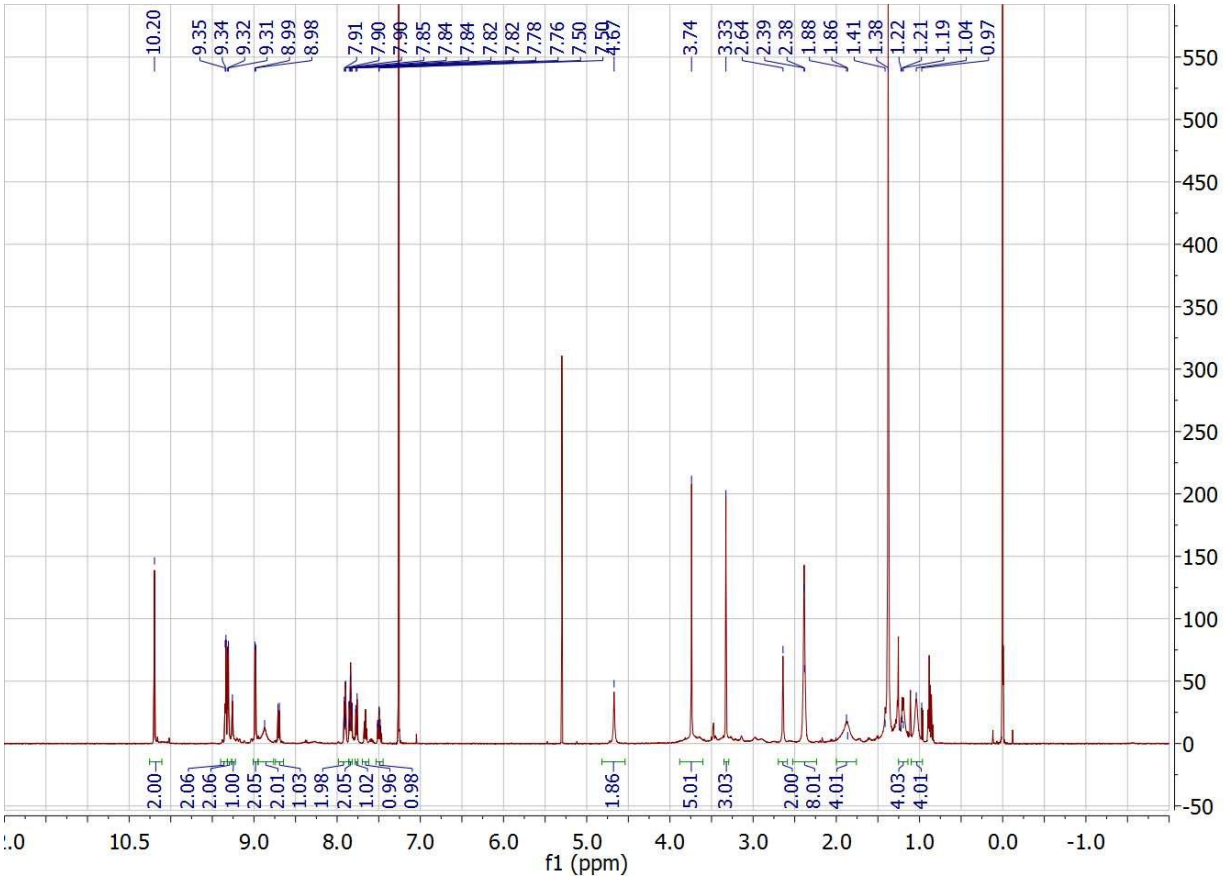

Residual signals: residual $CHCl_3$ (7.26 ppm); residual CH_2Cl_2 (5.29 ppm); residual H_2O (1.41 ppm); adventitious aliphatic grease (1.25, 0.88)

5.17 ^{1}H NMR spectra of porphyrin 8a in DMSO-d_6

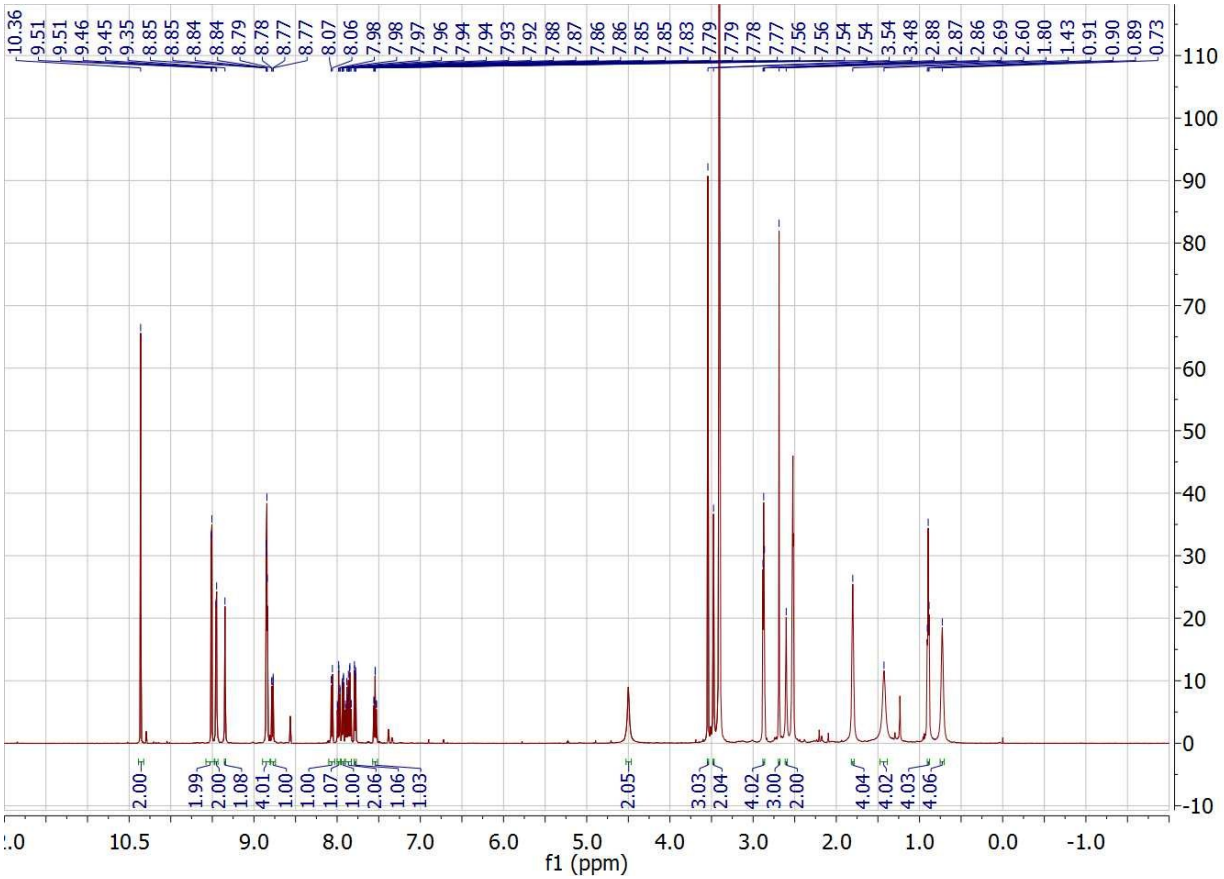

Residual signals: residual H_2O (3.30 ppm); residual DMSO (2.50 ppm); adventitious aliphatic grease (1.25, 0.88)

5.18 ^{1}H NMR spectra of porphyrin 8b in $CDCl_3$

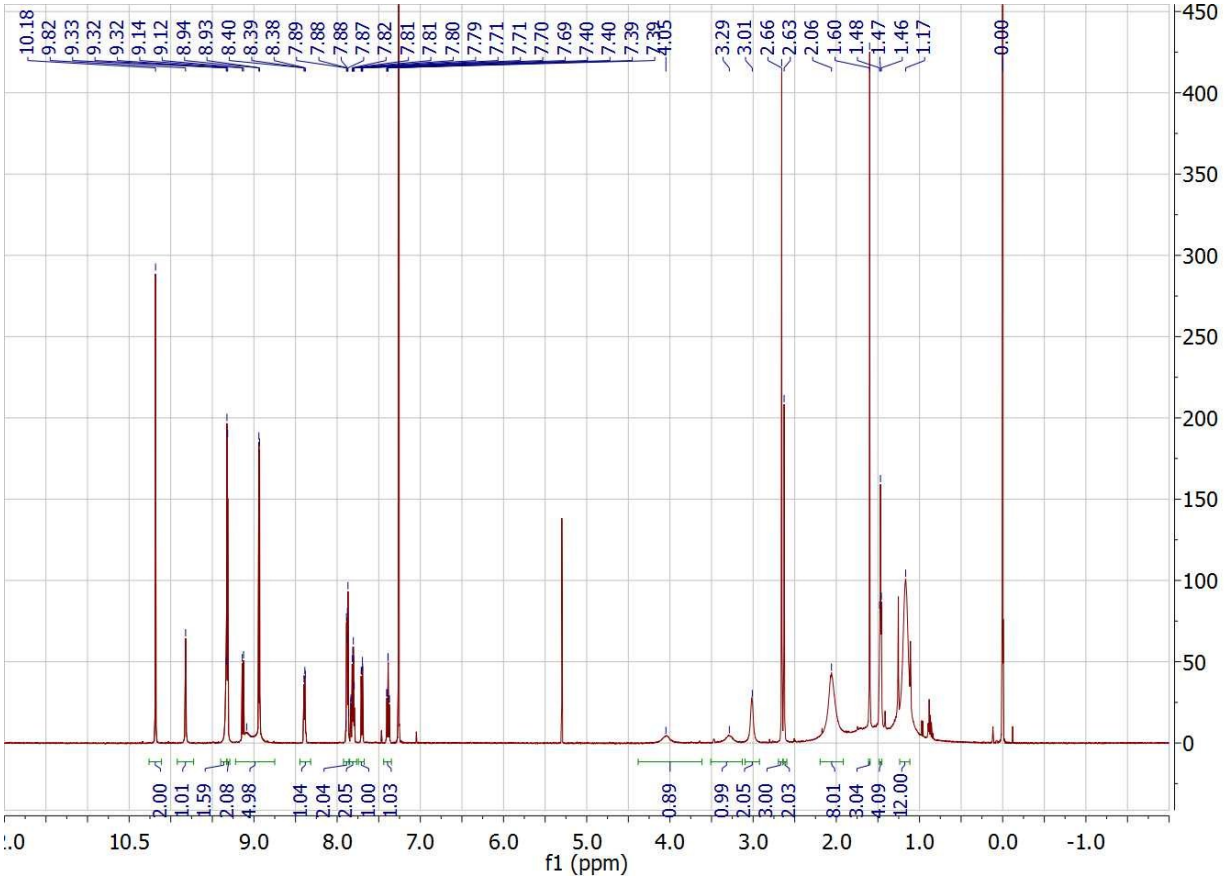

Residual signals: residual $CHCl_3$ (7.26 ppm); residual CH_2Cl_2 (5.32 ppm); adventitious aliphatic grease (1.25, 0.88)

5.19 ^{1}H NMR spectra of porphyrin 8b in DMSO-d_6

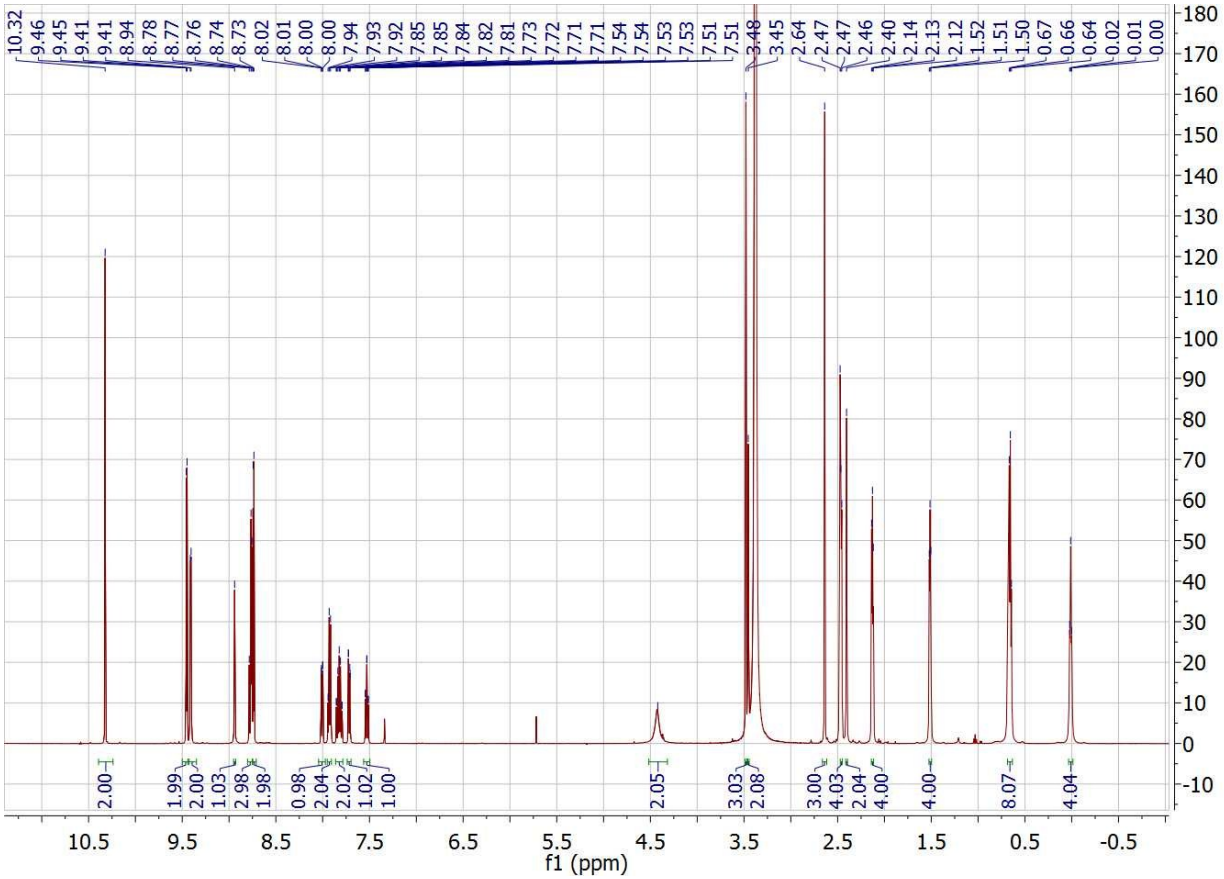

Residual signals: residual CH_2Cl_2 (5.75 ppm); residual H_2O (3.30 ppm); residual DMSO (2.48 ppm)

5.20 ^{1}H NMR spectra of porphyrin 2a in DMSO-d_6

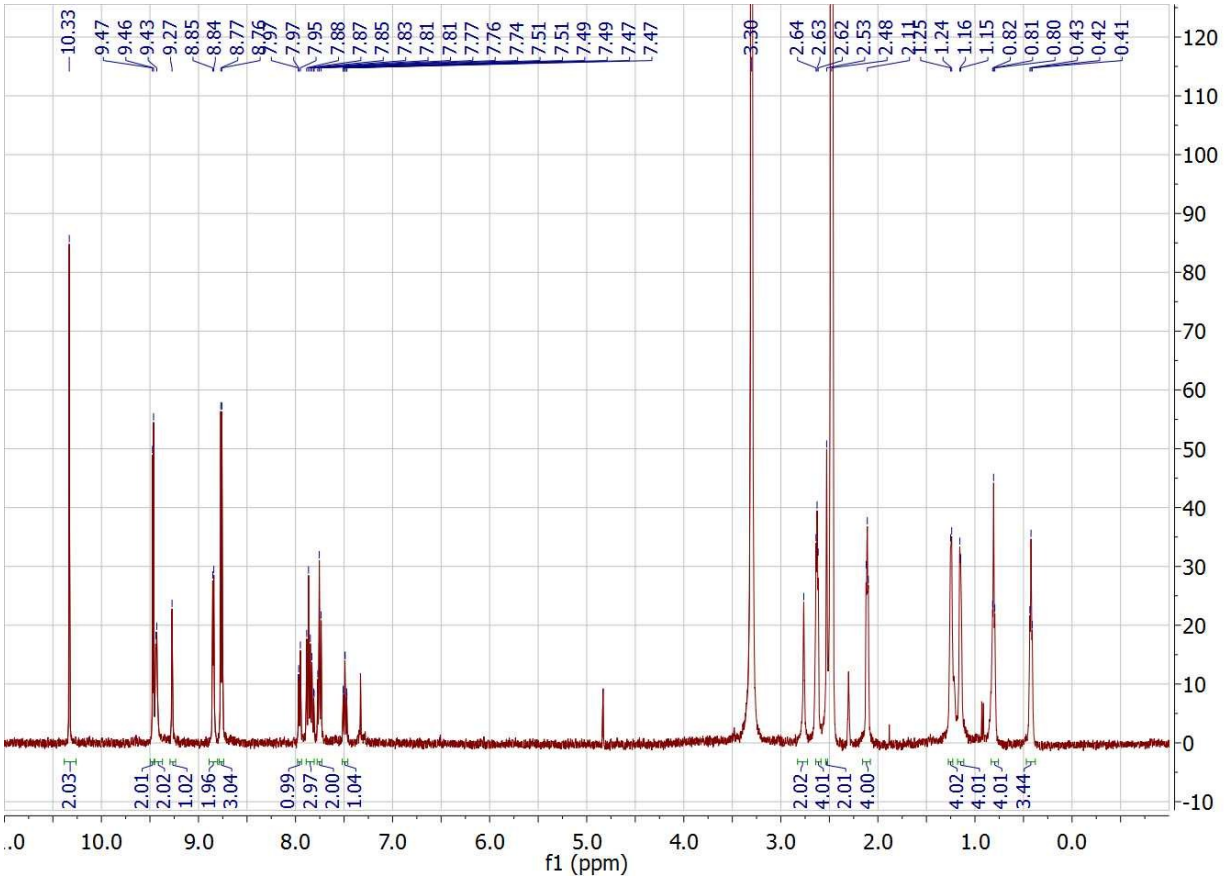

Residual signals: residual H_2O (3.30 ppm); residual DMSO (2.48 ppm)

5.21 ^{1}H NMR spectra of porphyrin 2b in DMSO-d_6

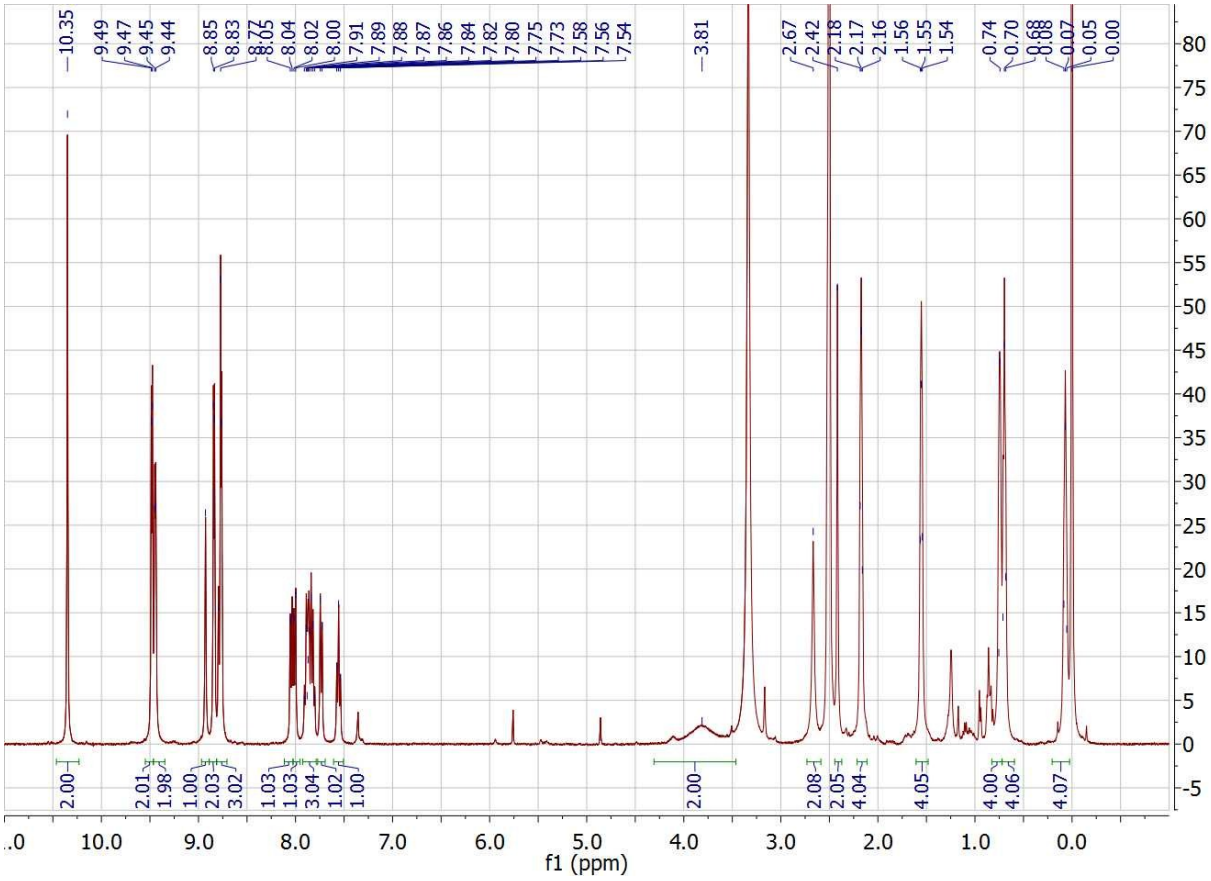

Residual signals: residual H_2O (3.32 ppm); residual DMSO (2.48 ppm); adventitious aliphatic grease (1.25, 0.88)

5.22 ^{1}H NMR spectra of 5-phenyl-15-(2-nitrophenyl)porphyrin 17 in $CDCl_3$

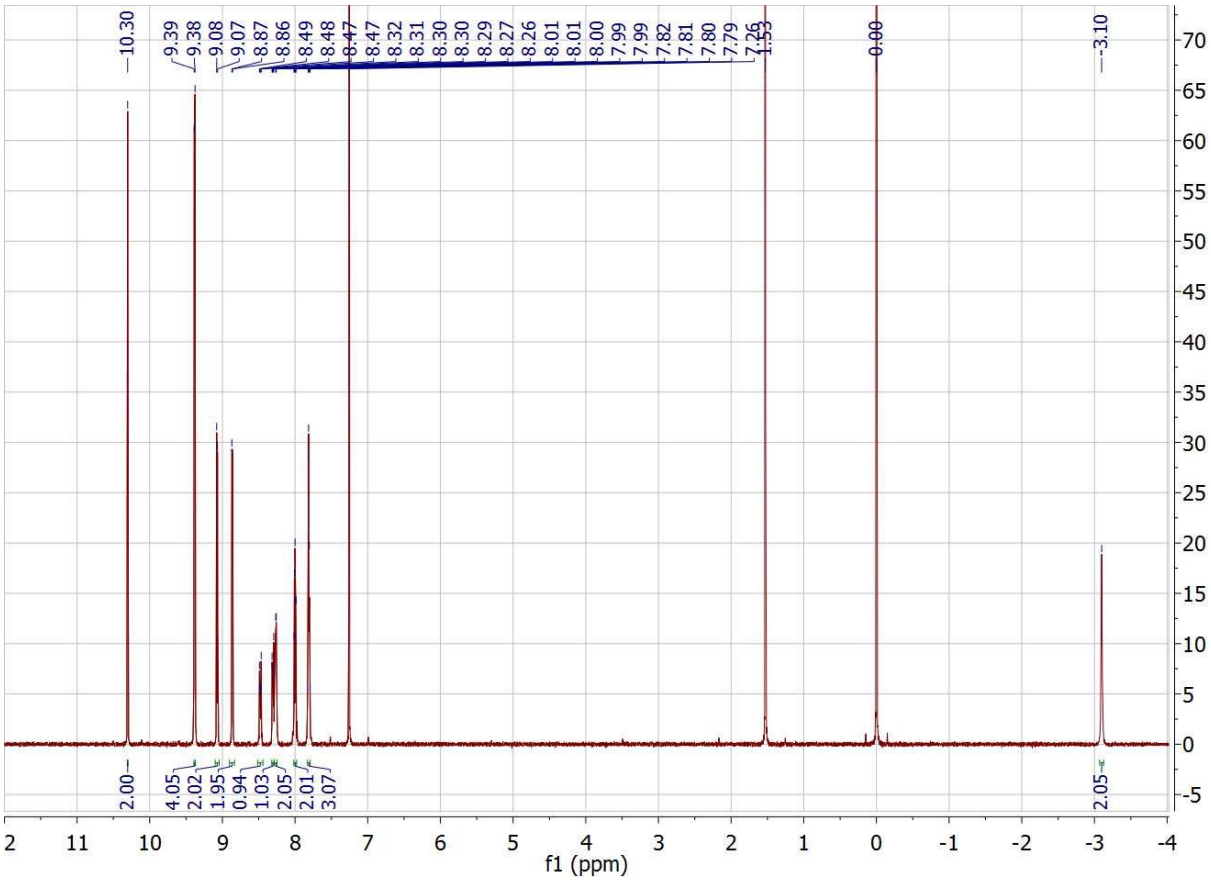

Residual signals: residual $CHCl_3$ (7.26 ppm); residual H_2O (1.53 ppm)

5.23 ^{1}H NMR spectra of 5-phenyl-15-(2-aminophenyl)porphyrin 16 in $CDCl_3$

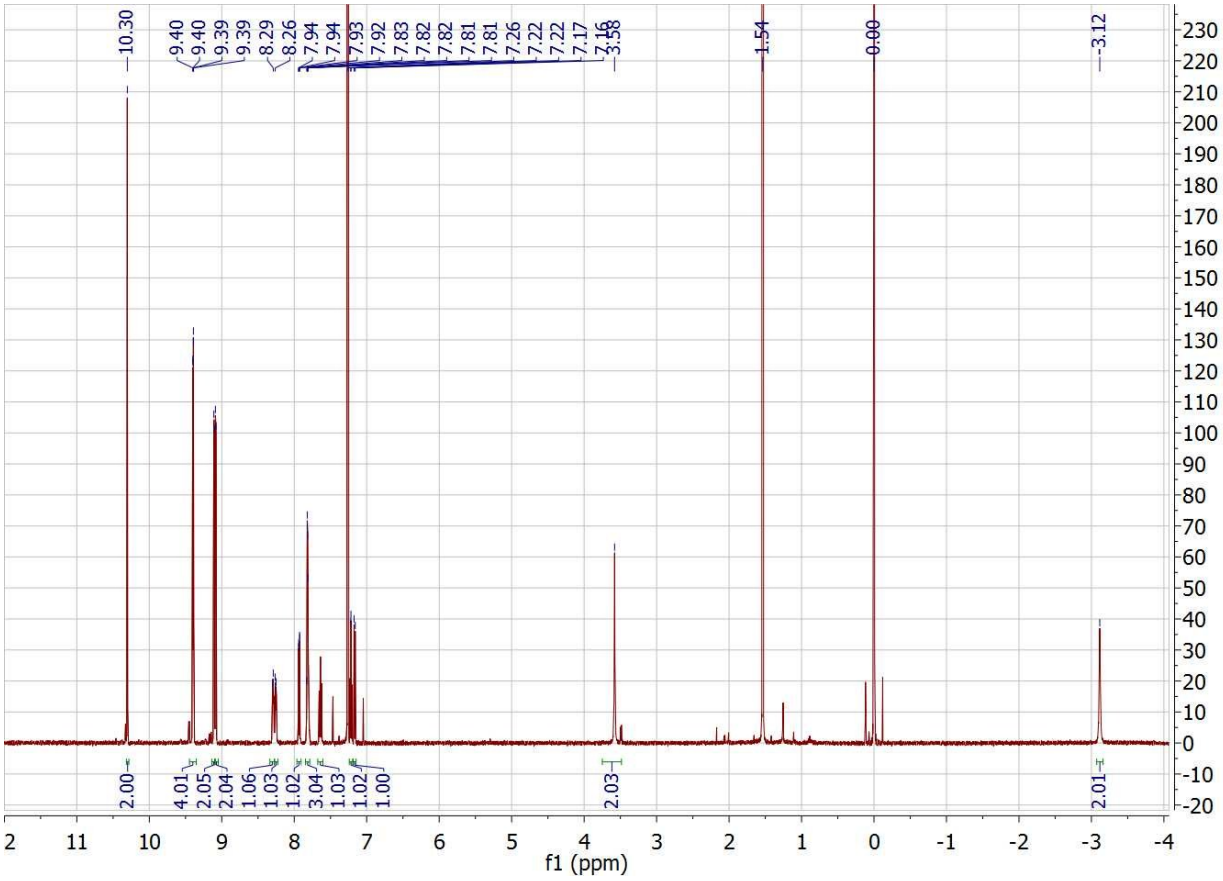

Residual signals: residual $CHCl_3$ (7.26 ppm); residual H_2O (1.53 ppm); adventitious aliphatic grease (1.25, 0.88)

5.24 ^{1}H NMR spectra of 5-phenyl-15-(2-(2-chloroacethylaminophenyl))porphyrin zinc(II) complex 15 in $CDCl_3$

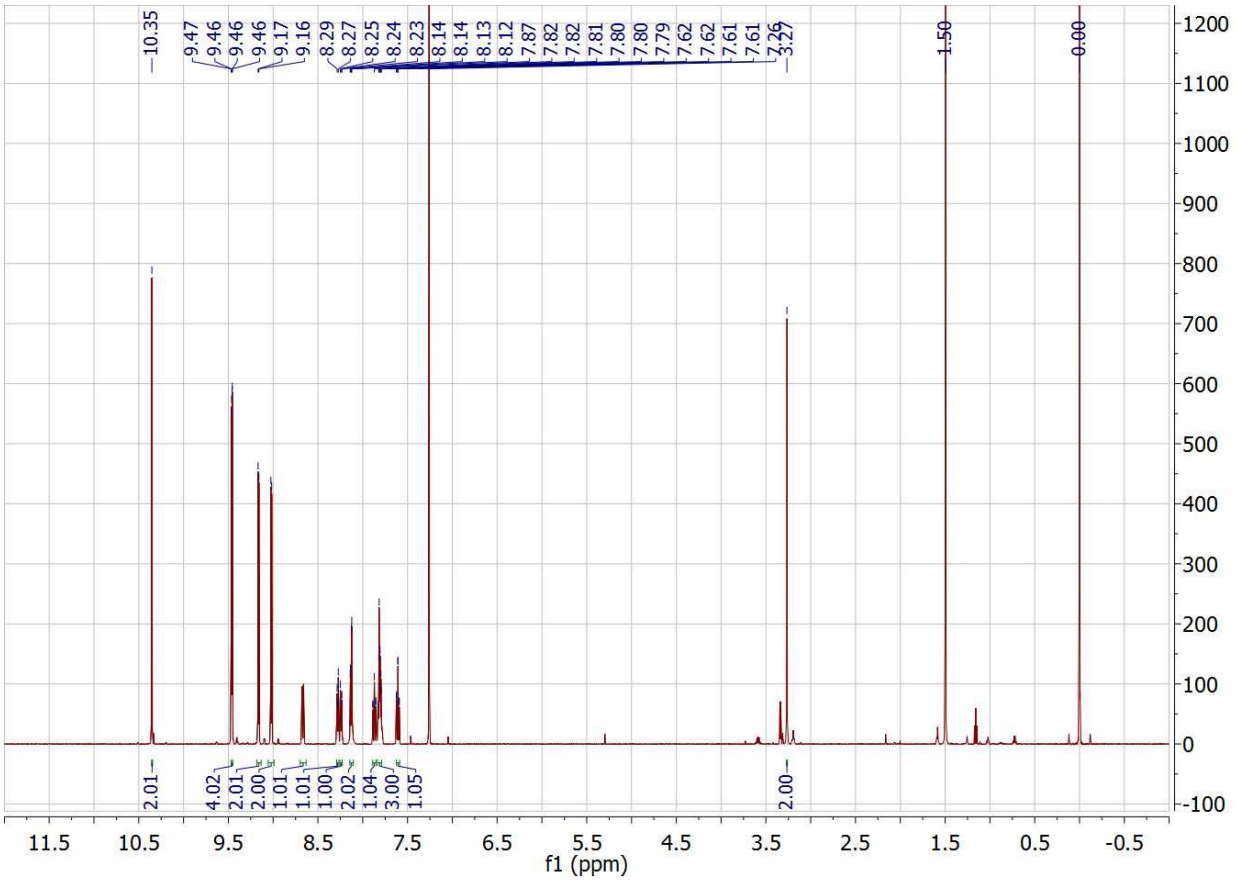

Residual signals: residual $CHCl_3$ (7.26 ppm); residual H_2O (1.50 ppm); adventitious aliphatic grease (1.25, 0.88)

5.25 ^{1}H NMR spectra of R2 in DMSO-d_6

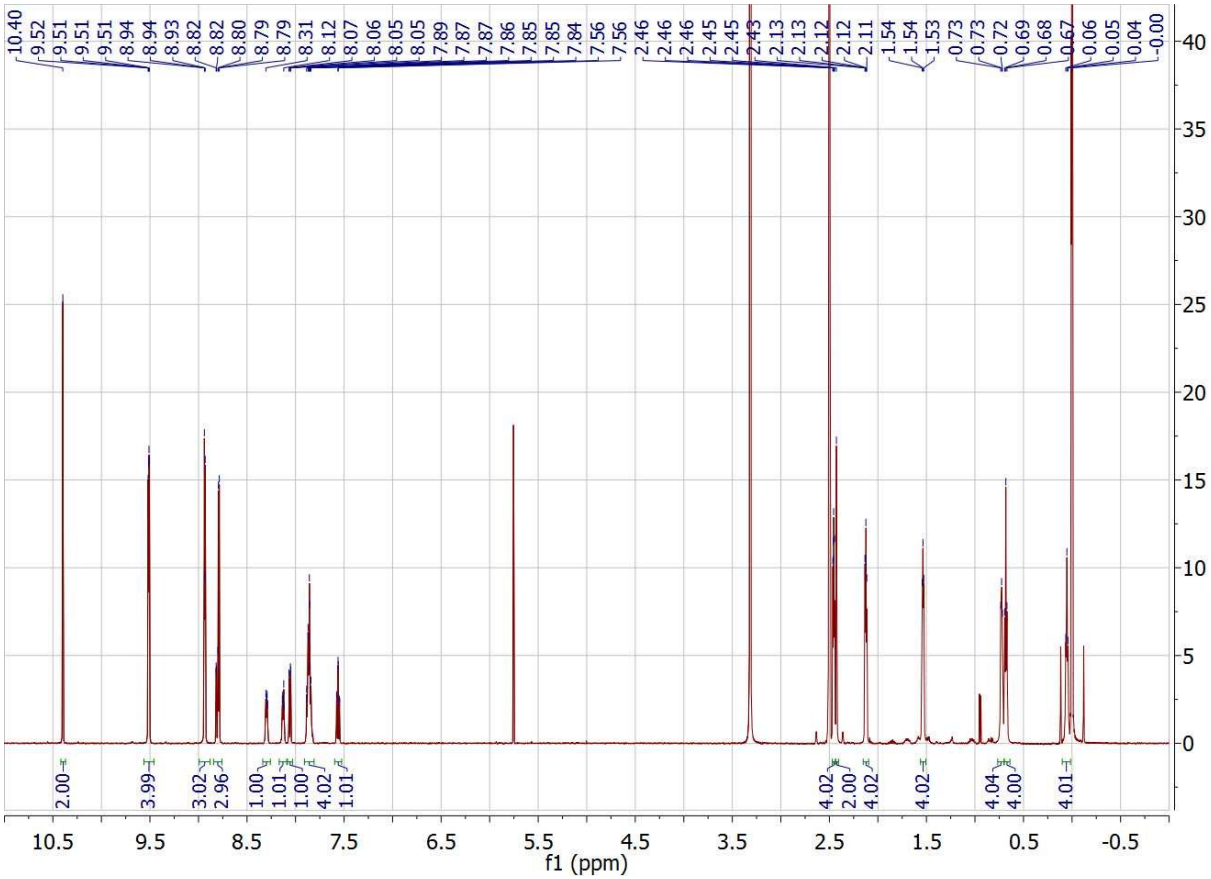

Residual signals: residual CH_2Cl_2 (5.75 ppm); residual H_2O (3.31 ppm); residual DMSO (2.48 ppm)

5.26 ^{1}H NMR spectra of R1 in MeOD-5% Pyridine-d_5

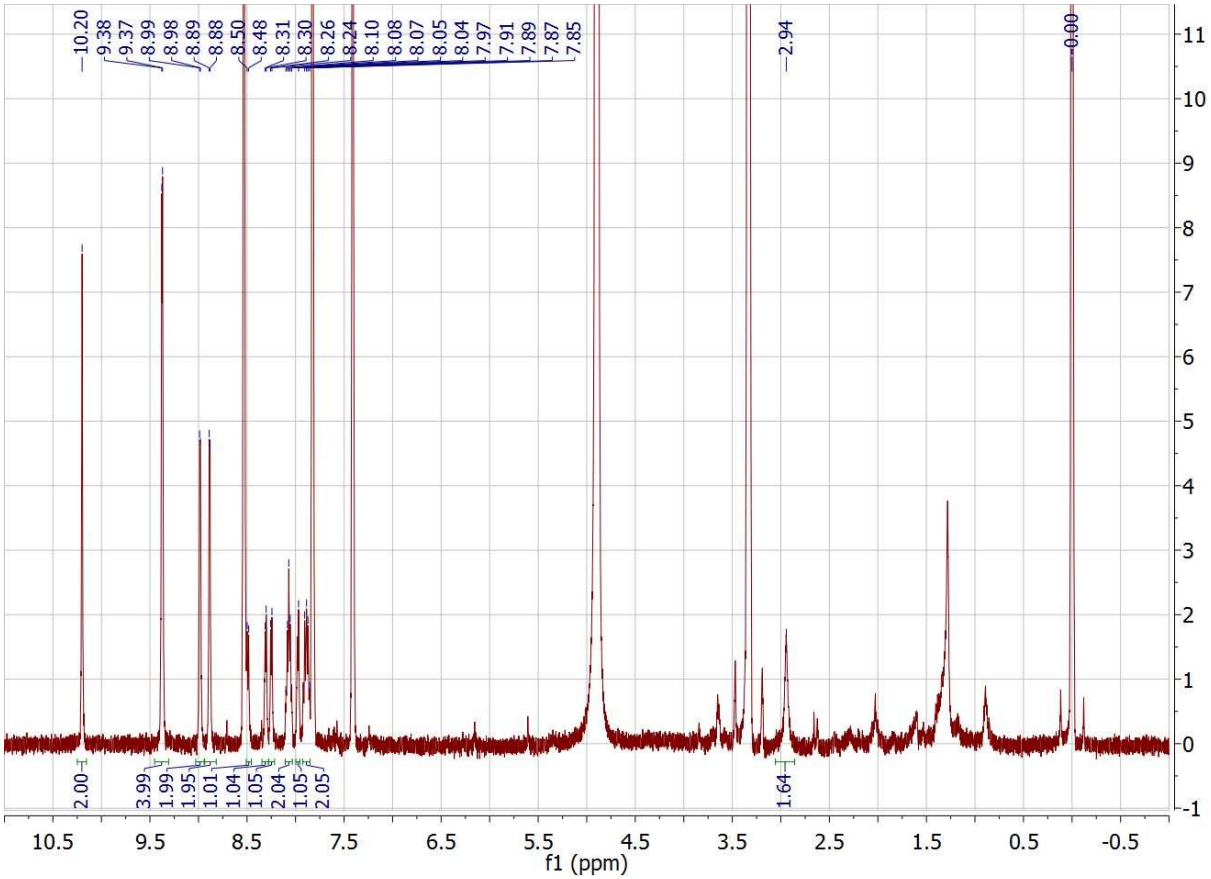

Residual signals: residual pyridine (8.53, 7.83, and 7.41 ppm); residual H_2O (4.90 ppm); residual MeOH (3.33 ppm)

5.27 ^{1}H NMR spectra of R1 in DMSO-d_6-5% Pyridine-d_5

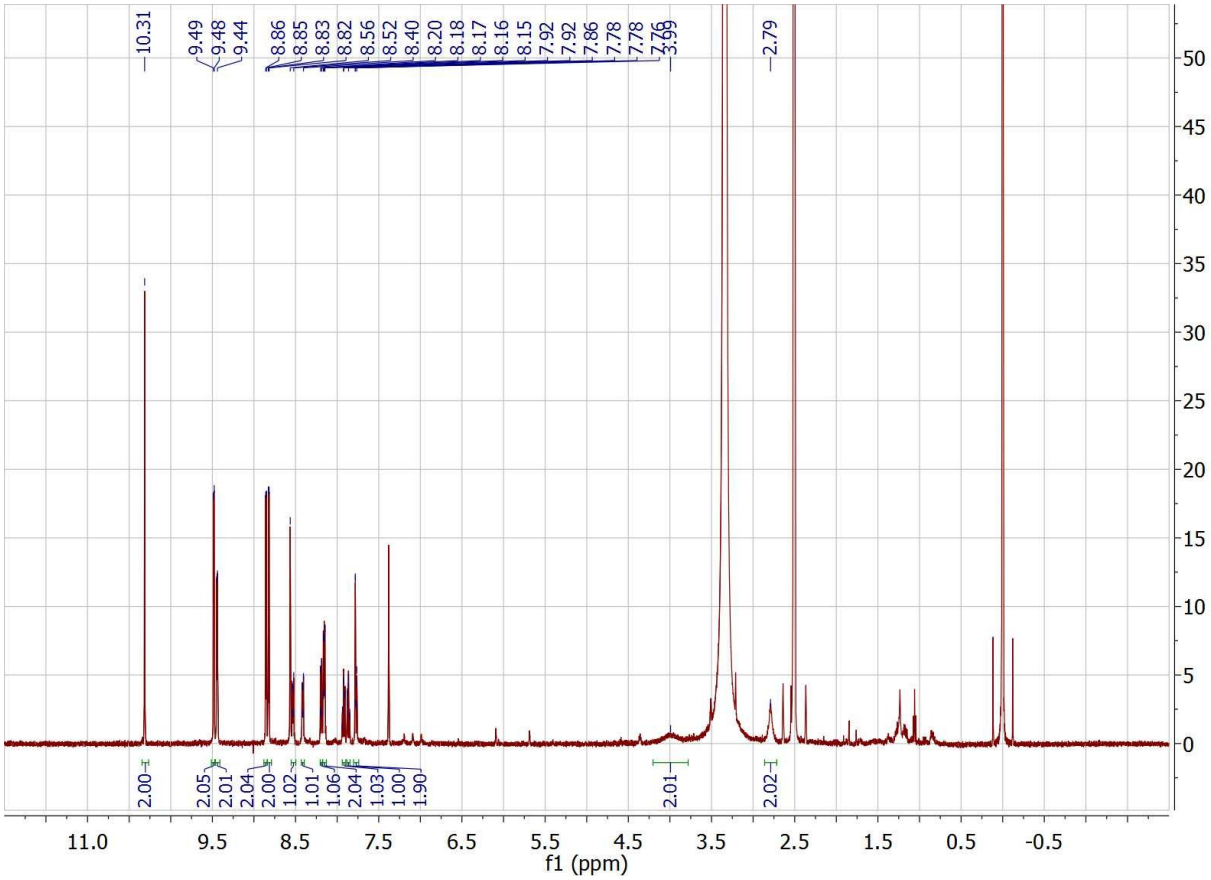

Residual signals: residual pyridine (8.56, 7.79, and 7.38 ppm); residual H_2O (3.34 ppm); residual DMSO (2.51 ppm)

6 References

[1] J. K. Laha, S. Dhanalekshmi, M. Taniguchi, A. Ambroise, J. S. Lindsey, *Org. Process Res. Dev.* **2003**, *7*, 799-812.

[2] J. K. Laha, S. Dhanalekshmi, M. Taniguchi, A. Ambroise and J. S. Lindsey, *Org. Process Res. Dev.*, 2003, **7**, 799-812.

[3] J. Lindsey, *J. Org. Chem.*, 1980, **45**, 5215-5215.

[4] J. S. Manka, D. S. Lawrence, *Tetrahedron Lett.* **1989**, *30*, 6989-6992.

[5] A. Brown, M. J. Langton, N. L. Kilah, A. L. Thompson, P. D. Beer, *Chemistry – A European Journal* **2015**, *21*, 17664-17675.

[6] a) J. R. Lakowicz, *Principles of Fluorescence Spectroscopy*, 3 ed., Springer Science+Business Media, New York, **2006**; b) B. Valeur, Wiley-VCH, Weinheim, Germany **2002**.

[7] P. Debye, *Polar Molecules*,The Chemical Catalogue Company **1929.**